

# **An investigation of the importance of the ATM protein in the endothelium and its role in the signalling pathways of NO production**

by  
Natalie Chantel Collop

*Thesis presented in fulfilment of the requirements for the degree of Master of Science in Medical Sciences in the Faculty of Medical and Health Science at Stellenbosch University*



Supervisor: Prof. Barbara Huisamen  
Co-supervisor: Prof. Hans Strijdom

March 2015

## **Declaration**

By submitting this thesis electronically, I declare that the entirety of the work contained therein is my own, original work, that I am the sole author thereof (save to the extent explicitly otherwise stated), that reproduction and publication thereof by Stellenbosch University will not infringe any third party rights and that I have not previously in its entirety or in part submitted it for obtaining any qualification.

December 2014

Copyright © 2015 Stellenbosch University

All rights reserved

**Abstract:**

Ataxia telangiectasia (AT) is a well-characterized neurodegenerative disease resulting from a genetic defect in the *Atm* gene causing an absence or very low expression of the ATM protein. As AT patients are prone to the development of insulin resistance and atherosclerosis, the aim of the current study was to investigate the importance of the ATM protein in the endothelium and its role in the signalling pathways of nitric oxide (NO) production. To accomplish this, the first objective was to establish an in-house endothelial cell isolation technique harvested from normal and insulin resistant animals. Unfortunately, these cultures, although staining positive with an endothelial cell specific stain, were not pure enough and did not express endothelial NO synthase (eNOS), the central enzyme in NO production.

The remainder of the study utilized commercial aortic endothelial cells (AECs) and found that there was a significant increase in NO production when the ATM protein was inhibited by the specific inhibitor, Ku-60019. The beneficial impact of increased NO production includes maintaining vascular homeostasis, promoting angiogenesis, initiating DNA repair by activating p53 and inhibiting smooth muscle cell proliferation. On the other hand, reactive oxygen species (ROS) and reactive nitrogen species (RNS) also generated by high levels of NO, can exert both protective and harmful effects. Examples of these include cell death due to high concentrations of ROS. However, Ku-60019 did not result in increased cell death of AECs.

We demonstrated for the first time, a relationship between endothelial ATM protein kinase and the generation of NO. The signalling pathways involved in NO production and glucose utilization form a network of interrelationships. Central to both pathways is the activity of

two protein kinases, PKB/Akt and AMPK. Both these kinases are known to phosphorylate the eNOS enzyme to produce NO on the one hand and AS160 to induce GLUT 4 translocation and glucose uptake on the other hand. Activation of the ATM protein is postulated to be a prerequisite for PKB/Akt activation and it may also result in activation of AMPK. However, using insulin to stimulate ATM, we could not show that inhibition of ATM in endothelial cells affected expression or insulin-stimulated activation of PKB/Akt while the PI3-K inhibitor wortmannin, inhibited the latter. In addition, inhibition of ATM negatively regulated the phospho/total ratio of AMPK. We therefore postulate that the NO production elicited by inhibition of ATM, may not be as result of eNOS activity.

A second important observation was that inhibition of ATM significantly enhanced phosphorylation of the p85 regulatory subunit of PI3-K. This would imply that ATM normally has an inhibitory effect on p85 phosphorylation and therefore PI3-K activation. We base this assumption on previous publications showing that Ku-60019 does not inhibit PI3K. This again indicates that ATM has a hitherto unexplored regulatory role in endothelial function.

## Opsomming:

Ataxia telangiectasia (AT) is a goed-gekarakteriseerde neurodegeneratiewe siekte a.g.v. 'n genetiese afwyking in the *Atm* geen wat lei tot 'n afwesige of lae uitdrukking van die ATM proteïen. Aangesien AT pasiënte geneig is om insulienweerstandigheid en aterosklerose te ontwikkel, was die doel van hierdie studie om die belang van die ATM proteïen in die endoteel, en sy rol in die seintransduksiepaaie betrokke by stikstofoksied (NO) produksie, te ondersoek. Om dit te bereik, was die eerste mikpunt om 'n eie endoteelsel isolasietegniek (ge-oes van normale en insulienweerstandige diere) te vestig. Ongelukkig was hierdie selkulture nie suiwer genoeg nie. Ten spyte daarvan dat hulle positief getoets het met 'n endoteelsel-spesifieke kleurstof kon geen uitdrukking van eNOS, die sentrale ensiem verantwoordelik vir NO produksie, waargeneem word nie.

Die res van die studie het van kommersiële aorta endoteelselle (AES) gebruik gemaak, en daar is gevind dat die inhibisie van die ATM proteïen met die spesifieke inhibitor, Ku-60019, tot 'n beduidende toename in NO produksie gelei het. Die voordelige impak van verhoogde NO produksie sluit die handhawing van vaskulêre homeostase, bevordering van angiogenese, inisiëring van DNA herstel deur p53 aktivering en inhibisie van gladdespiersel proliferasie in. Reaktiewe suurstofspesies (ROS) en reaktiewe stikstofspesies (RNS) wat ook a.g.v. verhoogde NO gegenereer word, kan egter beide beskermende sowel as skadelike effekte uitoefen. Voorbeelde sluit seldood a.g.v. hoë ROS konsentrasies in. Ku-60019 het egter nie tot 'n toename in seldood van die AES gelei nie.

Hierdie studie het vir die eerste keer aangetoon dat daar 'n verwantskap tussen die endoteel ATM proteïen kinase en die produksie van NO bestaan. Die seintransduksie

paaie betrokke by NO produksie en glukose verbruik vorm 'n interafhanklike netwerk. Die aktiwiteit van twee proteïen kinases, PKB/Akt en AMPK, is sentrale rolspelers in beide paaie. Albei hierdie kinases is daarvoor bekend dat hulle die eNOS ensiem fosforileer om NO te produseer, maar terselfdertyd ook lei tot AS160 fosforilering, wat tot GLUT 4 translokering en glukose opname lei. Dis is voorgestel dat aktivering van die ATM proteïen 'n voorvereiste vir PKB/Akt aktivering mag wees en verder kan dit ook tot aktivering van AMPK lei. Ons kon nie aantoon dat inhibisie van ATM in endoteelselle die uitdrukking of insulien-geïnduseerde aktivering van PKB/Akt onderdruk nie, terwyl die PI3-K inhibitor, wortmannin, wel laasgenoemde geïnhibeer het. Verder het die inhibisie van ATM die fosfo/totale AMPK verhouding negatief gereguleer. Ons postuleer dus dat die NO produksie waargeneem tydens ATM inhibisie, moontlik nie die gevolg van eNOS aktiwiteit was nie.

'n Tweede belangrike waarneming was dat die inhibisie van ATM die fosforilering van die p85 regulatoriese subeenheid van PI3-K beduidend laat toeneem het. Dit impliseer dat ATM normaalweg 'n inhibitoriese effek op p85 fosforilering, en dus PI3-K aktivering, het. Hierdie aanname word gemaak n.a.v. vorige publikasies wat getoon het dat Ku-60019 nie PI3-K inhibeer nie. Dit dui weer eens daarop dat ATM 'n tot nog toe onbekende regulatoriese rol in endoteelfunksie het.

## Acknowledgements

I would like to dedicate this MSc thesis to my Mother Linda and my sister Cindy for always standing by me, encouraging me and believing in me. Without you, none of this would be possible.

Thank you to God above for all he has done and for giving me this opportunity to complete my MSc degree; I truly live a blessed life.

I would like to express my gratitude to my supervisors Prof. B. Huisamen and Prof. H. Strijdom for their mentorship, guidance, support and advice during the past two years.

I would like to give thanks and recognition to the following institutions; the University of Stellenbosch, NRF, Harry Crossley Research Grant and the Harry Truter bursary fund for without their funding this project would not be have been complete.

Thank you to my colleagues Corli Westcott, Dr Amanda Genis, Dr Erna Marias, Mashuda Mthethwa, Rafee'ah Kaskar, Dirk Loubser, Dumisile Lumkwana, Yolandi Espach, Michelle Smit van Schalkwyk and my fellow MSc students for all your encouragement, laughs and support over the past two years.

Thank you to my friends and family, especially the Willemse family for your kind words, support and prayers they have meant a lot to me and touched my heart.

## Table of Contents

Declaration.....	I
Abstract: .....	II
Opsomming: .....	IV
Acknowledgements .....	VI
List of Figures:.....	XIII
List of Tables: .....	XVII
Abbreviations.....	XVIII
<b>Chapter 1: Introduction</b> .....	<b>1</b>
1.1. The metabolic syndrome, diabetes mellitus and atherosclerosis: risk factors for the development of cardiovascular disease (CVD) development.....	3
1.1.1. The metabolic syndrome.....	3
1.1.2. Type 2 diabetes mellitus.....	4
1.1.2.1. Activation of the PI3-K pathway in an insulin dependent manner.....	6
1.1.2.2. Glucose uptake .....	6
1.1.2.3. Insulin insensitivity.....	9
1.1.3. Atherosclerosis development .....	10
1.2. The importance of the endothelium in vascular health .....	13



1.2.1. Endothelial dysfunction and cardiovascular disease .....	13
1.2.2. The function and importance of aortic endothelial cells (AECs) in vascular health .....	13
1.3. Conclusion .....	16
<b>Chapter 2: Literature review .....</b>	<b>18</b>
2.1. The ATM protein .....	18
2.2. Activating the ATM protein – the nuclear function of ATM.....	21
2.2.1. The DNA damage response .....	22
2.2.2. Proteins involved in the DDR.....	25
2.2.3. DNA damage and heart disease.....	31
2.2.4. DNA damage and cell pathology .....	33
2.3. Oxidative stress .....	35
2.3.1. Mitochondrial uncoupling .....	36
2.3.2. The NADPH oxidase.....	37
2.3.2.1. Ox-LDL induced ROS production and ATM .....	40
2.3.3. Atherosclerosis development in relation to ATM <sup>-/-</sup> and ATM <sup>+/-</sup> genotypes.....	40
2.3.3.1. ROS, ATM and the induction/expression of HIF1 $\alpha$ .....	40
2.3.3.2. The ATM protein and NF $\kappa$ B in response to oxidative stress.....	41

2.3.3.3. The effects of antioxidant treatment for mitochondrial dysfunction in an ATM-/- mouse model.....	41
2.3.4.Regulation of ROS by ATM and p53.....	42
2.3.5.Pathologies associated with increased ROS production .....	43
2.4. ATM in the cytoplasm .....	43
2.4.1.Protein translation .....	43
2.4.2.The impact of the expression and activation of ATM on insulin growth factor-1 and insulin receptor substrate-1 .....	46
2.4.3.The role of ATM in the glucose uptake pathway and insulin resistance.....	50
2.4.4.Inhibitors of ATM .....	53
2.5. Motivation.....	55
2.6. Aims and objectives .....	57
<b>Chapter 3: Methods</b> .....	<b>58</b>
3.1. Aortic endothelial cell (AEC) isolation techniques:.....	58
3.1.1.Vascular ring method.....	58
3.1.2.Collagenase method.....	60
3.1.3.Validation of endothelial cell purity: Acetylated low density lipoprotein (Ac-LDL) .....	63
3.2. Western blots .....	63
3.3. Commercial Aortic endothelial cells (AECs).....	70

3.4. AEC treatment groups: .....	72
3.4.1. Insulin Dose response curve: .....	72
3.4.2. Stimulation and inhibition of the phosphatidylinositol-3 kinase (PI3-K) signalling pathway with emphasis on the ATM protein .....	72
3.4.3. 4,5-diaminofluorescein-2/diacetate (DAF-2/DA).....	73
3.4.4. Propidium iodide.....	74
3.4.5. Statistical analysis:.....	75
<b>Chapter 4: Isolation of aortic endothelial cells .....</b>	<b>76</b>
4.1. The vascular ring method.....	78
4.2. Collagenase method .....	84
4.2.1. Cell morphology.....	85
4.2.2. Dil-Ac-LDL staining .....	85
4.2.3. Cell cultures stained with Dil-Ac-LDL: Microphotographic analysis.....	90
4.2.4. Western blot analysis.....	95
4.3. Discussion and Conclusion.....	97
<b>Chapter 5: Flow Cytometry Results .....</b>	<b>98</b>
5.1. AEC viability: Propidium iodide staining (necrosis).....	99
5.2. NO-production.....	103

5.3. Discussion and conclusion.....	105
<b>Chapter 6: Western blot analysis.....</b>	<b>106</b>
6.1. Insulin dose response experiments.....	107
6.1.1. PKB/Akt .....	107
6.1.2. eNOS .....	108
6.2. Stimulation and inhibition of the phosphatidylinositol-3 kinase (PI3-K) signalling pathway in aortic endothelial cells with emphasis on the ATM protein .....	111
6.2.1. PI3-K/P85.....	111
6.2.2. PTEN .....	111
6.2.3. PKB/Akt .....	114
6.2.4. GSK3 $\beta$ .....	114
6.2.5. AMPK.....	118
6.2.6. ATM.....	118
6.2.7. eNOS activation and inhibition.....	121
6.2.8. AS160 .....	122
6.3. Discussion and conclusion .....	125
<b>Chapter 7: Discussion and conclusion.....</b>	<b>128</b>
7.1. Literature review .....	128

7.2. Aortic endothelial cell (AEC) isolation .....	129
7.3. Nitric oxide production and AEC viability in response to insulin, Ku-60019 and wortmannin .	130
7.4. The relationship between ATM and eNOS function in the insulin signalling pathway.....	131
7.5. Conclusion.....	132
References.....	133

## List of Figures:

Figure 1.1: Diagram of the ATM protein [Stracker et al., 2013]. ATM has four autophosphorylation sites namely S367, S1893, S1981 and S2996. The ATM protein has two <i>FKBP12-rapamycin-associated protein</i> (FRAP), <i>ataxia-telangiectasia mutated</i> (ATM), Transformation/transcription domain-associated protein (TRRAP; FAT) domains, FAT 1963-2566 and FAT C-terminal (FATC).....	2
Figure 1.2: A diagram listing the different signalling pathways in which PKB/Akt plays a role in; [ <a href="http://what-when-how.com/cardiomyopathies-from-basic-research-to-clinical-management/insulin-resistance-and-cardiomyopathy-metabolic-and-drug-induced-cardiomyopathies-part-1/">http://what-when-how.com/cardiomyopathies-from-basic-research-to-clinical-management/insulin-resistance-and-cardiomyopathy-metabolic-and-drug-induced-cardiomyopathies-part-1/</a> ] .....	5
Figure 1.3: Insulin mediated glucose uptake pathway [Jensen et al., 2011]. .....	8
Figure 1.4: Atherosclerotic plaque development and progression [Dandona and Aljada, 2002].....	11
Figure 1.5: Diagram showing the structure and domains of an eNOS enzyme in a dimer conformation. The diagram depicts the pathway the electrons follow during NO formation. [Stuehr et al., 2005] .....	15
Figure 1.6: A proposed mechanism on how an inactive ATM protein could influence the onset of atherosclerosis [Mercer et al., 2010]. .....	17
Figure 2.1: Dimer dissociation and activation of the ATM protein [Stracker et al., 2013]. .....	19

Figure 2.2:	Diagram depicting the many proteins activated by ATM in response to DNA double strand breaks..	20
Figure 2.3:	The role of ATM in response to DNA damage [Watters, D.J., 2003].	24
Figure 2.4:	DNA damage repair mechanisms [Khalil et al., 2012].	27
Figure 2.5:	Cytoplasmic activation of ATM by ROS and its role in cell growth and autophagy [Ditch and Paull, 2012].	30
Figure 2.6:	The role of ATM in the vasculature..	32
Figure 2.7:	The role of ATM in response to DNA damage and ROS [Guo et al., 2010].	34
Figure 2.8:	Oxidative stress produced by the NADPH oxidase and the antioxidants which target ROS production [Khalil et al., 2012].	39
Figure 2.9:	Cap dependent protein translation by eIF-4E. [Yang and Kastan, 2000].	45
Figure 2.10:	mTOR mediated protein translation. [Greife et al., 2001].	49
Figure 2.11:	Activators of the ATM protein [Ditch and Paull, 2012].	52
Figure 2.12:	Diagram of ATM inhibitors Ku-60019 and Ku-55933, respectively [Golding et al., 2009].	54
Figure 3.1:	Diagram of the protocol used in the vascular ring method.	59
Figure 3.2:	Isolated male Wistar rat thoracic aortas being bound to a 26-gauge needle	62

Figure 3.3: Diagram depicting the procedure used to passage and label the cells [A. Genis, 2014]. .....	71
Figure 4.1: Validation of the endothelial cell purity of commercially purchased AECs with flow cytometric analysis of fluorescence intensity after staining with the endothelial-specific marker, Dil-Ac-LDL. ....	81
Figure 4.2: (A) Representative scatterplot of the commercial endothelial cells with forward scatter (cell size) and side scatter (cell granularity) on the x-axis and y-axis respectively. ....	82
Figure 4.3: Validation of the endothelial cell purity by comparing the endothelial cells isolated from rat thoracic aorta with commercially purchased AECs with flow cytometric analysis of fluorescence intensity after staining with the endothelial-specific marker, Dil-Ac-LDL. ....	83
Figure 4.4: Cells isolated from the lumen of the thoracic region of male Wistar rats. ....	87
Figure 4.5: Validation of the endothelial cell purity of commercially purchased AECs and AECs isolated using the collagenase method with flow cytometric analysis of fluorescence intensity of the endothelial-specific marker, Dil-Ac-LDL. ....	88
Figure 4.6: Isolated endothelial cells in culture after being stained with Dil-Ac-LDL. ....	91
Figure 4.7: AECs (experimental control) were cultured in an eight chamber borosilicate coverglass system (Nunc, NY, USA) stained with Dil-Ac-LDL, the bar is 10 $\mu$ m and the magnification 60x. ....	92



Figure 4.8: Cells stained with Dil-Ac-LDL, 60x magnification. AECs (experimental control) were cultured in an eight chamber borosilicate coverglass system and stained with Dil-Ac-LDL, the bar is 10 µm. ....	93
Figure 4.9: Commercial AECs stained with Dil-Ac-LDL, 60x magnification. ....	94
Figure 4.10: Total eNOS expression differences among the commercially purchased AECs and the experimental cells (endothelial cells isolated using the collagenase method).....	96
Figure 4.11: Total PKB-Akt expression in experimental cells isolated from the thoracic region of the rat aorta.....	96
Figure 5.1: Density plot used to determine the percentage of viable and non-viable cells in a total AECs population.. ....	101
Figure 5.2: The effects of insulin, Ku-60019 and wortmannin on the development of necrosis (% cells staining positively with propidium iodide) in AECs. ....	102
Figure 5.3: The effects of insulin, Ku-60019 and wortmannin on the production of NO (as determined by the arithmetic mean of the fluorescence intensity) in AECs. ....	104
Figure 6.1: PKB/Akt insulin dose response. ....	109
Figure 6.2: eNOS insulin dose response. ....	110
Figure 6.3: P85 protein activation and inhibition.....	112
Figure 6.4: PTEN protein activation and inhibition. ....	113

Figure 6.5: PKB/Akt protein activation and inhibition .....	116
Figure 6.6: GSK3 $\beta$ protein activation and inhibition .....	117
Figure 6.7: AMPK protein activation and inhibition.....	119
Figure 6.8: ATM protein activation and inhibition (A) Phosphorylated ATM.....	120
Figure 6.9: eNOS protein activation and inhibition.....	123
Figure 6.10: AS160 protein activation and inhibition.....	124

## List of Tables:

Table 3.1: The table below consist of a list of different SDS-PAGE gels used and their respective compositions.	66
Table 3.2: Proteins probed in this research project are listed below along with their molecular weights (kDa) and optimization conditions	68

## Abbreviations

4E-BP1:	4E binding protein 1
ACE :	Angiotensin converting enzyme
Ac-LDL:	Acetylated low density lipoprotein
AEC:	Aortic endothelial cell
AGE:	Advanced glycation end-products
AMPK:	AMP-activated protein kinase
ApoE:	Apolipoprotein E
AS160:	Akt substrate, 160 kDa
AT:	Ataxia telangiectasia
ATM <sup>-/-</sup> :	ATM null phenotype
ATM:	Ataxia telangiectasia mutated
ATM <sup>+/-</sup> :	ATM heterozygous phenotype
ATM <sup>+/+</sup> :	ATM wild type phenotype
ATR:	ATM and RAD3-related protein
BH4:	Tetrahydrobiopterin
BRCA1:	Breast cancer gene 1

Ca <sup>2+</sup> :	Calcium
CaM:	Calmodulin
cAMP:	<i>Cyclic adenosine monophosphate</i>
CDK:	Cyclin-dependent kinase
cGMP:	Cyclic guanosine monophosphate
CVD:	Cardiovascular disease
DAG:	Diacylglycerol
DDR:	DNA damage response
DHA:	Dehydroascorbic acid
Dil:	1,1'-dioctadecyl-1,3,3,3',3'-tetramethyl-indocarbocyanine
DNA-PK:	DNA-dependent protein kinase
DNA-PKcs:	DNA protein kinase catalytic subunit
DSB:	DNA double strand break
EC:	Endothelial cell
ECGF:	Endothelial cell growth factor
EDRF:	Endothelium-derived relaxing factor
eNOS/NOS3:	Endothelial NOS
EPC:	Endothelial progenitor cells

ETC:	Electron transport chain
FACS:	Fluorescent activated cell sorting
FAD:	Flavin adenine dinucleotide
FAT:	FRAP-ATM-TRRAP
FATC:	FAT C-terminal
FMN:	Flavin mononucleotide
FRAP:	FKBP12-rapamycin-associated protein
GAP:	GTPase activating protein
GDP:	Guanosine diphosphate
GLUT:	Glucose transporter
GSK3 $\beta$ :	Glycogen synthase 3 beta subunit
GTP:	Guanosine-5'-triphosphate
H <sub>2</sub> O <sub>2</sub> :	Hydrogen peroxide
HDL:	High density lipoprotein
HIF1 $\alpha$ :	Hypoxia induced factor 1 alpha
HMG-CoA:	3-hydroxy-3-methylglutaryl coenzyme A
HR:	Homologous recombination
Hsp90:	Heat shock protein 90

ICAM-1:	Intracellular adhesion molecule
IGF-1:	Insulin-like growth factor 1
iNOS/NOS3:	Inducible NOS
IP <sub>3</sub> :	Inositol trisphosphate
IRS-1:	Insulin receptor substrate-1
LDL:	Low-density lipoprotein
LKB1:	Liver kinase B1
LPL:	Lipoprotein lipase
MAPK:	Mitogen activated protein kinase
mCAT:	Catalase target of mitochondria
MCP-1:	Monocyte chemo-attractant protein -1
MDA:	Malondialdehyde
MnSOD:	Manganese superoxide dismutase
Mre11:	Meiotic recombination 11
MRN:	MRE11, RAD0 and NBS1
mtDNA:	Mitochondrial DNA
mTOR:	Mammalian target of rapamycin
mTORC:	mTOR-containing multiprotein complex-1/2

NADPH:	Nicotinamide-adenine-dinucleotide phosphate
NBS1:	Nijmegen breakage syndrome
NER:	Nucleotide excision repair
NFκB:	Nuclear factor kappa B
NHEJ :	Non-homologous end joining
nNOS/NOS1:	Neuronal NOS
NO:	Nitric oxide
NO <sub>2</sub> <sup>-</sup> :	Nitrite
NO <sub>3</sub> <sup>-</sup> :	Nitrate
NOS:	Nitric oxide synthase
Nox:	NADPH oxidase
O <sub>2</sub> <sup>-</sup> :	Superoxide anion radical
O <sub>2</sub> :	Oxygen
OH:	Hydroxyl radicals
ONOO <sup>-</sup> :	Peroxynitrite
Ox-LDL:	Oxidized low-density lipoprotein
p53 <sup>S18A</sup> :	Absent p53 ATM phosphorylation site
PDK:	Phosphatidylinositol dependent kinase

PI3-K:	Phosphatidylinositol 3 kinase
PIKK:	PI3-K related kinases
PIP2:	Phosphatidylinositol 4,5-biphosphate
PIP3:	Phosphatidylinositol 3,4,5-trisphosphate
PKB/Akt:	Protein kinase B
PKC:	Protein kinase C
PVAT:	Perivascular adipose tissue
Q:	Glutamine
RAD50:	DNA repair protein Rad50
RNS:	Reactive nitrogen species
ROS:	Reactive oxygen species
S/Ser:	Serine
S6K:	70-kDa ribosomal protein S6 kinase
SMC:	Smooth muscle cells
SSB:	DNA single strand break
T/Thr:	Threonine
TRRAP:	Transformation/transcription domain-associated protein
UV:	Ultraviolet light



VCAM-1: Vascular cell adhesion molecule

VEGF: Vascular endothelial cell growth factor

VLDL: Very low-density lipoprotein

## Chapter 1: Introduction

Ataxia telangiectasia (AT) is an autosomal recessive disease with an early onset in children. The disease is characterized by the presence of telangiectasias (red focal lesions due to the dilatation of small blood vessels) in the conjunctivae of the eye and body as well as an unsteady gait caused by muscle atrophy [Li, Y. and Yang, 2010]. Patients with this disease also show symptoms of neurodegeneration, an increased risk of cancer development, sensitivity to ionizing radiation, and, of importance to the current study, insulin resistance [Yang and Kastan, 2000].

Ataxia telangiectasia occurs when the ataxia telangiectasia mutated (ATM) protein is absent or inactive [Yang et al., 2011]. ATM is a 350-kDa protein and encoded by the *Atm* gene (figure 1.1). This protein is a member of the phosphatidylinositol-3 kinase related kinase (PIKK) family and phosphorylated at a conserved serine-threonine region followed by a glutamine (S/T/Q) [Bensimon et al., 2011]. Often the lack of ATM activity is caused by a mutation during protein translation or during the cell cycle.

On average, AT patients have a lifespan of approximately 30 years and often die from cancer. In the general population insulin resistance, glucose intolerance and type 2 diabetes mellitus usually develop at the age of 40-50 years. In contrast, many AT patients present with insulin resistance and glucose intolerance at a younger age (second to third decade of life), and are undiagnosed in most cases [Yang et al., 2011]. In the literature, it is reported that some AT patients present with symptoms and signs of the metabolic disease, including obesity, increased low-density lipoprotein (LDL) cholesterol levels, and low concentrations of high-density lipoprotein (HDL), [Schneider et al., 2006].

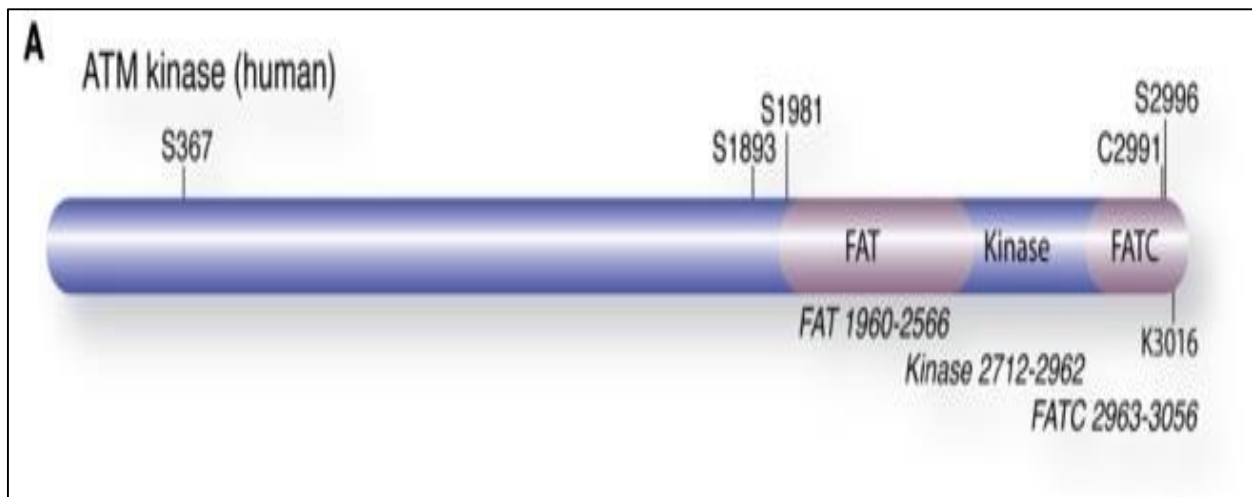


Figure 1.1: Diagram of the ATM protein [Stracker et al., 2013]. ATM has four autophosphorylation sites namely S367, S1893, S1981 and S2996. The ATM protein has two *FKBP12-rapamycin-associated protein* (FRAP), *ataxia-telangiectasia mutated* (ATM), Transformation/transcription domain-associated protein (TRRAP; FAT) domains, FAT 1963-2566 and FAT C-terminal (FATC).

## **1.1. The metabolic syndrome, diabetes mellitus and atherosclerosis: risk factors for the development of cardiovascular disease (CVD) development**

### **1.1.1. The metabolic syndrome**

Many lifestyle factors, which include diet, smoking or excessive alcohol intake can contribute to the development of the metabolic syndrome [Mercer et al., 2010]. Individuals are diagnosed with the metabolic syndrome when they present with at least three of the following risk factors: hypertension, decreased HDL, increased LDL, central obesity and a high fasting blood glucose concentration [Mercer et al., 2010]. The metabolic syndrome is closely associated with other risk factors such as insulin resistance, glucose intolerance, diabetes and cardiovascular disease. The metabolic syndrome is a complex disorder, and affects multiple organ systems in the body. In some cases, the disease can be reversed by lifestyle changes with or without therapeutic treatment, whereas in other cases, if untreated, it can be fatal [Zreikat et al., 2014; Chen, B. et al., 2012].

Two different studies conducted in South Korea and Finland assessed the risk of developing both diabetes and cardiovascular disease in individuals presenting with the metabolic syndrome. In the study by Khang et al. (2010), the risk of developing cardiovascular disease and diabetes was measured in Asian individuals with the metabolic syndrome using a national longitudinal data set (Harmonization definition) [Khang et al., 2010].; In their results section their study indicated that the metabolic syndrome was independently and significantly associated with the development of CVD and diabetes [Khang et al., 2010]. Conversely, in the study conducted in Finland by Pajunen et al. (2010) the development of heart disease and diabetes was evaluated in individuals who met the different definitions of metabolic syndrome as well as the relatively new

Harmonization definition. The study included both baseline and follow-up metabolic measurements (height, weight, waist circumference and blood pressure). Their results indicated that in people who have the metabolic syndrome, there is a greater risk of developing diabetes than cardiovascular disease at the follow-up consultation [Pajunen et al., 2010].

### **1.1.2. Type 2 diabetes mellitus**

In a healthy individual, insulin is secreted by the pancreatic beta cells. Insulin mediates the uptake and metabolism of glucose in tissue types like skeletal muscle. Diabetes occurs when the body is unable to respond to the secretion of insulin (insulin resistance) resulting in hyperglycaemia. Under healthy conditions when insulin is released by the pancreatic beta cells, the phosphatidylinositol-3 kinases (PI3-K) pathway is activated in insulin-sensitive peripheral tissue. Following this downstream proteins like PKB/Akt are phosphorylated, which activate a host of downstream signalling pathways involved in glucose uptake, nitric oxide (NO) production, angiogenesis as well as playing an important role in controlling the cell cycle and cell survival (figure 1.2).

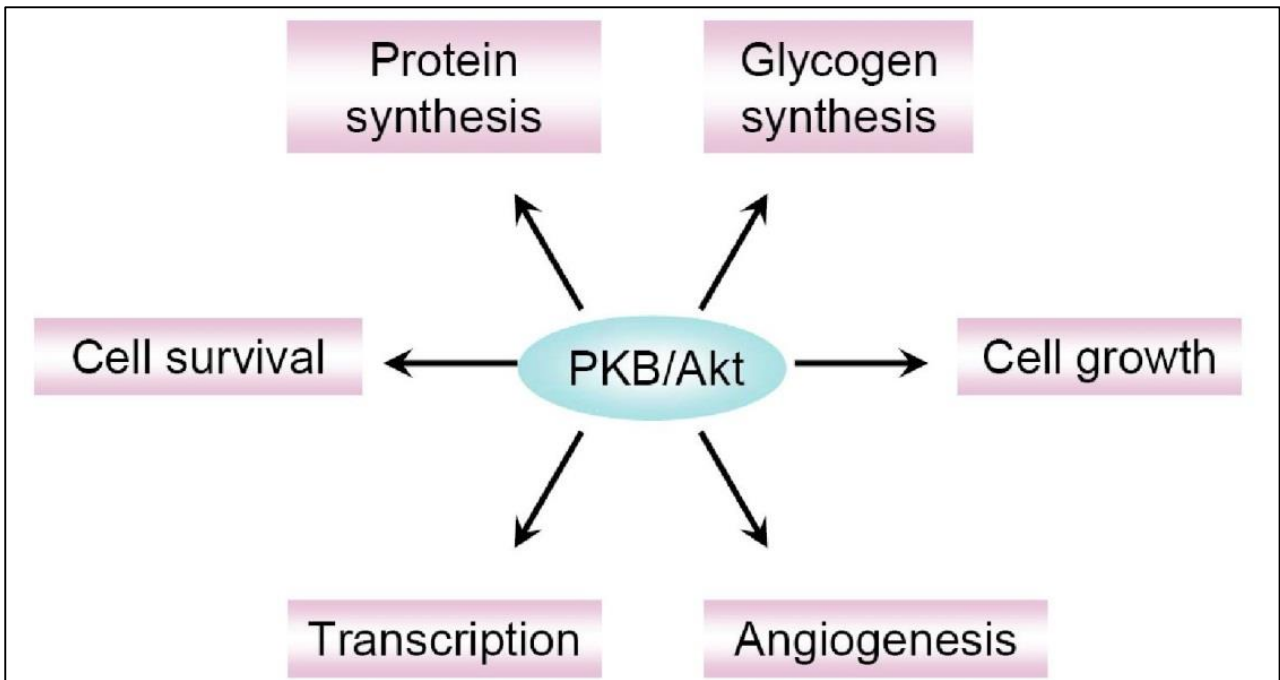


Figure 1.2: A diagram listing the different signalling pathways in which PKB/Akt plays a role in; <http://what-when-how.com/cardiomyopathies-from-basic-research-to-clinical-management/insulin-resistance-and-cardiomyopathy-metabolic-and-drug-induced-cardiomyopathies-part-1/>

### **1.1.2.1. Activation of the PI3-K pathway in an insulin dependent manner**

Insulin binds to its receptor tyrosine kinase and stimulates the autophosphorylation of the tyrosine residues on the  $\beta$ -subunit, leading to insulin receptor substrate (e.g. IRS-1) phosphorylation [Hotamisligil et al., 1996 and Liu et al., 2009]. IRS-1 binds the PI3-K protein, which has been recruited, to the inner wall of the cell membrane. There are three classes of PI3-K, including Class IA, which has a regulatory subunit (P85) and catalytic subunit (P110), [Irarrazabal et al., 2006]. PI3-K is phosphorylated at the P85 regulatory subunit when treated with insulin. Once activated, PI3-K phosphorylates the membrane-bound protein phosphatidylinositol 4,5-bisphosphate (PIP<sub>2</sub>) into phosphatidylinositol 3,4,5-trisphosphate (PIP<sub>3</sub>). PIP<sub>3</sub> mediates the phosphorylation of PKB/Akt at Thr308, through activation of phosphatidylinositol dependent kinase 1 (PDK1). Following this PKB/Akt is immediately phosphorylated at Ser473 by phosphatidylinositol dependent kinase 2 (PDK2) to elicit its full function. PDK2 is an unidentified protein and researchers speculate that this protein can either be mammalian target of rapamycin (mTOR), DNA-PK or ATM as all of these proteins form part of the PIKK (figure 1.3), [Jensen et al., 2011 and Wymann and Morone, 2005].

### **1.1.2.2. Glucose uptake**

Once insulin mediated activation of PKB/Akt occurs, PKB/Akt phosphorylates the Akt substrate (AS160) protein at Ser588 (AS160 has six phosphorylation sites, Ser588 is the phosphorylation site which is most responsive to insulin). AS160 is a Rab GTPase activating protein (GAP). Rab GAP proteins are responsible for controlling the transfer of proteins through the membrane and for hydrolysing Guanosine-5'-triphosphate (GTP) binding proteins (considered the active state) to the Guanosine diphosphate (GDP) form (the inactive state). AS160 prevents glucose transporter-4 (GLUT4) vesicle translocation to the cell membrane and phosphorylation of AS160 alleviates this inhibitory effect [Jensen et

al., 2011; Treebak et al., 2006; He et al., 2007]. There are 13 various GLUT proteins; GLUT4 is the main glucose transporter that is activated by insulin. GLUT4 translocates to the cell membrane, fuses with the plasma membrane and mediates the uptake of glucose into the cells (Figure 1.3), [He et al., 2007; Egeuz et al., 2005].

Simultaneously, glycogen synthase kinase 3 $\beta$  (GSK3 $\beta$ ) is another protein downstream PKB/Akt. GSK3 $\beta$  plays a role in many signalling proteins including protein synthesis, glycogen metabolism and regulating the cell cycle [Vara et al., 2004 and Yang and Li, 2008]. In response to insulin GSK3 $\beta$  is inactivated by phosphorylation at Ser9 by PKB/Akt [Razani et al., 2010; Jensen et al., 2011]. Glycogen synthase (GS) is a protein responsible for the conversion of unused glucose into glycogen and its subsequent storage. The activity of glycogen synthase is inhibited by GSK3 $\beta$ . Thus when GSK3 $\beta$  is deactivated more glucose is converted to glycogen due to the increase in GS activity [Jensen et al., 2011].



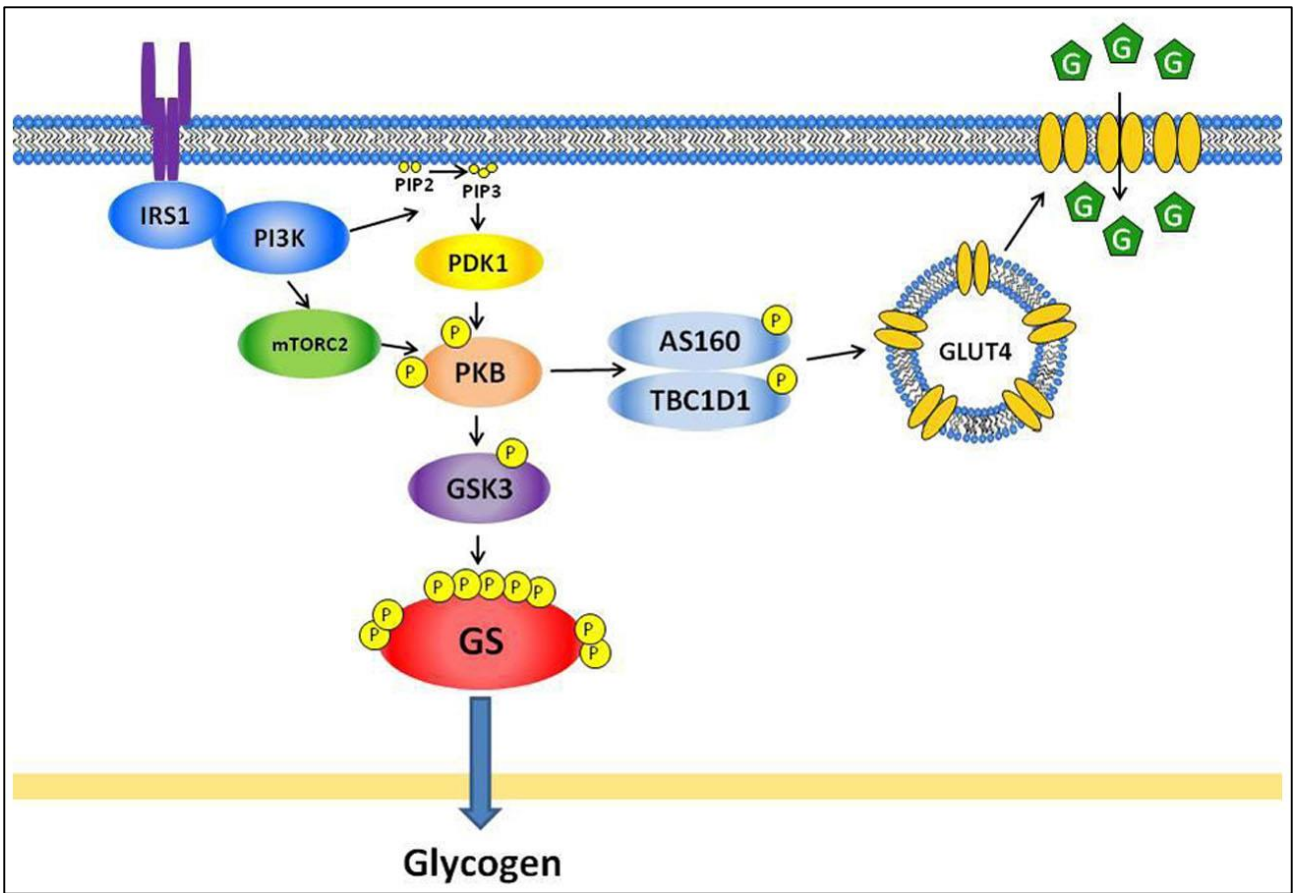


Figure 1.3: Insulin mediated glucose uptake pathway [Jensen et al., 2011].

### 1.1.2.3. Insulin insensitivity

As mentioned, AT patients display insulin insensitivity and glucose intolerance, which poses interesting questions about the importance of the ATM protein in insulin sensitivity and glucose homeostasis. In patients with the metabolic syndrome and in AT patients insulin is present in skeletal muscle and brown adipose [Mookerjee et al., 2010] as well as the vasculature at basal concentrations but the cells are not responding, and therefore cellular processes mediated by insulin are left incomplete.

During insulin resistance, it is over active phosphatase and tensin homologue deleted on chromosome 10 (PTEN) which contributes to the development of this disease. PTEN has dual function as both a lipid and a protein. When active PTEN dephosphorylates PIP3 [Vara et al., 2004 and Mukherjee et al., 2013] at its D3 position, thereby negatively regulating the insulin mediated PI3K and PKB/Akt pathway [Weichhart and Säemann, 2008]. PTEN often defined as a tumour suppressor protein plays a role in many signalling pathways including cell motility, cell senescence and chromosomal stability. When inactivated, PTEN has been discovered to promote cancer progression [Wymann and Marone et al., 2005], and enhances GLUT4 translocation to the cell membrane to increase glucose uptake and increases insulin sensitivity [Hirsch et al., 2007].

ATM, a known member of the PIKK family, plays a role in the activation of PKB/Akt at Ser473 in response to insulin treatment. When ATM is inhibited or absent in cells there is a decrease in PKB/Akt activation and glucose uptake and an increase in insulin resistance [Yang et al., 2011]. Various studies have investigated the effects of silencing AS160 on insulin mediated glucose uptake via GLUT4 as well as the role of other glucose transporters in ATM deficient cell types. According to Halaby et al. glucose uptake by GLUT4 mediated by insulin was inhibited in L6 muscle cell lines when treated with the ATM inhibitor Ku-55933 [Halaby et al., 2008]. Andrisse et al. (2014) confirmed that GLUT1 is expressed and fully functional in the absence of a functional ATM protein and observed

that when this occurs there is an increase in insulin resistance in skeletal muscle cells [Andrisse et al., 2014].

### **1.1.3. Atherosclerosis development**

Insulin resistance and type 2 diabetes are independent risk factors for atherosclerosis, which is labelled an inflammatory disease [Ray et al., 2009]. Endothelial dysfunction, characterised by reduced NO bioavailability and hence reduced ability of blood vessels to dilate, is an early biomarker of atherosclerosis [Li and Keaney, 2010]. There are various factors that contribute to the development of endothelial dysfunction and atherosclerosis, which include oxidative stress, oxidation of low-density lipoprotein (LDL) and inflammation [Semlitsch et al., 2011].

An atherosclerotic plaque develops when a lesion occurs in the endothelium exposing the smooth muscle cells in the vasculature. When this occurs, chemo-attractants are released and monocytes are drawn to and adhere to the injured site. Proteins involved in the inflammatory process of atherosclerosis are monocyte chemo-attractant protein-1 (MCP-1), vascular cell adhesion molecule-1 (VCAM-1) and intracellular adhesion molecule-1 (ICAM-1), [Nickenig and Harrison, 2002]. When drawn to the injured site monocytes differentiate into macrophages and these monocyte-derived macrophages turn into foam cells. Foam cells develop when the macrophage-derived monocytes take up oxidized low-density lipoprotein (ox-LDL), forming fatty streaks [Nickenig and Harrison, 2002; Kuo et al., 2009].

Oxidized LDL is produced by 3-hydroxy-3-methylglutaryl coenzyme A (HMG-CoA) or lipoprotein lipase (LPL) under various conditions. During foam cell formation the monocyte derived macrophages express lipoprotein lipase (LPL). LPL, which is up-regulated in diabetes, is responsible for membrane synthesis and hydrolyses chylomicrons and very

low-density lipoprotein (VLDL), [Basu et al., 1976]. The free cholesterol generated by the hydrolysis process is taken-up by macrophages. The ox-LDL is insoluble and it takes longer for the smooth muscle cells to remove the lipids from the intimal space, which results in the over accumulation of these cells and foam cell formation (Figure 1.4), [Mead and Ramji, 2002].

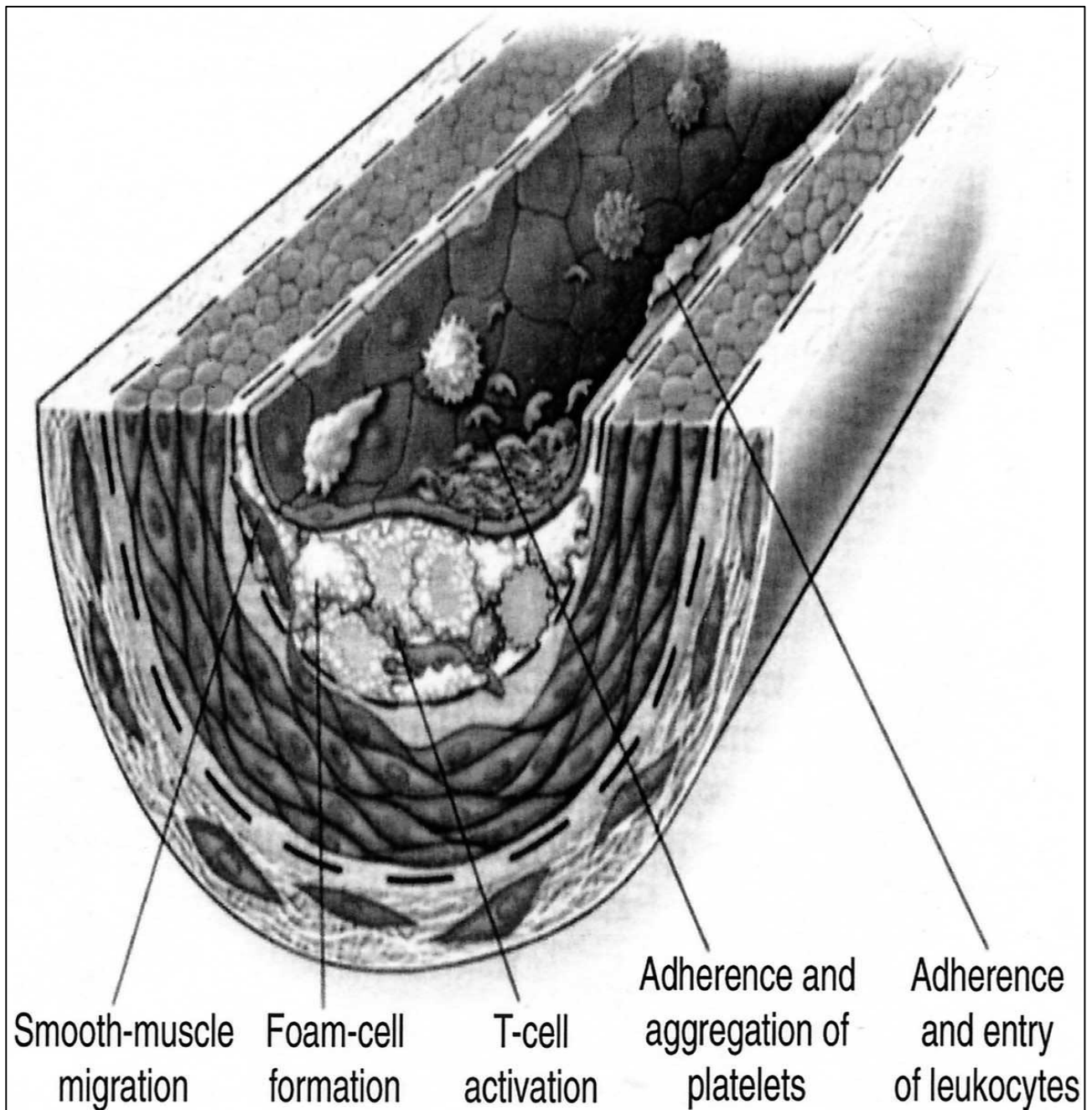


Figure 1.4: Atherosclerotic plaque development and progression [Dandona and Aljada, 2002].

Atherosclerosis development and progression is accompanied by oxidative stress, whereby the amount of reactive species exceeds the availability of antioxidants (for example manganese super oxide dismutase (Mn-SOD) and malondialdehyde (MDA)) in the cell [Yin, et al., 2007]. The most common reactive species is superoxide anion ( $O_2^-$ ). In addition to traditional ROS sources such as NADPH-oxidase and mitochondria, dysfunctional vascular endothelial cells generate superoxide anions via endothelial nitric oxide synthase (eNOS) when it uncouples due to, among others, the loss of its cofactor tetrahydrobiopterin (BH4). When BH4 is absent or inactive, electrons are transferred to an oxygen molecule instead of L-arginine [Nickenig and Harrison, 2002]. Other mechanisms of ROS formation include damage to the mitochondrial respiratory system [Semenkovich, 2006] and the NADPH oxidase.

Apoptosis of smooth muscle cells (SMC) in the atherosclerotic plaque leads to plaque instability and rupture. Often the onset of SMC apoptosis is caused by the activation of angiotensin receptor AT1 [Nickenig and Harrison, 2002]. Both insulin resistance and atherosclerosis can cause DNA damage, which leads to the activation of the protein ATM [Semenkovich, 2006]. ATM is inactive in AT patients and it was observed that people with a single copy of the defective ATM gene (carriers) are susceptible to developing cardiovascular disease. This was demonstrated in a study completed by Yang et al.; whereby mice heterozygous for ATM<sup>+/-</sup> and who were also Apolipoprotein E null (ApoE<sup>-/-</sup>) were found to have a higher incidence of developing atherosclerosis, insulin resistance and glucose intolerance. These pathologies were induced after the mice were fed a high fat diet compared to ATM<sup>+/+</sup>ApoE<sup>-/-</sup> mice fed the same diet [Yang et al., 2011; Hammond and Giaccia, 2004 and Schneider et al., 2006].

## **1.2. The importance of the endothelium in vascular health**

### **1.2.1. Endothelial dysfunction and cardiovascular disease**

Vascular endothelial cells have been the topic of research for many years. Without the endothelial cells and their role in vascular homeostasis, people would be at a higher risk of developing cardiovascular disease (CVD) and dying from a CVD related pathology.

According to Kuliszewski et al. (2013), mature endothelial cells that have differentiated from endothelial progenitor cells (EPC) play an important role in repair and tissue regeneration when damage occurs in the vasculature [Kuliszewski et al., 2013]. Under hypoxic conditions and during peroxynitrite ( $\text{ONOO}^-$ ) formation in the endothelial cells, AMP-activated protein kinase (AMPK) is activated. AMPK is an energy sensor that is activated by increased concentrations in AMP and maintains intracellular homeostasis under stressful conditions (e.g. DNA strand breaks and oxidative stress), [Wang, S. et al., 2012]. The endothelial cells constitutively express the enzyme eNOS which produces NO. NO is responsible for vasodilation and inhibits the proliferation of smooth muscle cells (SMCs), [Venugopal et al., 2002]. A decrease in eNOS activity is associated with cardiovascular pathologies such as hypoxia, oxidative stress and is often a precursor for atherogenesis [Li, H. et al., 2014 and Razani et al., 2008]. It has been suggested that the endothelial cell may play an important role in the insulin-induced uptake of glucose by the skeletal muscle [Kubota et al., 2011].

### **1.2.2. The function and importance of aortic endothelial cells (AECs) in vascular health**

The vascular endothelium (ECs) plays a pivotal role in the maintenance of vascular homeostasis [Jaffe et al, 1973]. They fulfil this role by, among others, regulating the transfer of molecules across the semi-permeable endothelial layer, and releasing NO and



other vasoactive factors [Sumpio et al, 2002]. NO is synthesised by a family of enzymes, called the NO synthases (NOS). There are three different NOS isoforms, namely neuronal NOS (nNOS or NOS1), inducible NOS (iNOS or NOS2) and endothelial NOS (eNOS or NOS3) [Carnicer et al., 2013; Förstermann and Sessa, 2012]. The NOS isoforms are located in various parts of the body and in different subcellular regions, and they release NO in concentrations that range in the nano- and micro- molar range [Strijdom et al., 2009 and Mian et al., 2013].

In AECs, the protein PKB/Akt phosphorylates eNOS in response to insulin [Taguchi et al. 2012]. eNOS, which is constitutively expressed in both vascular endothelial cells and cardiomyocytes, is responsible for the release of NO from the amino acid substrate L-arginine in the presence of oxygen. In order to generate NO, eNOS requires phosphorylation (and therefore activation) at Ser1177, as well as the presence of substrates (L-arginine, tetrahydrobiopterin), co-substrates (oxygen and NADPH: nicotinamide-adenine-dinucleotide phosphate), cofactors (FAD: flavin adenine dinucleotide and FMN: flavin mononucleotide) and a calmodulin (CaM) binding site [Carnicer et al., 2013; Förstermann and Sessa, 2012]. The carboxy-terminal of eNOS is responsible for the transfer of electrons from NADPH to the haeme group via FAD and FMN. At the amino-terminal oxidase; tetrahydrobiopterin (BH<sub>4</sub>), oxygen and L-arginine bind. The electrons transferred from NADPH are used to reduce oxygen and oxidize (catabolize) L-arginine to form L-citrulline and release NO (figure 1.5).

Collectively, the endothelial cells are important for angiogenesis and are responsible for cell survival, proliferation and migration [Levine et al., 2003 and Joshi et al., 2013].





### 1.3. Conclusion

For many years endothelial cells have been the topic of research ranging from the first endothelial cell isolation by Jaffe and his colleagues (1973) to the unknown endothelium-derived relaxing factor (EDRF) later known as NO. Endothelial cell dysfunction disrupts the maintenance of vascular homeostasis. This disruption leads to the development of various forms of cardiovascular disease, increases ROS production, negatively impacts glucose uptake and activates inflammatory responses. Due to these reasons and the increasing prevalence of CVD, research on endothelial cells remains relevant in this present age.

There is a limited amount of data available on the presence and function of the ATM protein in AEC. Although few studies have explored the role of the ATM protein in ApoE<sup>-/-</sup> mice and the development of atherosclerosis [Mercer et al. 2010], it has not been determined whether or not AT patients have a higher incidence of developing cardiovascular disease due to the mutation in the *Atm* gene. Some studies suggest that the lack of ATM protein present in AT patients could promote the onset of atherosclerosis and mitochondrial dysfunction (increasing ROS production), [D'Souza et al., 2013]. A study completed by Mercer et al. investigated the prevalence of atherosclerosis development in heterozygous carriers of the mutated *Atm* gene. In this study, the possible mechanisms by which ATM heterozygosity could lead to atherosclerosis development were outlined (figure 1.6).

The role of the ATM protein and its function has been researched extensively especially in relation to PKB/Akt. PKB/Akt is a diverse protein that plays a role in different cellular processes. In this research topic, the role of PKB/Akt mediated by ATM in response to insulin treatment is of great interest concerning endothelial dysfunction and vascular pathology.

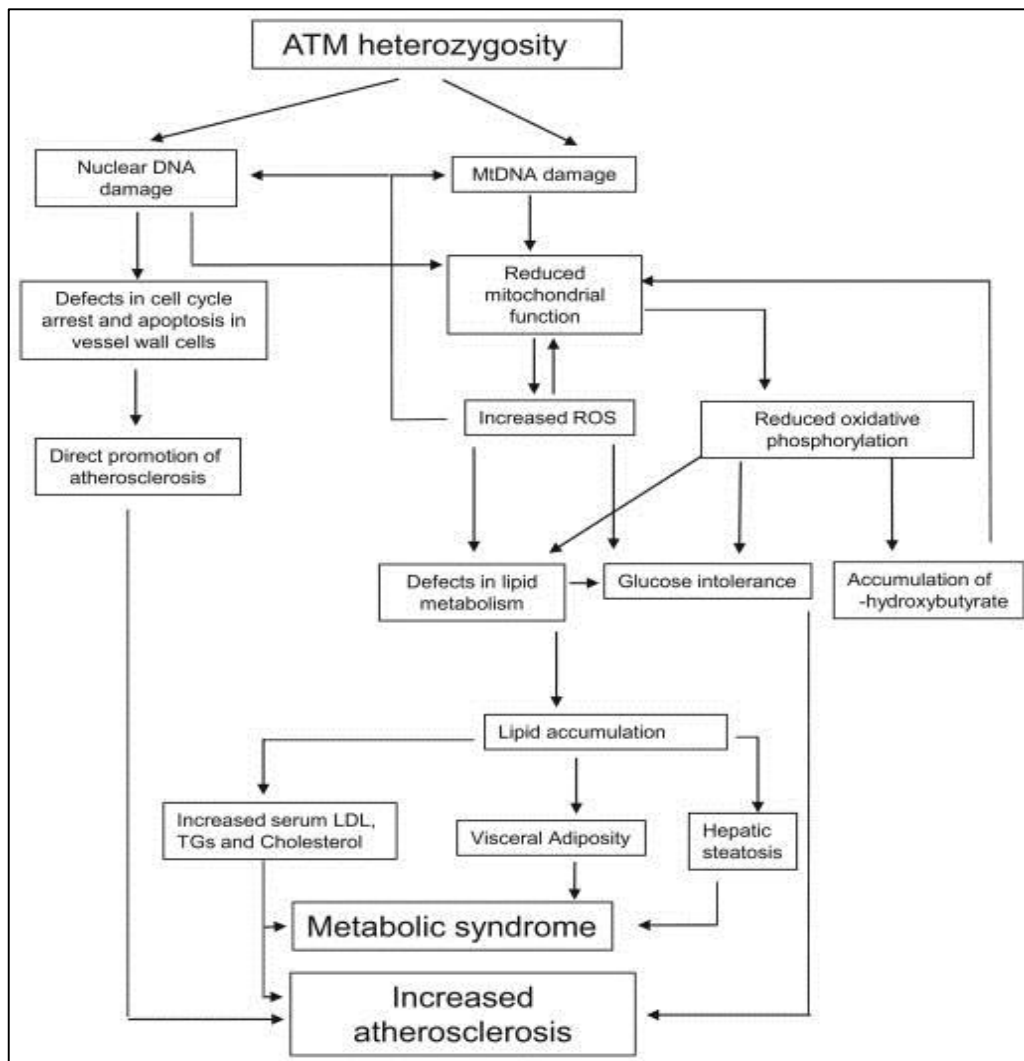


Figure 1.6: A proposed mechanism on how an inactive ATM protein could influence the onset of atherosclerosis [Mercer et al., 2010].

## Chapter 2: Literature review

### 2.1. The ATM protein

The gene encoding the ataxia telangiectasia mutated (ATM) protein was first discovered in 1995 [Savitsky et al., 1995]. In addition to muscle atrophy and telangiectasia's, patients with ataxia telangiectasia (AT) are known to age prematurely, have stunted growth, display chromosomal instability, be predisposed to cancer, have increased requirements for serum growth factors and show sensitivity towards ionizing radiation. On average an AT patient has a lifespan of 20-30 years [Savitsky et al., 1995].

The ATM protein is a dimer when it is inactive and monomerizes when activated by DNA damage (figure 2.1). ATM is mostly localized in the nucleus where it stimulates and activates many other proteins involved in various cellular processes (figure 2.2). Due to the nature of these proteins and their localization in other parts of the cell, many research groups have not only investigated the nuclear function of the ATM protein but also the localization and function of the protein in the mitochondria and the cytoplasm.

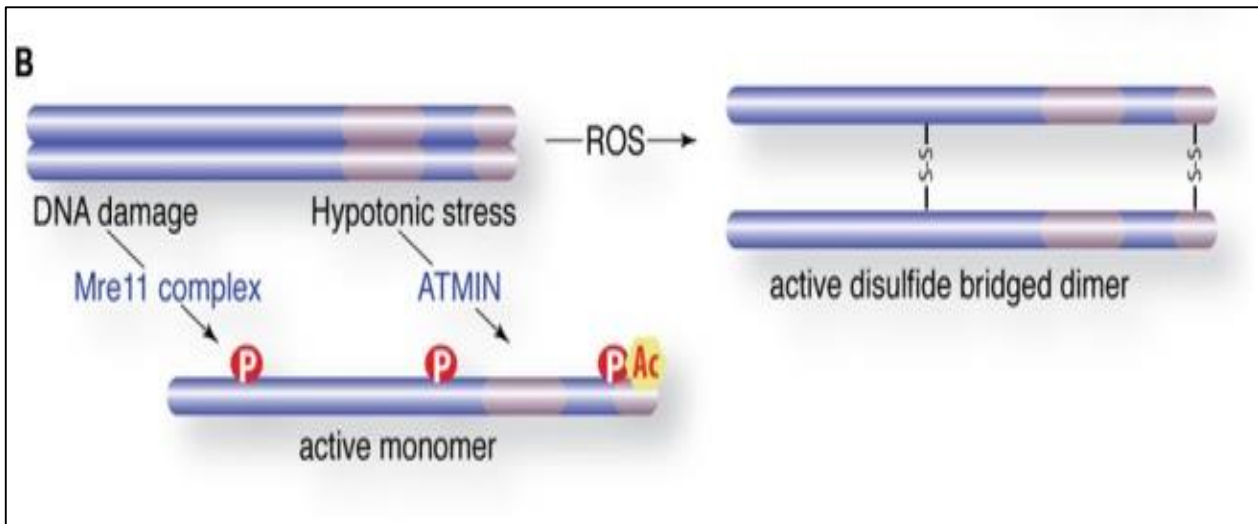


Figure 2.1: Dimer dissociation and activation of the ATM protein [Stracker et al., 2013]. The ATM dimer protein is activated by DNA damage and oxidative stress. DNA damage causes autophosphorylation at Ser181 in humans. Oxidative stress causes dimerization and sulphur bonds between two ATM monomers.

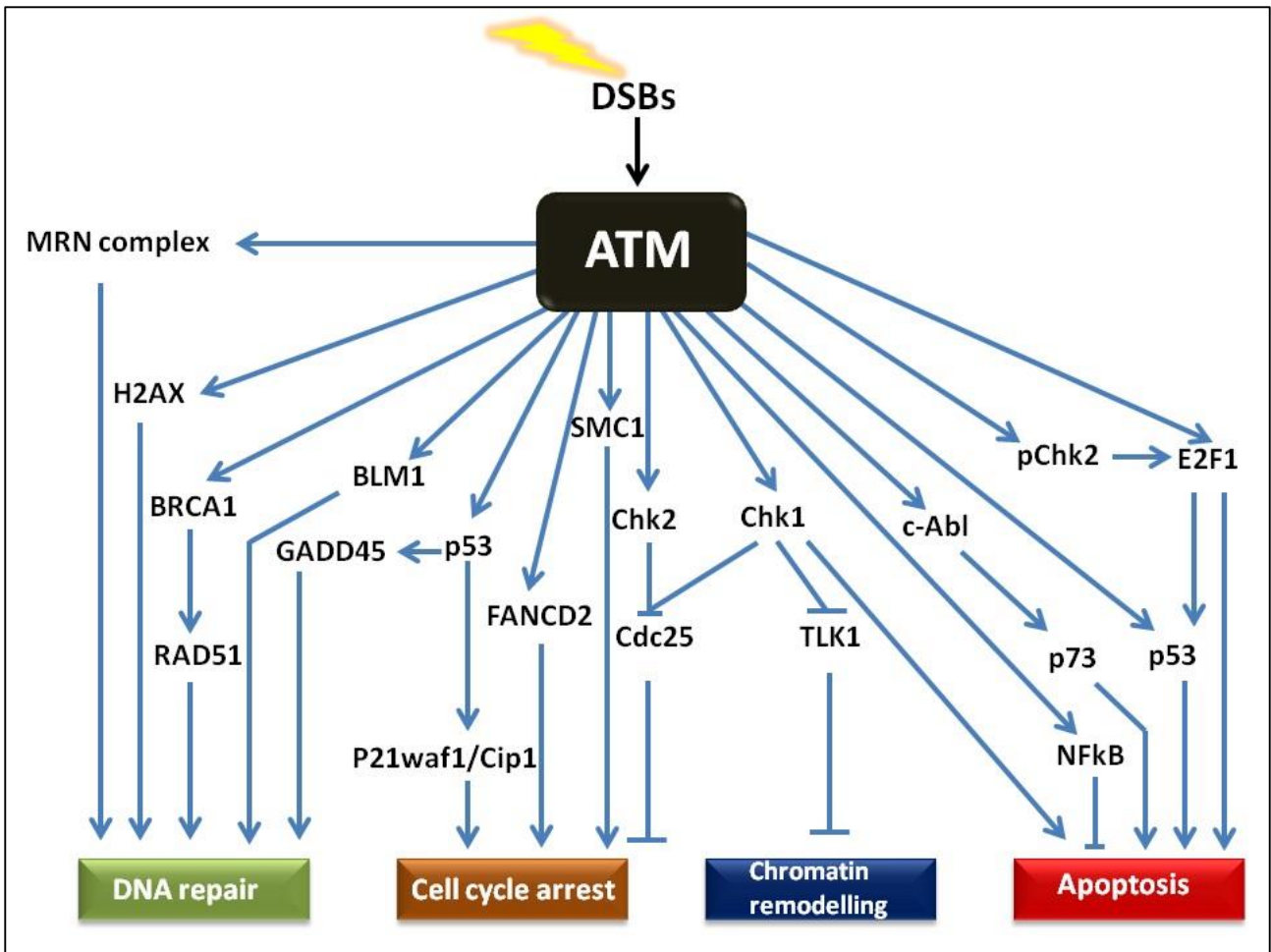


Figure 2.2: Diagram depicting the many proteins activated by ATM in response to DNA double strand breaks. Each protein or multiple proteins play a role in signalling pathways involving DNA repair, cell cycle arrest, apoptosis and chromatin remodelling within the nucleus [Khalil et al., 2012].

## 2.2. Activating the ATM protein – the nuclear function of ATM

DNA damage is an event that occurs due to abnormalities in the synthesis of DNA. Often these abnormalities occur under physiological conditions or can be induced by various treatments and environmental stress [Shiloh, 2003]. Physiological conditions include base mismatches, which occur during DNA replication, inactivation of topoisomerases I and II, formation of cell lesions, oxidative stress caused by reactive oxygen species (ROS), and depurination. Drug induced DNA damage is believed to be a result of the Fenton reaction facilitated by excessively high concentrations of metals. Often these compounds either lead to single strand breaks (SSBs) or double strand breaks (DSBs). Of these two, DSBs occur seldom, are hard to repair and can be fatal [Mahmoudi et al., 2006].

It has been described that DSBs arise when two SSBs occur near to each other or when there is one SSB and a lesion in close proximity. These lesions include impaired base pairing, inhibition of DNA replication and transcription as well as base loss [Jackson and Bartek, 2009]. Other factors involved with the onset of DNA damage include smoking, diabetes mellitus and ionizing radiation. Smoking and DNA damage occur due to the ability of tobacco-related toxins to inhibit DNA repair, promote oxidative stress and stimulate the production of advanced glycation end-products (AGEs) which are believed to cause DNA mutations. Selenium-treatment has also been found to promote oxidative stress, which induces DNA damage [Rocourt et al., 2013]. Exposure of cells to ionizing radiation can also induce DSBs. It is believed that ionizing radiation not only causes DNA strand breaks, but can also alter the formation of chromatin structure. Chromatin structure is known to be altered by the induction of various agents which include hypotonic conditions, chloroquine and histone deacetylase inhibitors. Although none of these agents cause DNA strand breaks, they are thought to stimulate the phosphorylation of proteins in the DNA damage response. Furthermore, it has been observed that DSBs can occur during both meiotic and

V(D)J recombination [Bakkenist and Kastan, 2003; Khanna et al., 2001 and Bensimon et al., 2011].

### **2.2.1. The DNA damage response**

The cellular DNA damage response (DDR) aims to repair DNA lesions, both SSBs and DSBs and is known for controlling the cell cycle checkpoints [Bensimon et al., 2011; Jackson and Bartek, 2009]. The DDR has been shown to utilize different and distinct repair mechanisms.

The first mechanism is the so-called mismatch repair, which is commonly used to repair mismatches or insertion/deletion loops by enzymes like nuclease, polymerase and ligase.

The second is the base excision repair mechanism, which not only consists of the above mentioned enzymes, but additionally also DNA glycosylase responsible for removing unwanted base pairs. Base excision repair can also be used in the repair of SSBs. The third repair mechanism is nucleotide excision repair (NER) which consists of two sub-mechanisms namely; transcription-coupled NER and global genome NER. Both of these target lesions [Jackson and Bartek, 2009].

In the case of DSBs the cells have two mechanisms to combat these breaks, the first is non-homologous end joining (NHEJ) and the second is homologous recombination (HR). Some of the other mechanisms employed to combat DNA damage are antioxidants such as ascorbic acid, glutathione and others, which fight DNA damage caused by oxidative stress [Mahmoudi et al., 2006; Jackson and Bartek, 2009]. When the DNA damage becomes irreparable, it could lead to cell death through apoptosis (Figure 2.3), [Khalil et al., 2012].

There are various proteins involved with the DDR, which either control, or are involved in the cell life cycle. According to Mahmoudi et al. (2006) there are three steps in the DDR to

repair DNA damage, these steps consists of sensors, transducers and effectors. Sensors are responsible for detecting lesions and changes in chromatin structure after DNA damage has occurred. Sensors are a group of proteins called the meiotic recombination 11 (Mre11), DNA repair protein Rad50 (RAD50) and Nijmegen breakage syndrome (NBS1), also known as the MRN complex [C. Chen et al., 2013]. Transducers are proteins that initiate a host of signalling events that reverse the DNA damage. Mahmoudi et al. (2006) identified two transducer proteins namely; ATM and ATM Rad3-related protein (ATR) [Mahmoudi et al., 2006]. Lastly, are the effectors that are considered to complete the DDR, as they are responsible for carrying out the final response relayed by the sensors to the transducers. Both Chk1 and Chk2 proteins have been labelled as effectors as they are both downstream from the ATM and ATR proteins.



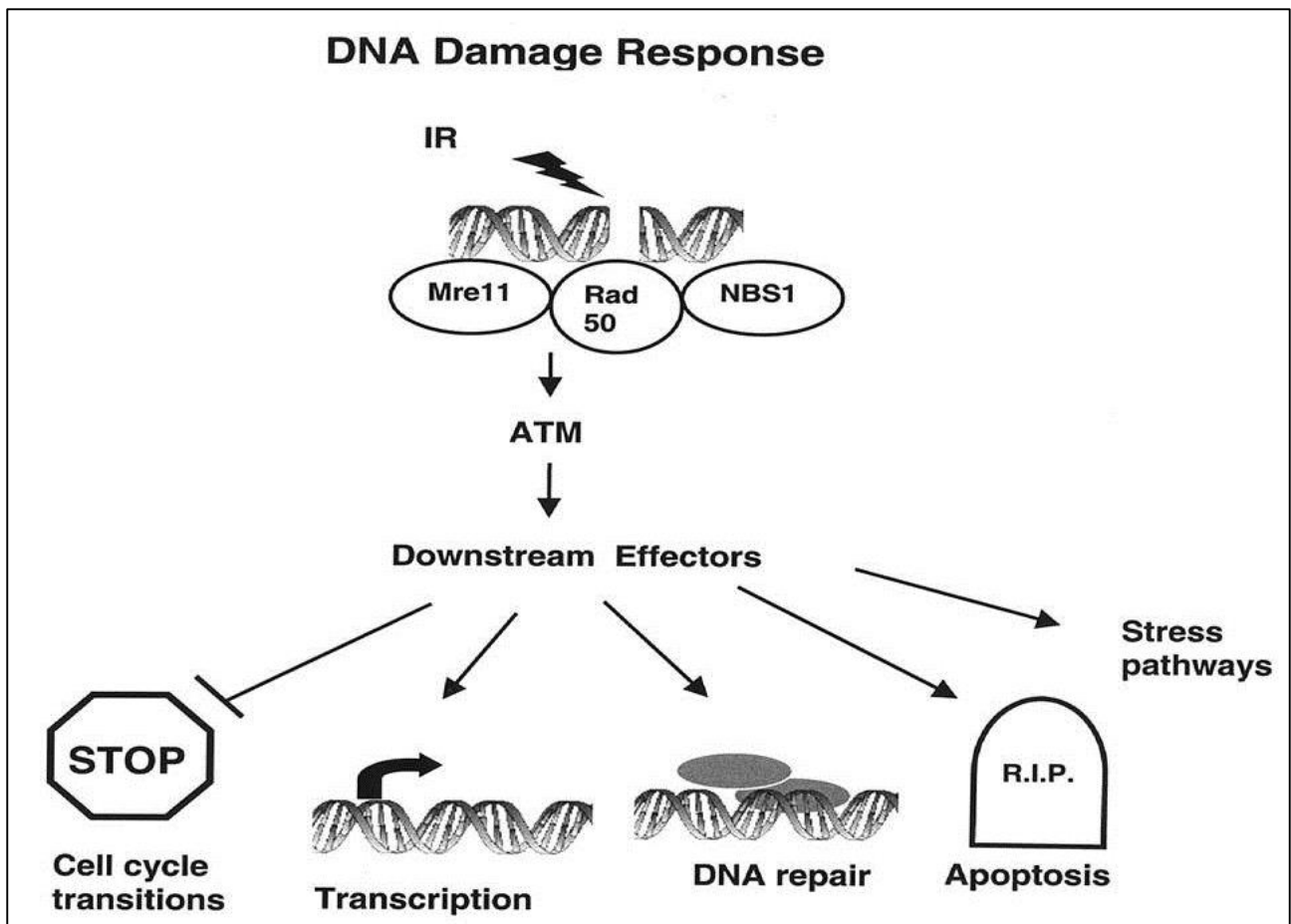


Figure 2.3: The role of ATM in response to DNA damage [Watters, 2003]. ATM is considered a transducer protein as it activates many proteins involved in controlling the cell cycle, DNA repair and apoptosis.

### 2.2.2. Proteins involved in the DDR

There is a wide spectrum of proteins involved in the DDR. As mentioned earlier some of these include the MRN complex, the ATM protein, ATR protein and Chk1 and Chk2. But other proteins involved with the DDR include DNA-dependent protein kinase (DNA-PK), Ku, PKB/Akt, the mitogen activated protein kinase (MAPK) family and many more, each with their own functions. It has been proposed that the MRN complex stimulates homologous recombination, which responds to SSBs [Jackson and Bartek, 2009]. Each protein in the MRN complex has a specific role to play. MRE11 has both endonuclease (for both single and double stranded DNA) and exonuclease activity, but most importantly, it possesses the binding domain for NBS1. The RAD50 protein is considered to function as a dimerization domain as it comprises of an ATP cassette accompanied by two coiled-coil domains. The NBS1 is critical for the transportation of the MRN to the nucleus and the binding of phospho-H2AX at sites of DSBs [Mahmoudi et al., 2006].

The H2AX histone protein is an indicator of DNA damage as it is rapidly phosphorylated after cell exposure to ionizing radiation [Bakkenist and Kastan, 2003]. Both ATM and DNA-PKcs at Ser-139 can phosphorylate the H2AX protein [Rocourt et al., 2013]. Once DNA damage occurs, aggregates of phospho-H2AX assemble at the locations of DNA damage, at which point the damaged DNA recruits the MRN complex and activates the DDR [Shiloh, 2003].

The ATM protein is recruited to the site of DSB by the MRN complex and is auto-phosphorylated at Ser1981 [Rocourt et al., 2013]. The ATM protein in turn phosphorylates downstream proteins, involved in the cell cycle (Figure 2.4). The first of these proteins are Chk1 (activated by ATR) and Chk2. Chk1 and Chk2 with ATM have been observed to reduce or inhibit the activity of cyclin dependent kinases (CDKs). According to Y. Shiloh (2003) both Chk1 and Chk2 phosphorylate CDC25A, a phosphatase protein. CDC25A is responsible for the dephosphorylation of the cyclin dependent kinases and maintains the

activity of CDK1 and CDK2. The dephosphorylation of CDK2 activity brings about a halt in the cell cycle at the G1-S phase which will provide enough time for damaged DNA to be repaired before DNA replication occurs and mitosis completes which is promoted by CDK1 [Shiloh, 2003; Jackson and Bartek, 2009; Mercer et al., 2010 and Bensimon et al., 2011]. The tumour suppressor p53, is known to play an integral role in detaining the cell cycle at the G1/S phase [Bakkenist and Kastan, 2003]. The ATM protein is known to activate the tumour suppressor gene, p53 by phosphorylating it at Ser15. Chk2 is also thought to activate p53 at Ser20 by phosphorylation, which impedes binding between p53 and MDM2 (figure 2.4), [Shiloh, 2003]. P53 is known to promote apoptosis in cells where the DDR could not be effective, or where senescence induced either by DNA-PKcs or selenium, is not successful [Rocourt et al., 2013].

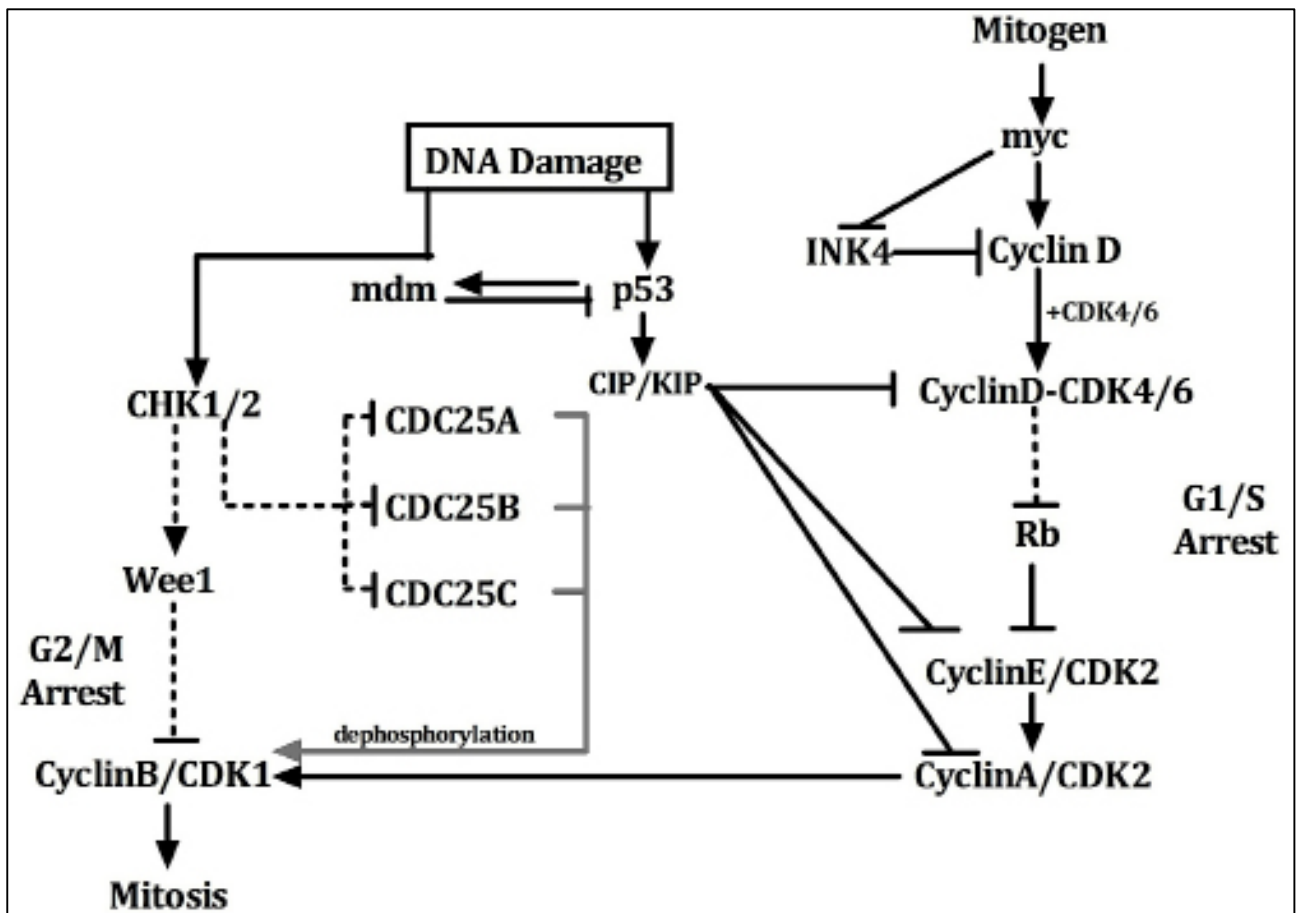


Figure 2.4: DNA damage repair mechanisms [Khalil et al., 2012]. The DNA damage response pathway activates p53 and the Chk1/2 proteins to arrest the cell cycle at the G1/S phase and G2/M phase respectively. Inhibition of cyclin dependent kinases (CDKs) and phosphorylation of the protein phosphatases are required for the repair mechanisms to occur.

In DSBs the non-homologous end joining (NHEJ) is identified by the Ku heterodimer (Ku70 and Ku80) which forms the catalytic subunit of the DNA-PK referred to as DNA-PKcs. The Ku heterodimer is responsible for binding to the DNA-PK and activating it to attract polymerases and DNA ligase IV to the damaged DNA site in order to repair it. The DNA-PKcs protein can be phosphorylated in two ways. The first is auto-phosphorylation at Ser-2056 which aims to repair NHEJ. The second is phosphorylation by ATM at Thr-2647, often due to ionizing radiation [Shiloh, 2003; Bensimon et al., 2011 and Rocourt et al., 2013]

The ATM protein is a member of the PI3-K-related family of kinases (PIKK). There are several other proteins that are a part of this family namely, ATR, mTOR/FRAP, TRRAP and DNA-PK [Bensimon et al., 2011].

Y. Shiloh suggested that proteins commonly involved in stress response pathways might play a role in the DDR. The activation of these proteins is normally independent of ATM, but when they are stimulated by the DDR their activity is ATM dependent. Examples of these proteins include MAPK and NF $\kappa$ B [Shiloh, 2003]. Once activated MAPK in turn activates ERK1/2. Subunits of the MAPK, p38 is known to be activated more dynamically by UV radiation than by ionizing radiation [Shiloh, 2003].

In addition to the DDR response, ATM activates other proteins as well; most of them have more than one function within the cell. These proteins are PKB/Akt and BRCA1. The ATM protein activates PKB/Akt during DNA damage caused by ionizing radiation. PKB/Akt is a member of the PI3-K signal transduction pathway and has many functions in the cell related to glucose uptake, cell progression and signalling pathways activated by insulin or IGF-1. The BRCA1 protein plays a role in the S-phase and the G2/M checkpoint of the cell cycle and initiates the expression of various DDR genes [Shiloh, 2003]. AMPK has been found to be activated by ATM in response to DNA damage. Activation of AMPK occurs independently from liver kinase B1 (LKB1) [Amatya et al., 2012]. Although LKB1 does not

activate AMPK it does result in the activation of mTOR complex 1 (mTORC1) and its signalling pathway together with TSC2 and hypoxia induced factor 1 alpha (HIF1 $\alpha$ ). The ATM protein is responsible for the activation of mTORC1 via this pathway (figure 2.5), [Guo et al., 2010].

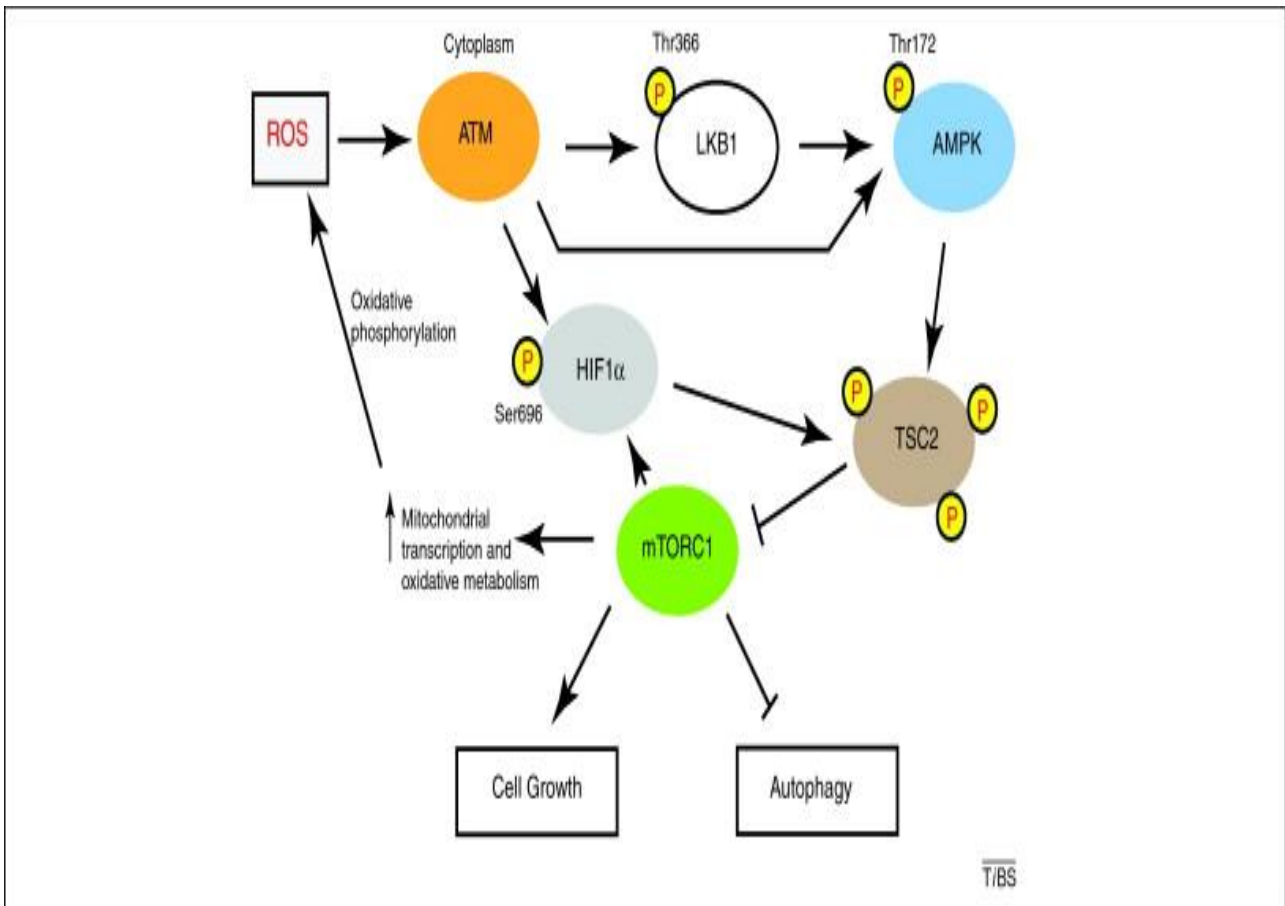


Figure 2.5: Cytoplasmic activation of ATM by ROS and its role in cell growth and autophagy [Ditch and Paull, 2012].

### 2.2.3. DNA damage and heart disease

Jackson and Bartek (2009) described that the activation of p53 is damaging in pathologies such as strokes and heart attacks. They also reported that the activation of p53 due to DNA damage could contribute to the development of atherosclerosis. The latter was attributed to senescence of vascular cells or cell death, which leads to the atherosclerosis lesion formation when the DDR is ineffective [Jackson and Bartek, 2009]. Similarly, Mercer et al. (2010) stated that there is a direct correlation between DNA damage and atherosclerosis (endothelial dysfunction; figure 2.6), and that either atherosclerosis or DNA damage will increase as the other progresses [Mercer et al., 2010]. Mahmoudi et al. (2006) argued that DNA damage occurs in both circulating cells and cells within the atherosclerotic plaque. They highlighted that early onset of atherosclerosis is an indication of failed DNA repair and pathologies like Werner syndrome, which is characterized by patients often showing signs of atherosclerosis, premature aging, cancer, osteoporosis, cataracts and diabetes [Mahmoudi et al., 2006].



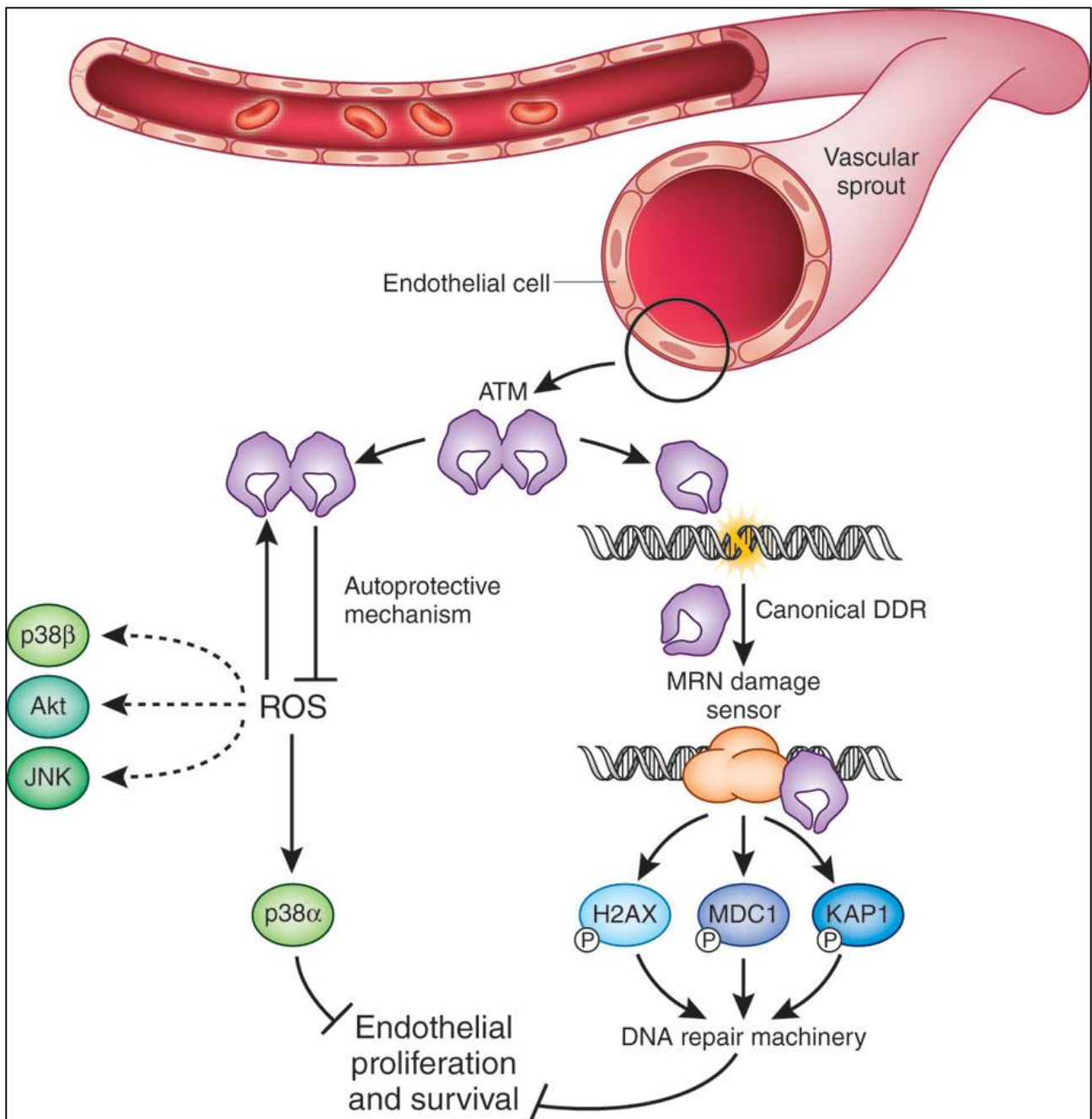


Figure 2.6: The role of ATM in the vasculature. First ATM is activated by the MRN complex in response to DNA damage caused by ionizing radiation. The ATM protein s dimer formation monomerizes into the active state. Secondly, ATM is activated by ROS and does dissociate from each other. Both ROS and DNA damage inhibit the proliferation and survival of endothelial cells [Kerr and Byzova, 2012].

#### **2.2.4. DNA damage and cell pathology**

Various studies have investigated several aspects of DNA damage. Throughout all of this, there appears to be a general theme, which includes the role of oxidative stress and the ATM protein. It is generally accepted that oxidative stress can cause DNA damage (cell nucleus or mitochondrial DNA; figure 2.7). This stems from the fact that the mitochondria are mainly responsible for cellular respiration, which releases reactive oxygen species (ROS) as a by-product. ROS is produced by different processes and contributes to the formation and progression of atherosclerotic plaques. DNA damage, which mostly occurs due to abnormally high levels of ROS, has been linked to atherosclerosis development [Mahmoudi et al., 2006]. This 'theory' is supported by the fact that in patients where the DDR is ineffective, few of the repair proteins will be activated, replication and mitosis will continue resulting in increased coding of mutated genes. This inevitably results in severe pathologies like that of Werner syndrome and Ataxia telangiectasia, as well as a much higher risk of developing cardiac disease, diabetes mellitus and the metabolic syndrome. In addition, there is a greater risk of developing cancer.

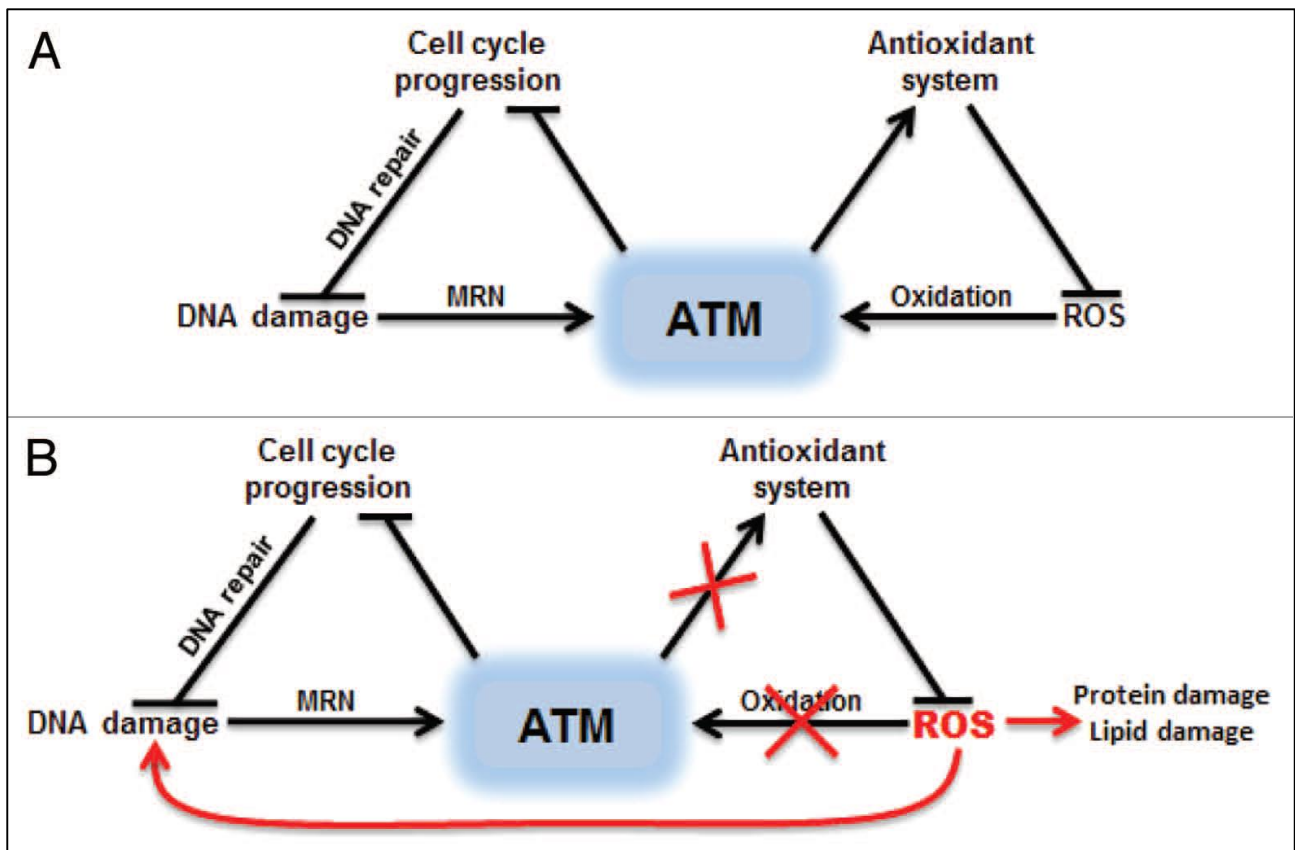


Figure 2.7: The role of ATM in response to DNA damage and ROS. (A) diagram depicting the dual role of ATM in response to both DNA damage and oxidative stress. (B) Indicates the adverse effects of ROS in the system when the protective role of ATM is inhibited [Guo et al., 2010].

### 2.3. Oxidative stress

The ATM protein is known not only as a sensor of DNA damage but also as a sensor for oxidative stress and oxidative damage [Chen, B et al., 2012 and Andrisse et al., 2014]. There are different types of oxidative stress, which activates the ATM protein at ser-1981. The mechanism by which ROS is generated is divided into endogenous and exogenous production. ROS is produced endogenously by various cellular mechanisms, which include mitochondrial respiration, xanthine oxidase and the NADPH oxidase [Coyle et al., 2006]. ROS produced by these mechanisms include superoxide anion ( $O_2^-$ ), hydrogen peroxide ( $H_2O_2$ ), reactive nitrogen species (RNS) and hydroxyl radicals (OH). ROS is known to play an important role in maintaining cell signalling and gene expression. ROS is generated exogenously by the addition of chemicals (chemotherapeutic drugs, hydrogen peroxide ( $H_2O_2$ )) or exposure to ionizing radiation or ultraviolet (UV) light. ROS production and release occur during cellular stress, hypoxic conditions or as a result from pathologies such as insulin resistance and diabetes [Chen, B. et al., 2012].

High cellular ROS concentrations are scavenged by antioxidants such as manganese superoxide anion dismutase (MnSOD), glutathione reductase, metal chelation thioredoxin and many more. When the concentration of ROS exceeds that of the antioxidants, the cellular redox homeostasis is lost, and oxidative stress ensues [Semlitsch et al., 2011].

ATM is an oxidative stress sensor and a deficiency in the activity of ATM is associated with high cellular concentrations of ROS, often observed in ataxia telangiectasia patients. The role of ATM as an oxidative stress sensor hints at the possible localization of the ATM protein in the mitochondria [D'Souza, et al., 2013].

### 2.3.1. Mitochondrial uncoupling

Type 2 diabetes mellitus and atherosclerosis have several commonalities, one of them being oxidative stress, whereby the presence of ROS in a cell exceeds the protective effects of antioxidants, resulting in impaired glucose uptake [Mookerjee et al., 2010] and atherosclerosis development. Vascular endothelial cells possess mitochondria in the cytosol. The mitochondria is responsible for the energy status of the cell by maintaining the levels of ATP and it is also responsible for regulating processes like apoptosis, calcium signalling and the production of ROS [Mookerjee et al., 2010].

The mitochondria possess their own DNA (mtDNA) which encodes for the proteins involved in the electron transport chain (ETC) namely, complex I, III, IV and V (the ATP synthase). Within the ETC, electrons are donated to NAD<sup>+</sup> and ubiquinone to generate NADH and ubiquinol. Both these molecules enter the ETC donating their electrons, which flows down a negative energy potential gradient in the mitochondrial inner membrane. The electrons enter the intermembrane space via complex I and are passed on to complex III and IV. Thereafter the protons are returned to the mitochondrial matrix by the proton motive force through complex V when ATP is generated [Mookerjee et al., 2010].

Once ATP is generated, the electrons are donated to oxygen (O<sub>2</sub>) to generate H<sub>2</sub>O. In some cases, the electrons are believed to “escape” the ETC at complex I and III [Mookerjee et al., 2010 and Yu, E. et al., 2013]. These electrons bind to O<sub>2</sub> and generate ROS in the form of superoxide anions (O<sub>2</sub><sup>-</sup>). The O<sub>2</sub><sup>-</sup> can form OH<sup>-</sup> radicals, which leads to extensive oxidative damage in cells.

Damage to mtDNA causes mitochondrial dysfunction and stimulates inflammation in the cell as well as cell death and senescence. According to Yu, E. et al. (2013) the aortas of patients with atherosclerosis have a higher incidence of mtDNA oxidative lesions

compared with control groups, thereby lowering the effects of antioxidants and promoting the onset of atherosclerosis [Yu, E. et al., 2013].

### **2.3.2. The NADPH oxidase**

The NADPH oxidase (Nox) consists of seven catalytic subunits namely, Nox1, Nox2, Nox3, Nox4, Nox5, Duox1 and Duox2 [Schramm et al., 2012]. The Nox enzymes are transmembrane proteins that transfer electrons from NADPH to  $O_2$  and produce  $O_2^-$ . Factors that activate the NADPH oxidase include growth factors and mechanical forces. One example includes the activation of the angiotensin II receptor, AT1. Once angiotensin II binds to AT1 it causes phospholipase C (PLC) activation, which results in the release of both diacylglycerol (DAG) and inositol trisphosphate ( $IP_3$ ).  $IP_3$  with DAG are considered to activate protein kinase C (PKC) by facilitating the release of calcium intracellularly. PKC is then believed to activate the NADPH oxidase through its activation subunit p47phox [Nickenig and Harris, 2002; Huang et al., 2011; Schramm et al., 2012].

Only Nox1, 2, 4 and Nox5 are thought to be present in vascular tissue. Nox1 is present in vascular smooth muscle cells (VSMC), Nox2 and Nox5 in ECs, Nox2 in adventitial fat and VSMC whereas Nox4 is localized in all cell types. It has been described that Nox1, 2, 3 and Nox4 possess a structural/functional subunit called p22phox and that Nox5 is calcium dependent [Huang et al., 2011]. Furthermore, Nox4 is the most abundantly expressed in ECs compared to the other Nox subunits. Nox4 activity is only dependent on p22phox and not p47phox, it was suggested that Nox4 is the least related member of the Nox family [Bretón-Romeros and Lamas, 2014].

In endothelial cells the NADPH oxidase produces  $O_2^-$ . Superoxide anions react with NO to produce peroxynitrite ( $ONOO^-$ ; figure 2.8).  $ONOO^-$  is considered one of the most effective

markers of endothelial dysfunction. Concurrently,  $O_2^-$  reacts with enzymes that stabilize the ROS by converting it into  $H_2O_2$ .  $H_2O_2$  may further be broken down into a volatile form, which affects both HDL and LDL and promotes atherosclerosis plaque formation. It has been described that both iNOS, the inducible NOS isoform responsible for the generation of high amounts of NO, and Nox4 play a role in atherosclerosis; Nox4 in atherosclerosis development and Nox2 in atherosclerosis progression [Wang, H. et al., 2014]. Atherosclerosis progression occurs by the formation of foam cells due to the excess uptake of ox-LDL by monocyte-derived macrophages.

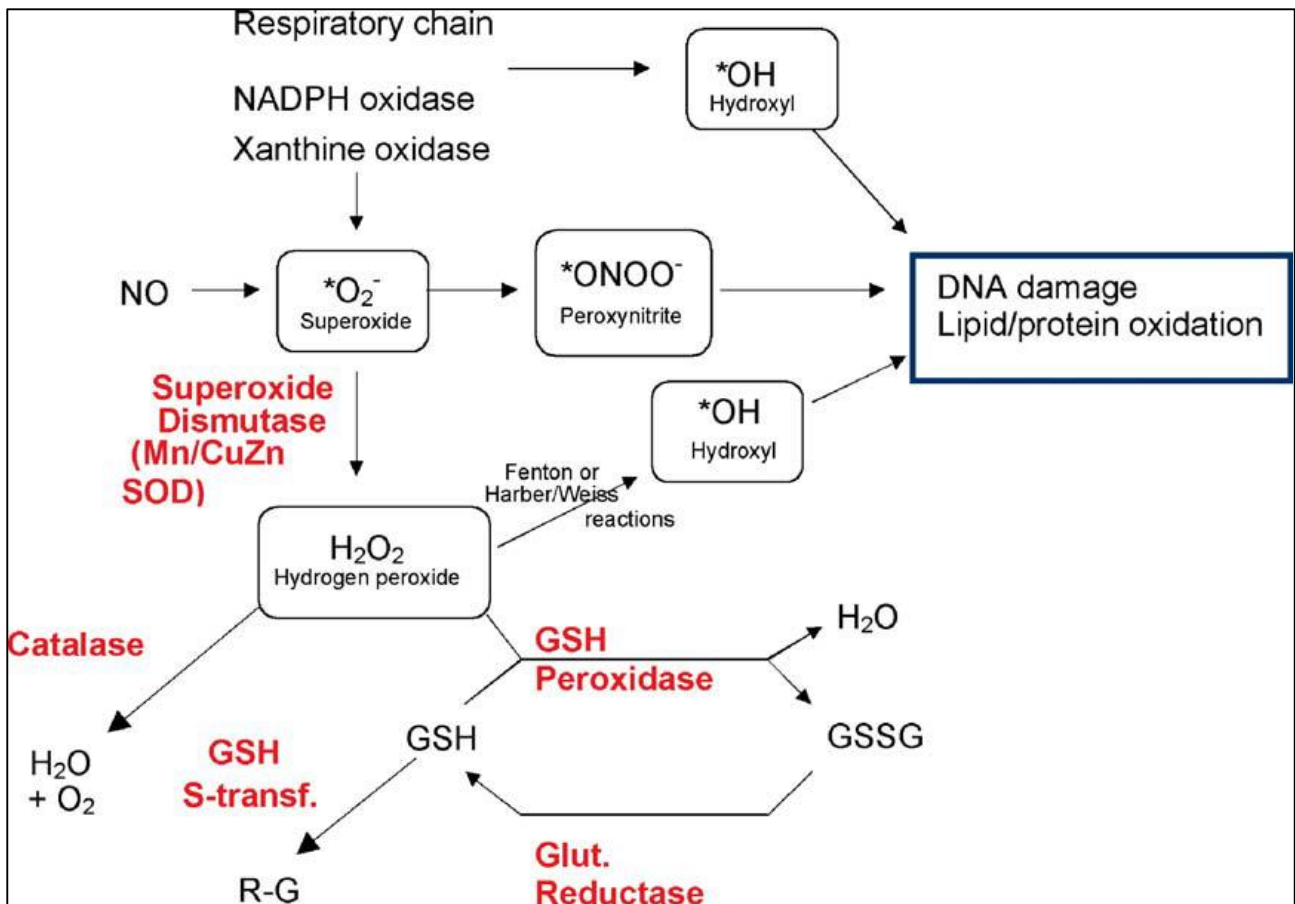


Figure 2. 8: Oxidative stress produced by the NADPH oxidase and the antioxidants which target ROS production [Khalil et al., 2012].



### **2.3.2.1. Ox-LDL induced ROS production and ATM**

Many studies have explored the relationship between the ATM protein, ROS and RNS. Semlitsch et al. (2011) studied the putative protective role of ATM against ROS in the presence of oxidized low-density lipoprotein (oxLDL) and the looming onset of atherosclerosis. Their results showed that ox-LDL activated ATM in a time dependent manner and this activation was abrogated in cells treated with an ATM inhibitor. Furthermore, although ox-LDL inhibited the growth of ATM<sup>+/+</sup> AND ATM<sup>-/-</sup> cell types, it had no effect on the survival of these cells. Ox-LDL was observed to increase ROS production in ATM<sup>-/-</sup> cell lines and cells inhibited with a specific ATM inhibitor. When functional ATM was activated by ox-LDL, ATM was found to elicit a protective effect against ROS production associated with the high levels of ox-LDL *in vitro* [Semlitsch et al., 2011].

### **2.3.3. Atherosclerosis development in relation to ATM<sup>-/-</sup> and ATM <sup>+/-</sup> genotypes**

#### **2.3.3.1. ROS, ATM and the induction/expression of HIF1 $\alpha$**

In ATM deficient patients, hypoxia-inducible factor 1 $\alpha$  (HIF1 $\alpha$ ) is up-regulated. HIF1 $\alpha$  is responsible for cellular adaptation to hypoxic conditions and promotes angiogenesis by regulating the expression of vascular endothelial cell growth factor (VEGF) and mediating the cell metabolism through glucose transporter 1 (GLUT1) [Ousset et al., 2010].

Ousset et al. (2010) hypothesized that HIF-1 biosynthesis was a result of the high levels of oxidative stress in ATM deficient cells [Ousset et al., 2010]. Their data suggested a direct link between the up-regulation of HIF1 $\alpha$  and oxidative stress in AT patients and that ROS produced by the mitochondria partially stabilizes HIF1- $\alpha$ . HIF-1 $\alpha$  stabilization leads to

increased tumour angiogenesis typical of cancer development in AT patients [Ousset et al., 2010].

### **2.3.3.2. The ATM protein and NF $\kappa$ B in response to oxidative stress**

NF $\kappa$ B is a transcription factor and regulates the oxidative stress response. NF $\kappa$ B activation is mediated by the presence of inflammation or by the ATM protein via I $\kappa$ B in response to DNA damage. In ATM deficient cells, the activation of NF $\kappa$ B was shown to be reduced [Watters, 2003].

### **2.3.3.3. The effects of antioxidant treatment for mitochondrial dysfunction in an ATM<sup>-/-</sup> mouse model**

Antioxidant therapy is a well-known and useful way of reducing intracellular ROS. In a study completed by D'Souza et al. (2013), the antioxidant effects of catalase targeted to mitochondria (mCAT) on the clinical symptoms of AT in an ATM<sup>-/-</sup> mouse model, with regards to thymic function, a deficiency in the bone marrow hematopoiesis and dysfunctional memory CD8<sup>+</sup> T-cells were investigated. Their data demonstrated that mitochondrial ROS production is responsible for the oxidative stress observed in AT. They observed an increase in thymocytes due to mCAT activity, but in the presence of cancer in the ATM<sup>-/-</sup> mice model, mCAT had no effect on the function of the thymus. It was also observed that the CD8<sup>+</sup> T-cell function was partially restored. Lastly, although not significantly and irrespective of mCAT treatment, the bone marrow hematopoiesis declined in an age-dependent manner [D'Souza et al., 2013]. The data presented by this study indicated that although antioxidant therapy was successful in alleviating or postponing the symptoms of AT, it did not prevent morbidity or mortality arising from AT associated pathologies.

### 2.3.4. Regulation of ROS by ATM and p53

Ataxia telangiectasia and ATM deficiency lead to oxidative stress. P53 is believed to have a dual role in the regulation of ROS and oxidative stress homeostasis [Armata et al., 2010]. They believed that p53 had a twofold role in maintaining ROS. They argued that the same pathologies related to p53 activation also induced its phosphorylation at Ser15, which is known as the ATM phosphorylation site. Some of these pathologies include atherosclerosis, hypoxia and shear stress [Armata et al., 2010]. Armata and colleagues (2010) first suggested a link between p53 and glucose homeostasis in 2010. They furthermore described the role of p53 in regulating the expression of GLUT-1 and -4 by cancer cells. It is believed that animals deficient in p53 protein are more susceptible to developing type 1 diabetes in a streptozotocin-induced model compared to control animals. Using this information, and the fact that AT patients display symptoms of type 2 diabetes, they investigated the effect p53 had on the glucose homeostasis and insulin resistance by exploring the PKB/Akt activation in both wild type and ATM phosphorylation site absent p53 mice models (p53<sup>S18A</sup>) [Armata et al., 2010]. In addition, their study compared the expression of the naturally occurring antioxidant Sestrin and the amount of ROS produced by the different models. They concluded that the p53 ATM phosphorylation site has a defensive role in maintaining glucose levels, as they observed a higher rate of glucose intolerance, insulin resistance and ROS in the p53<sup>S18A</sup> models. They also concluded that the ATM phosphorylation site on p53 is necessary for p53-antioxidant dependent gene expression [Armata et al., 2010].

S. Ditch and T.T. Paull (2012) hypothesized that the ATM protein and p53 may be working together to maintain glucose homeostasis. They ascribed this to an observed increase in ROS levels as a result of a deficit in the ATM phosphorylation sites on the p53 protein (Ser15). An increase in ROS leads to an increase in glucose intolerance and insulin

resistance, often also leading to the development of type 2 diabetes and a decrease in functional antioxidant activity mediated by p53. Concerning this, theoretically in the absence of ATM and p53 phosphorylation, the insulin-signalling pathway is undoubtedly disrupted [Ditch and Paull, 2012].

### **2.3.5. Pathologies associated with increased ROS production**

Neuro-degeneration, Parkinson's disease and Alzheimer's disease are associated with oxidative stress [Marinoglou, 2012] but a discussion of these pathologies falls outside the scope of this thesis.

It was found that, when the ATM protein is inactive, there is a mutation in the GLUT1 ATM activation site (S490 from alanine to aspartate) coupled to a decrease in ROS production. This is explained by an increased activation of GLUT1 in the absence of ATM. GLUT1 takes up glucose (glucose-6-phosphate) and dehydroascorbic acid (DHA) into the cells. Glucose-6-phosphate and DHA both contribute electrons to antioxidant pathways [Andrisse et al., 2014]. These observations are absent with GLUT4 as, unlike GLUT1, it does not have an ATM activation site.

## **2.4. ATM in the cytoplasm**

### **2.4.1. Protein translation**

As mentioned above, it has been established that the ATM protein is present in both the nucleus and the mitochondria. The nuclear function of ATM has been closely linked to the DNA damage response and the mitochondrial function of ATM has been linked to combating effects of oxidative stress. In addition to this, Yang and Kastan (2000)

described the cytoplasmic function of ATM as being a direct mediator of protein translation in response to insulin treatment. The eukaryotic initiation factor 4E (eIF-4E) protein carries out protein translation in a rapamycin insensitive manner and in the presence of insulin. In the inactive state eIF-4E is bound to 4E-binding protein 1 (4E-BP1). 4E-BP1 is a protein phosphorylated by ATM at its Ser111 phosphorylation site [Yang and Kastan, 2000]. The mammalian target of rapamycin (mTOR), which is a part of the ATM related kinase (figure 2.9) can also activate 4E-BP1, [Gingras et al., 1998 and Greiwe et al., 2001]. Ser111 has a glutamine next to it, which is consistent with the target phosphorylation sites of ATM. According to Yang and Kastan (2000) 4E-BP1 has three different phosphorylation sites that can be activated by many different stimulators. One of them is mTOR, which is rapamycin sensitive, but only Ser111 is phosphorylated by the ATM protein. Phosphorylation of 4E-BP1 at Ser111 was confirmed when Yang and Kastan studied the phosphorylation of 4E-BP1 and initiation of protein translation by eIF-4E in cell cultures with an inactive ATM protein. In their study 293T cells, A38 (ATM<sup>-/-</sup>) and A29 (ATM<sup>+/+</sup>) cells were used. Additionally, Yang and Kastan (2000) sought to silence the *Atm* gene in cells expressing functional ATM or to insert a vector containing the functional *Atm* gene to reverse the lack of ATM activity as a way to confirm their previous results [Yang and Kastan, 2000].

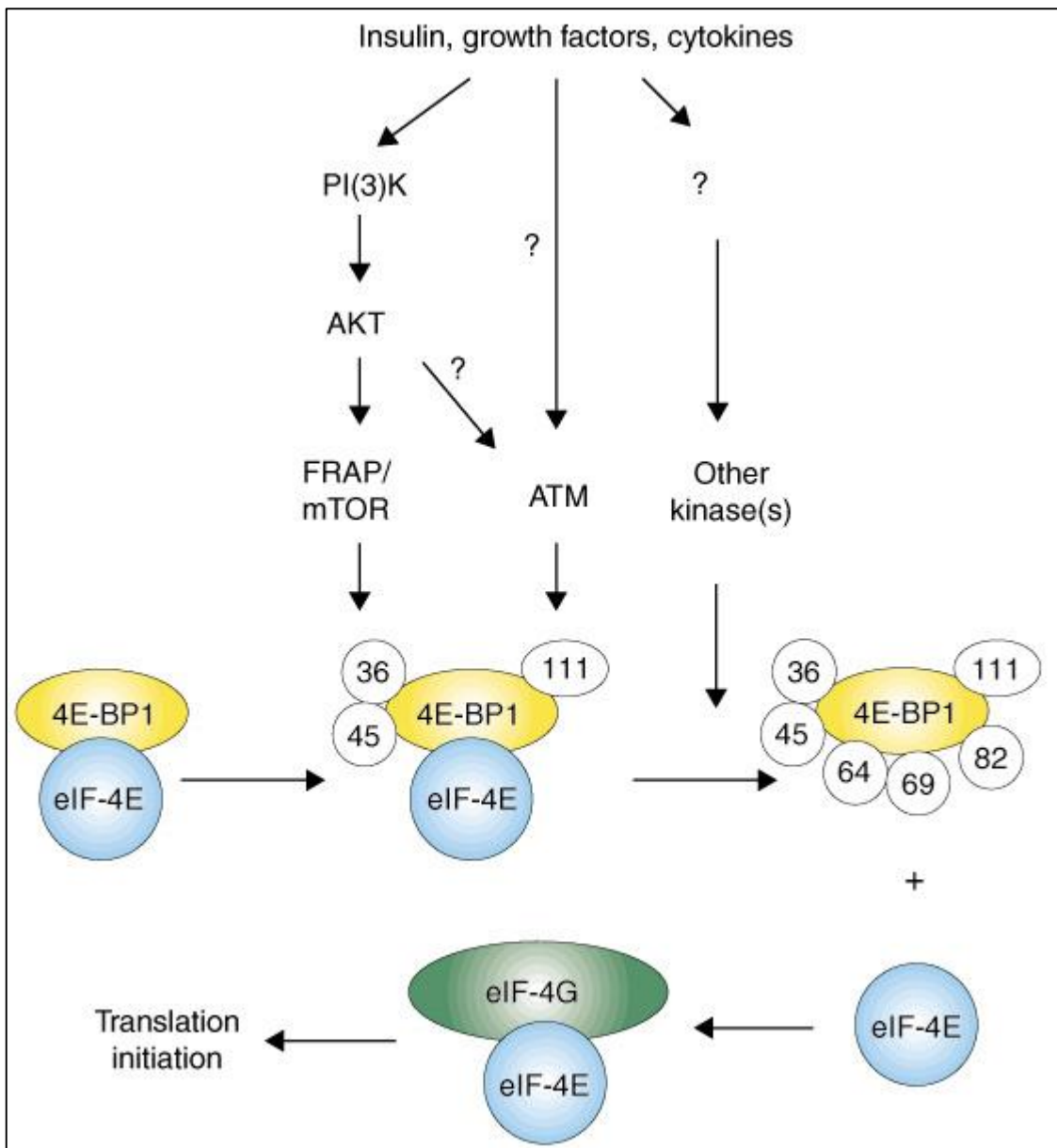


Figure 2.9: Cap dependent protein translation by eIF-4E. The ATM protein phosphorylates 4E-BP1 at Ser111, which then dissociates from eIF-4E. Free eIF-4E binds to eIF-4G and initiates protein translation [Yang and Kastan, 2000].

#### **2.4.2. The impact of the expression and activation of ATM on insulin growth factor-1 and insulin receptor substrate-1**

The mTOR protein is the catalytic subunit for both mTOR-containing multiprotein complex-1 (MTORC1) and mTOR-containing multiprotein complex-2 (MTORC2), also known as the mTOR complex. Both mTORC1 and mTORC2 have four subunits but each complex has its own function. mTORC1 is responsible for protein translation whereas mTORC2 is responsible for cell survival [Zhang, D. et al., 2010]. Proteins targeted by mTORC1 include 4E-BP1 and 70-kDa ribosomal protein S6 kinase (p70 S6 kinase; figure 2.10).

Ching et al. (2013) investigated the significance of ATM protein expression in relation to the phosphorylation and activation of p70 S6 kinase (S6K) mediated by the insulin receptor substrate-1 receptor (IRS-1R) proposing that a different pathway could be available to activate S6K [Ching et al., 2013]. Ching et al. (2013) used both a cell culture model (C2C12 myotubes) and an animal model for their research. The cell culture was treated with short hairpin RNA (shRNA) or Ku-55933, an ATM inhibitor. The animal model was an ATM protein heterozygous mouse model fed a high-fat diet. Both the cell culture model and the animal model had age-matched controls. The C2C12 myotubes treated with shRNA expressed 22% of the total ATM observed in the control C2C12 myotubes. This value emulated the same amount of total ATM expressed in mice fed a high-fat diet compared to mice that were chow-fed [Ching et al., 2013]. Following this observation, Ching et al. (2013) found an increase in ATM phosphorylation at Ser1981 by IGF-1 after insulin treatment in the wild type mice (ATM+/+) but not the ATM+/- mice. IGF-1 is known to phosphorylate PKB/Akt in response to insulin but this signal transduction was down regulated in ATM+/- mice despite the fact that the total PKB/Akt expressed were the same in both mice models (control and high-fat fed mice), [Ching et al., 2013]. Secondly, there were no differences in the phosphorylation of IRS-1 by IGF-1 in heterozygous mice but a

decrease in the activation of PI3-K by IGF-1 in ATM<sup>+/-</sup> mice occurred. Lastly, changes in the phosphorylation of S6K were observed. IGF-1 activates S6K, which is a target protein of mTORC1. Inactive mTORC1 can be found in a complex with mTORC2. The phosphorylation of S6K was lower in ATM<sup>+/-</sup> C2C12 myotubes treated with shRNA. C2C12 myotubes treated with Ku-55933 also had less activation of S6K by IGF-1, the same effect was observed in the soleus of ATM<sup>+/-</sup> mice [Ching et al., 2013]. Furthermore Ching et al. (2013) concluded that, when ATM is inhibited or in ATM<sup>+/-</sup> mice, the activity of mTOR decreases. The data implies that if IGF-1 is activated by insulin then the ATM protein will fully mediate the activation of PKB/Akt. Since PKB/Akt can also be activated by other stimuli, Ching et al. (2013) concluded that the role of ATM to fully mediate PK/Akt phosphorylation in and ATM<sup>+/-</sup> mouse model is abolished. Based on the results obtained during their investigation, Ching et al. (2013) also concluded that ATM is distal from IRS-1 as this protein continued to be phosphorylated by IGF-1 while phosphorylation of PKB/Akt was reduced [Ching et al., 2013].

Peretz et al. (2001) explored the difference in insulin-like growth factor-1 receptor (IGF-1R) expression among three different ATM cell lines (ATM<sup>+/+</sup>, ATM<sup>+/-</sup> and ATM<sup>-/-</sup>). They observed a reduction in the expression of IGF-1R in ATM<sup>-/-</sup> cell lines compared to the heterozygous and wild type cells (ATM<sup>+/-</sup> and ATM<sup>+/+</sup>). They also observed that IGF-1R played a key role in regulating apoptosis induced by cytotoxic factors, including ionizing radiation [Peretz et al., 2001]. The lack of resistance towards ionizing radiation in ATM<sup>-/-</sup> cell lines were tested by transfecting ATM<sup>-/-</sup> with a cDNA encoding for IGF-1R and exposing these cells as well as ATM<sup>+/-</sup> and ATM<sup>+/+</sup> to different doses of ionizing radiation (1 Gy to 5 Gy). Contrary to these experiments, they also inhibited the function of the IGF-1R with anti-IGF-1R antibody in ATM<sup>-/-</sup> cells previously transfected with the IGF-1R vector cDNA and found an increase in ionizing radiation sensitivity in these cells [Peretz et al.,



2001]. Thereby, concluding that IGF-1 expression is necessary for an ATM<sup>-/-</sup> cell to display resistance towards ionizing radiation.

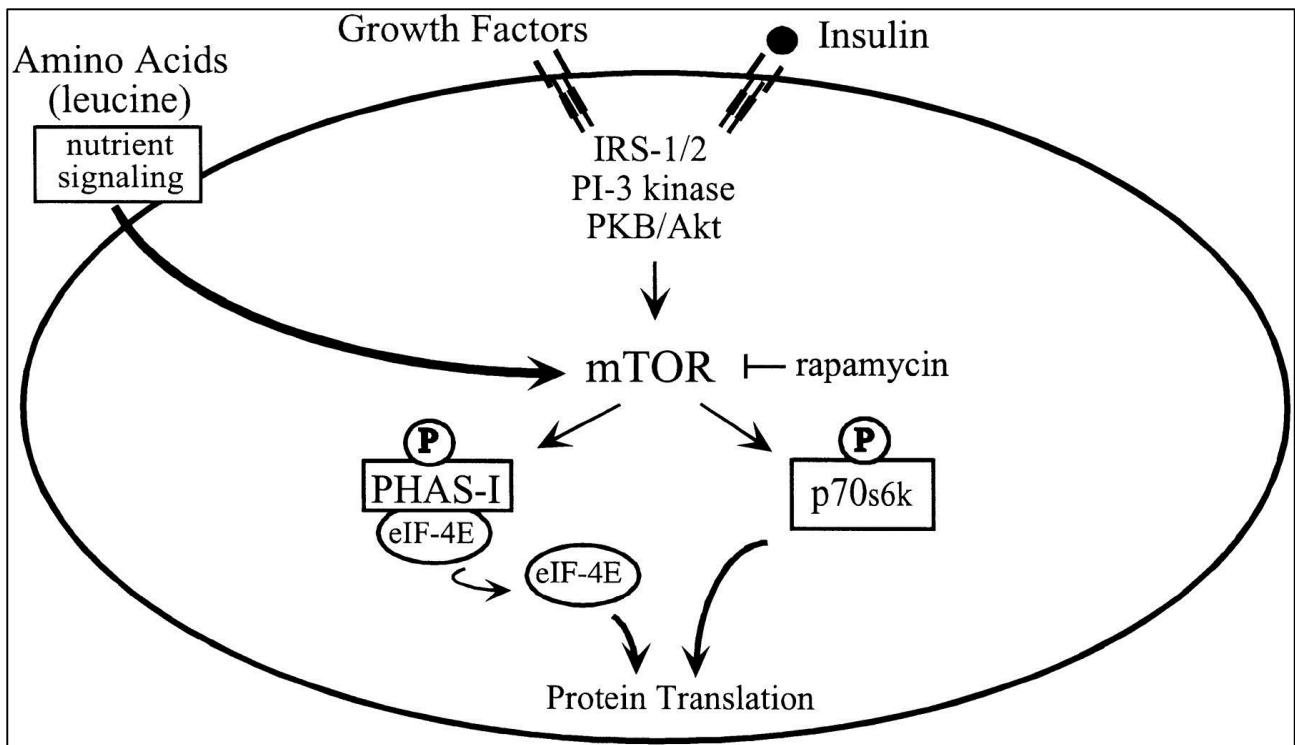


Figure 2.10: mTOR mediated protein translation. The mTOR protein can be activated in an insulin dependent manner or independent of insulin by amino acids such as leucine [Greiwe et al., 2001]. The mTOR protein phosphorylates both eIF-4E and S6K, thereby activating protein translation. mTOR activity is inhibited by rapamycin.

### 2.4.3. The role of ATM in the glucose uptake pathway and insulin resistance

As mentioned, one of the cytosolic functions of ATM includes the phosphorylation of 4E-BP1 in response to insulin treatment. Another function of the ATM protein in the cytoplasm includes facilitating glucose uptake in skeletal muscle. The protein PKB/Akt mediates both protein translation and glucose uptake. Insulin has proven to be a definite activator of ATM in the absence of DNA damage and oxidative stress (figure 2.11).

Various research groups have studied the localization of ATM in the cytoplasm, especially in the development of insulin resistance. In this regard, Halaby et al., (2008) has researched the role of the ATM protein in rats with high-fat diet induced insulin resistance [Halaby et al., 2008].

In the study completed by Halaby et al. (2008) they investigated the expression of the ATM protein and its impact on the expression and phosphorylation of PKB/Akt as well as the possible role of ATM in the glucose uptake pathway [Halaby et al., 2008]. Experiments were completed in both ATM<sup>+/+</sup> (A29) and ATM<sup>-/-</sup> (A38) cell lines to determine if the presence or absence of ATM had an effect on PKB/Akt expression and activation. Secondly, the difference in phosphorylation of PKB/Akt by ATM in the skeletal muscle of rats that were insulin resistant due to being fed a high-fat diet versus chow-fed rats was determined. Lastly, L6 muscle cells were treated with the ATM inhibitor with or without the addition of insulin to determine any differences in the phosphorylation of PKB/Akt and GLUT4 translocation. Additionally, proteins such as IRS-1 and its phosphorylation at tyrosine 612 were determined in cells with or without functional ATM that were either treated with insulin or not. Their data indicated that a lack of ATM activity was associated with a decrease in PKB/Akt phosphorylation. This decrease could not be accounted for by the lack of PKB/Akt expression as total PKB/Akt remained uniform throughout the different tissue types (skeletal muscle from insulin resistant rats compared to control rats, ATM<sup>+/+</sup>

and ATM<sup>-/-</sup> as well as L6 muscle cells), [Halaby et al., 2008]. Secondly, the ATM protein is required to phosphorylate PKB/Akt in response to insulin at Ser473 and phosphorylation of Ser473 is required for the phosphorylation of Thr308. There was no difference in the expression of both the insulin receptor and IRS-1 and no differences were observed in the phosphorylation of IRS-1 when treated with insulin in both the ATM<sup>+/+</sup> and ATM<sup>-/-</sup> cell lines. Furthermore, it was observed that the ATM protein was necessary for the translocation of GLUT4 to the plasma membrane as inactive ATM resulted in a decrease in GLUT4 translocation, which can be associated with insulin resistance and glucose intolerance. Halaby et al. (2008) concluded that although the ATM protein is necessary for PKB/Akt phosphorylation in response to insulin, there are still uncertainties as to whether the ATM protein works parallel to the PI3-K and is activated by the IRS-1 or if it is the PI3-K protein as is 4E-BP1, a known substrate of both ATM and PI3-K in the presence of insulin [Halaby et al., 2008].

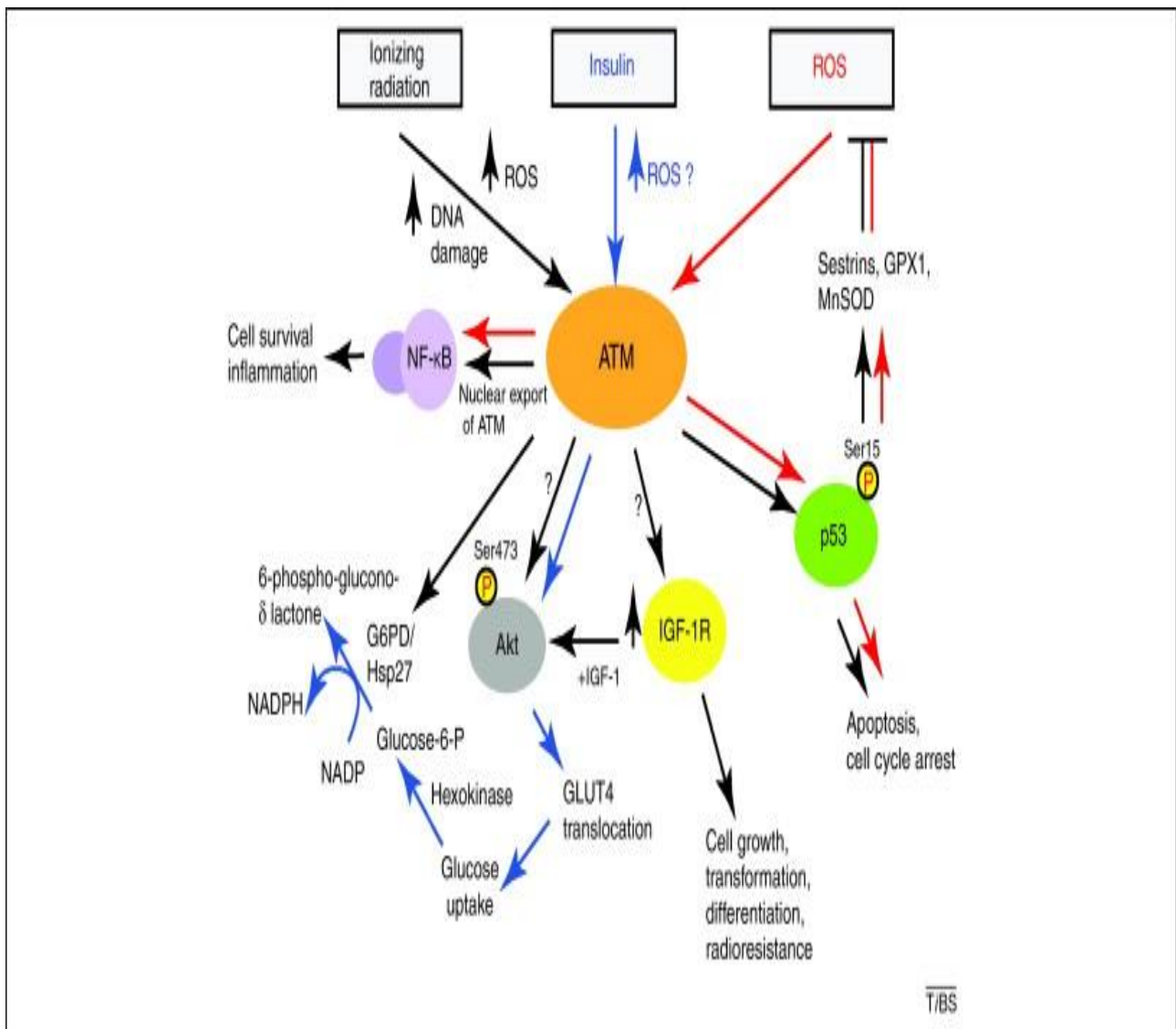


Figure 2.11: Activators of the ATM protein [Ditch and Paull, 2012]. The diagram shows the three known activators (DNA damage response (DDR), reactive oxygen species (ROS) and insulin) of the ATM protein and the different signalling pathways ATM is involved in. Each pathway has been assigned a colour (DDR: black, insulin: blue and ROS: red) to depict how ATM responds to the different stimuli.

#### 2.4.4. Inhibitors of ATM

There are two known ATM inhibitors present on the market namely, Ku55933 and Ku-60019 (figure 2.12). Many research projects involving the ATM protein have used the ATM inhibitor Ku-55933. Ku-60019 is an ATM inhibitor, which has a higher specificity for the ATM protein and to date only one article is available whereby researchers have used Ku-60019 to test the importance of the ATM protein in Glioma cells [Golding et al., 2009]. Presently the only known differences between Ku-55933 and Ku-60019 is the variation in IC<sub>50</sub> and K<sub>i</sub> for Ku-55933 has an IC<sub>50</sub> of 13 nM and a K<sub>i</sub> of 2.2 nM [Hickson et al., 2004]. and the solubility and IC<sub>50</sub> of the Ku-60019 inhibitor as it is a more water-soluble substance, has an IC<sub>50</sub> of 6.3 nM, and has been found to be a more potent inhibitor of the ATM protein than Ku-55933 [Golding et al., 2009].

Wortmannin is a non-specific PI3-K inhibitor, which targets many of the PI3-K related kinases (PIKK), [Hickson et al., 2004]. Considering ATM is a part of the PIKK family it has been proposed that treatment with this inhibitor will abolish the function of ATM in the cytoplasm.

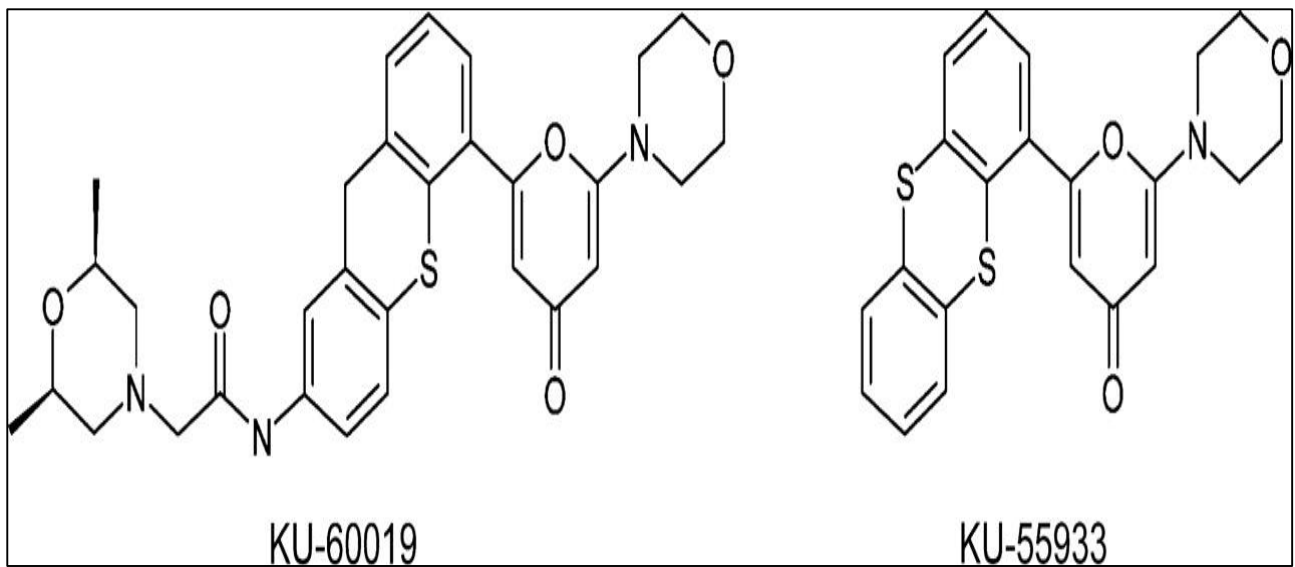


Figure 2.12: Diagram of ATM inhibitors Ku-60019 and Ku-55933, respectively [Golding et al., 2009].

## 2.5. Motivation

As mentioned previously, few studies have been performed to establish the role of the ATM protein in endothelial dysfunction and cardiovascular disease. In this literature review, it was established that the ATM protein is a key player in the DDR in the nucleus and that it is a sensor for oxidative stress in the mitochondria. Recently it has been proven that the ATM protein localized in the cytoplasm, also plays a role in protein translation and in the development of insulin resistance in AT patients.

Concerning atherosclerosis development and associated endothelial dysfunction, some of the common causes for these conditions include insulin resistance, hyperglycaemia, inflammation, oxidative stress and damaged DNA that cannot be repaired, leading to cell death by apoptosis. In a functional endothelial cell, the enzyme eNOS releases NO in order to maintain vascular homeostasis. In endothelial cells, insulin-induced activation of PKB/Akt is a major upstream activator of eNOS.

Currently, there is conflicting data as to whether the ATM protein mediates the full activation of PKB/Akt by phosphorylating both Ser473 and Thr308 or if ATM only activates Ser473 [Ching et al., 2013]. Conversely, Golding et al. (2009), believes that ATM does not directly activate PKB/Akt. As PKB/Akt does not have the conserved serine/threonine phosphorylation site, which is followed by the amino acid glutamine at targeted positions the ATM phosphorylates in other proteins [Golding et al., 2009].

Miles et al., (2007) believes that AT patients display normal sensitivity towards insulin but upon undergoing an oral glucose tolerance test they observed fleeting hyperglycaemia. Miles et al. (2007) ascribed this observation to ATM<sup>-/-</sup> cells having a delayed reaction in releasing insulin in response to glucose [Miles et al., 2007]. The delayed reaction of AT cells in response to glucose stimulation of insulin secretion is arguably a result of dysfunctional or a lack of pancreatic beta cells.



If ATM<sup>-/-</sup> mice have diminished functional pancreatic beta cells and thus cannot release insulin, there would be a decrease in PKB/Akt phosphorylation. However, if ATM<sup>-/-</sup> cells such as the A38 cell line are treated with insulin *in vitro* it has been observed that the activation of both IGF-1 and IRS-1 remains constant among ATM wild type and ATM null cells. The PKB/Akt protein is downstream from both IGF-1 and IRS-1 and thereby its activation is based on the phosphorylation of these two proteins in healthy cells. Ching et al. (2013) argued that if both IGF-1 and IRS-1 are activated by insulin in ATM<sup>-/-</sup> cells, then the ATM protein could be found downstream to these proteins in the signalling pathway. Hypothetically ATM is responsible for PKB/Akt phosphorylation at Ser473 and thus if there is no active ATM PKB/Akt cannot be activated. Furthermore, when a decrease in PKB/Akt phosphorylation occurs there will be a decrease in eNOS activation leading to a decrease in NO bioavailability and a disruption in vascular homeostasis as well as a decrease in glucose uptake resulting in hyperglycaemia.

Contrary to these explanations Yang and Kastan (2000) and Halaby et al. (2008) both concluded that the ATM protein may participate in signalling pathway which is activated by insulin but works parallel to the PI3-K signalling pathway. Therefore, for the purpose of this study, the position of the ATM protein in the PI3-K signalling pathway and the effect that ATM expression on glucose uptake and eNOS activation will be investigated.

## 2.6. Aims and objectives

Based on the literature review and the current motivation of the study; the aims and objectives of this research project are listed below.

Aim 1:

Identify a suitable model for the isolation and harvesting of AECs from male Wistar rats. The chosen isolation model will be determined by the following criteria: (i) highest possible yield of primary AECs; (ii) highest possible endothelial cell purity as measured by cell morphological appearance, positive staining with an endothelial cell-specific probe and detection of eNOS expression.

Aim 2:

Determine the difference in ATM protein expression by AECs in response to treatment with insulin, the ATM inhibitor Ku-60019 and the PI3-K signalling pathway inhibitor wortmannin.

Objectives for aim two includes:

Measuring the viability of the AECs after treatment with insulin, Ku-60019 and wortmannin.

Detecting any changes insulin, Ku-60019 and wortmannin may exert on the production of NO by the AECs.

Determining the role of ATM in the glucose uptake pathway and establishing a relationship between the ATM protein and the function of eNOS in the AECs.

## Chapter 3: Methods

### 3.1. Aortic endothelial cell (AEC) isolation techniques:

#### 3.1.1. Vascular ring method adapted from the article published by Hu et al., (2009)

Two male Wistar rats were anaesthetized with 160 mg/kg sodium pentobarbital (Bayer Healthcare, Leverkusen, Germany). The rats were sprayed from head to toe with 70% ethanol to ensure sterility before being placed in the laminar flow chamber. When deep anaesthesia, as confirmed by an absent foot pinch response, was achieved, the mid-section of the thoracic-abdominal region was opened by incision, and the thoracic region of the aorta was excised. The peri-vascular fat and connective tissue were removed and the aortas were placed in Dulbecco's Modified Eagle Medium (DMEM; Lonza, Basel, Switzerland) supplemented with fetal bovine serum (FBS; Highveld Biological, RSA). The full composition of the media consisted of 79% DMEM, 20% FBS and 1% penicillin-streptomycin (Gibco, CA, USA). Using a suture, the aortas were inverted to expose the endothelium. The aortas were cut into rings of 2-3 mm in length. The aortic rings were placed in a petri dish (previously coated with attachment factor (Gibco, CA, USA) for 1 hour) and incubated in DMEM under standard conditions (37°C, 5% CO<sub>2</sub>, 40-60% humidified). The aortic rings were removed on Day 4. Cells that have detached from the aortic rings onto the petri dish were allowed to grow until confluency and received fresh endothelial cell basal medium-2 (EGM-2MV; Lonza, MD, USA) supplemented with 20% FBS every two days (figure 3.1).

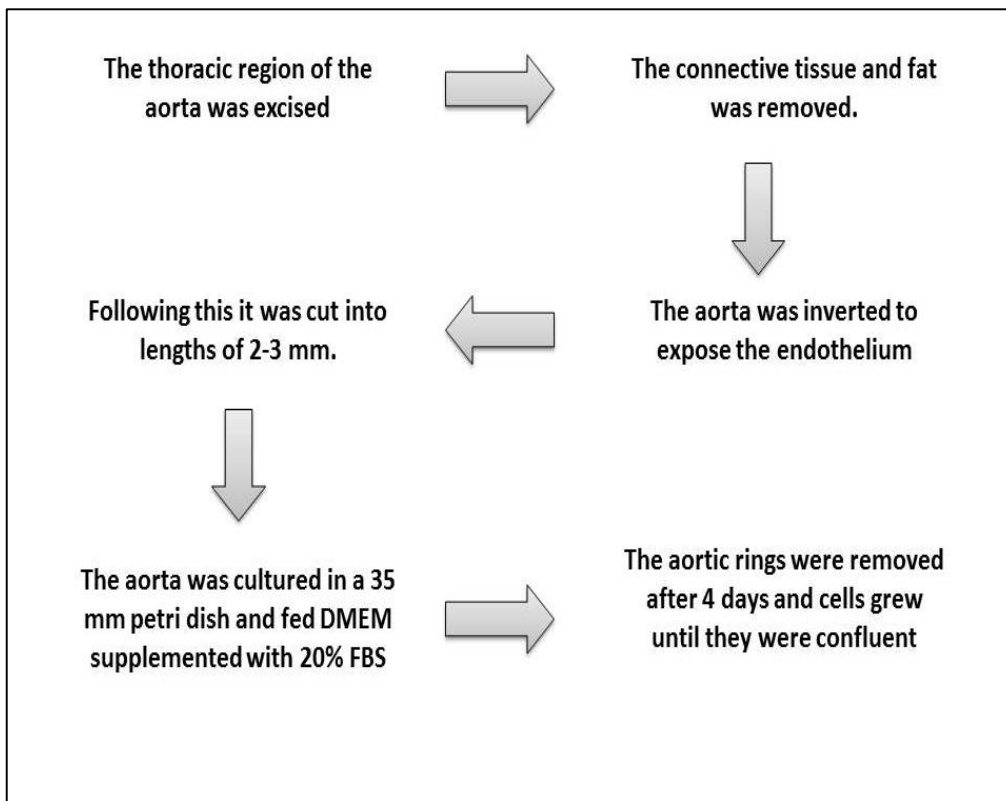


Figure 3.1: Diagram of the protocol used in the vascular ring method.

### **3.1.2. Collagenase method (adapted from the article by Kobayashi et al., 2005)**

Three male Wistar rats were anaesthetized with sodium pentobarbital (160 mg/kg) and sacrificed by exsanguination when deep anaesthesia, as indicated by the lack of response on a foot pinch, was reached. The animals were sprayed with 70% ethanol to sterilize them before placing their bodies in the laminar flow chamber. The aortas were cut above the left renal artery to release the blood. Heparin Sodium – Fresenius (5000 i.u./ml, Bodene (PTY) Limited trading as Intramed, PE, South Africa) was diluted in PBS (137 mM NaCl, 2.68 mM KCl, 8.33 mM Na<sub>2</sub>HPO<sub>4</sub> and 1.47 mM KH<sub>2</sub>PO<sub>4</sub>) to obtain a final concentration of 1000 i.u./ml. The Heparin PBS mixture was injected into the left ventricle of the heart to rinse the aorta. The portion of the aorta extending from the aortic arch to the renal artery was removed and placed in DMEM solution (DMEM + 1% penicillin-streptomycin + 20% FBS). The aorta was washed with 0.2 ml Heparin-PBS followed by a second wash step with 0.2 ml serum free DMEM. The abdominal region of the aorta was trimmed off, along with the aortic arch. The aorta was then bound to a 26 gauge needle and its distal end tied closed with a silk thread. The lumen was filled with a 0.3 g/ml collagenase solution (Worthington Type 2, Biochemical Corporation, NJ, USA) and incubated under standard conditions as described for the vascular ring method, for 45 minutes (figure 3.2). Thereafter the lumen was washed with 5 ml DMEM solution (DMEM + 1% penicillin-streptomycin + 20% FBS) and the effluent captured in a 15 ml conical tube. Following this, the contents of the tubes were centrifuged at 1200 rpm, 4°C for 5 minutes. The supernatant was aspirated and the pellet re-suspended in 2 ml DMEM solution (DMEM + 1% Pen-Strep + 20% FBS) and plated in a 35 mm petri dish previously coated with attachment factor for 1 hour. The cells were incubated under standard conditions. After 2 hours the media was removed and the cells were given EGM-2MV growth medium supplemented with 20% FBS. The cells received fresh growth medium 24 hours after the

initial isolation and allowed to grow freely. At day six post-AEC isolation, the AECs were detached with trypsin (2.5% Trypsin-EDTA diluted 10x in sterile PBS; Invitrogen, CA, USA) and re-seeded on a single 35 mm petri dish and once again allowed to grow until confluency. Once the cells reached confluency they were trypsinized and passaged in a 1:2 ratio, to the next generation. All cells were used at generation four to six for experimental purposes.

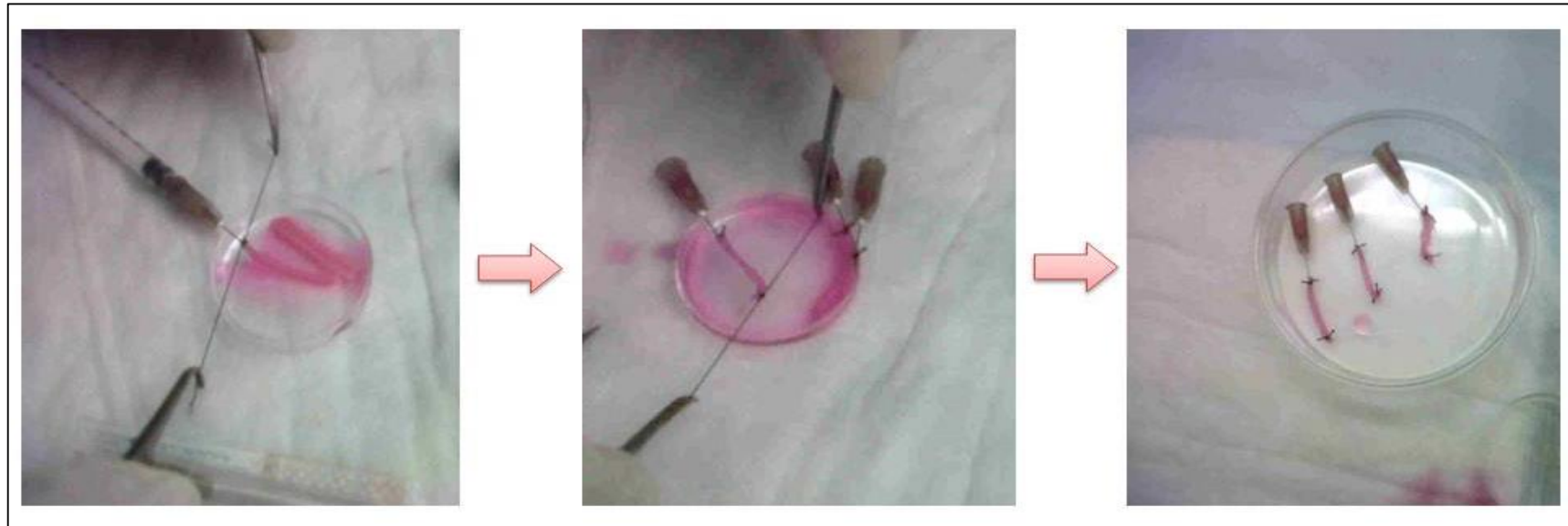


Figure 3.2: Isolated male Wistar rat thoracic aortas being bound to a 26-gauge needle (A) and its distal end ligated closed using a silk thread (B). (C) Thoracic aortas containing collagenase solution in the lumen prior to incubation at standard condition for 45 minutes.

### **3.1.3. Validation of endothelial cell purity: Acetylated low density lipoprotein (Ac-LDL)**

1,1'-dioctadecyl-3,3',3'-tetramethylindo-carbocyanine perchlorate (Dil) is a fluorescent probe attached to LDL after it has been acetylated. Dil-Ac-LDL (Biomedical Technology Inc., MA, USA) is an endothelial-specific marker used to stain endothelial cells in order to measure the purity of the culture.

Dil-Ac-LDL (50 µl) was added to 950 µl AEC media for a final concentration of 10 µg/ml according to the suppliers' instructions. The cells were washed twice with 2 ml sterile phosphate buffer saline (PBS) and incubated in 1 ml Dil-Ac-LDL/ EGM-2MV growth medium for 4 hours under standard conditions. After 4 hours, the cells were trypsinized and centrifuged at 1000 rpm, 4°C for 3 minutes. The supernatant was aspirated and the pellet re-suspended in 750 µl PBS. Positive staining of the cells with Dil-Ac-LDL was observed by fluorescence microscopy or flow cytometric analysis (FACS Calibur- Becton Dickinson; BD Biosciences, CA, USA). Data were expressed as the % cells that stained positively with the probe compared to unstained control cells.

## **3.2. Western blots**

### **i. Lysis buffer**

20.0 mM Tris-HCl (pH 7.5), 1.0 mM EGTA, 1.0 mM EDTA, 150 mM NaCl, 1.0 mM β-glycerophosphate, 2.5 mM sodium pyrophosphate, 0.1% sodium dodecyl sulfate (SDS), 1.0 mM sodium orthovanadate (Na<sub>3</sub>VO<sub>4</sub>), 1.0% Triton X-100, 10 µg/ml Leupeptin, 10 µg/ml Aprotinin, 50 nM sodium fluoride (NaF) and 50 µg/ml Phenylmethanesulfonyl Fluoride (PMSF).



ii. The growth medium was aspirated and AECs were washed twice with sterile PBS. The AECs were trypsinized with 0.25% trypsin as described earlier. The AECs from five 35 mm petri dishes were pooled into one 15 ml conical tube with 2 ml AEC media (AEC media supplemented with FBS) to prevent any further trypsin enzyme activity. The cells were centrifuged at 1000 rpm, 4°C for 3 minutes. The supernatant was aspirated and the pellet re-suspended in EGM-2MV growth medium. The re-suspended AECs were transferred to a 1.5 ml Eppendorf tube and subjected to further centrifugation at 1000 rpm, 4°C for 3 minutes. The supernatant was once again aspirated and zirconium oxide beads (0.5 mm diameter) were added to the pellet in a 1:1 ratio. Additionally, 800 µl of lysis buffer was added to the mixture. The sample was homogenized at 4°C using a bullet blender™ (Next Advance) for three cycles of 1 minute with a 5 minute rest period in between. Thereafter the samples were incubated on ice for 20 minutes. Following this, the samples were centrifuged at 14 000 rpm for 20 minutes at 4°C. The supernatant was transferred to another marked Eppendorf tube and stored on ice until further use, while the pellet was discarded. The amount of protein available in each sample was determined according to the method of Bradford (M. Bradford, 1976). Bovine serum albumin (BSA; Roche, Mannheim, Germany) was used to generate a standard curve of known concentrations. All samples were diluted 10-fold with distilled water in order to dilute the detergents in the lysis buffer as they will interfere with the Bradford method. Aliquots of the diluted sample were made up to 100ul with distilled water and assayed in duplicate to verify results. Double filtered Bradford reagent (900 µl) was added to both the standard curve and the protein samples, vortexed and incubated at room temperature for 15 minutes. The absorbance values were read at 595 nm. Once the protein concentrations of the samples have been obtained, protein lysates were brought to the same amount of protein per volume unit by addition of lysis buffer and Laemmli

sample buffer. The lysates were boiled for 5 min and stored away at -80°C until further use.

- iii. Protein lysates were loaded into a 4% stacking gel and separated on various percentage SDS-PAGE gels (Table 3.1). The SDS-PAGE gels were electrophoresed for 10 minutes at 100 V and 200 mA, followed by a second round of electrophoresis for 50 minutes at 200 V and 200 mA. The running buffer consisted of 25 mM Tris-Base, 192 mM Glycine and 0.1% SDS. All protein lysates were prepared as described above. Proteins involved in the insulin signalling pathway mediating glucose uptake were probed for (Table 3.2).

Table 3.1: The table below consist of a list of different SDS-PAGE gels used and their respective compositions.

Reagent	Stock	7.5%	10%	12%	4% (stack gel)
dH <sub>2</sub> O	Distilled	5.525 ml	4.9 ml	3.35 ml	3.05 ml
Tris (pH 8.8)	1.5 M	2.5 ml	2.5 ml	2.5 ml	
Tris (pH 6.8)	0.5 M				1.25 ml
SDS	10%	100 µl	100 µl	100 µl	50 µl
Acrylamide	40%	1.875 ml	2.5 ml	3.0 ml	0.5 ml
APS	10%	50 µl	50 µl	50 µl	50 µl
TEMED	99%	20 µl	20 µl	20 µl	10 µl

**iv. List of antibodies and their suppliers:**

*Cell Signaling* (MA, USA): Antibodies used in this research thesis: eNOS, phospho-eNOS (Ser1177), PKB/Akt, phospho-PKB/Akt (Ser473), ATM, phospho-ATM (Ser1981), AMPK, phospho-AMPK (Ser172), PI3-K/P85, phospho-PI3-K/P85 (Y458/p55), PTEN, phospho-PTEN (S380/T382), AS160, phospho-AS160 (Ser588), GSK3 $\beta$  and phospho-GSK3 $\beta$  (Ser9).

Table 3.2: Proteins probed in this research project are listed below along with their molecular weights (kDa) and optimization conditions

Protein	Phospho Site	MW	Gel %	1° Ab dilution	2° Ab dilution
eNOS	Ser1177	140	7.5	1:1000 TBS-Tween	1:4000 TBS-Tween
PKB	Ser473	60	10	1:1000 TBS-Tween	1:4000 TBS-Tween
ATM	Ser1981	350	4-15% gradient gel	1:1000 in signal boost	1:4000 in signal boost
AMPK	Ser172	62	10	1:1000 in 2.5% TBS-Tween milk	1:4000 in 2.5% TBS- Tween milk
P85- PI3-K	Y458/p55	85	10	1:1000 TBS-Tween	1:4000 TBS-Tween
PTEN	S380/T382	54	10	1:1000 TBS-Tween	1:4000 TBS-Tween
AS160	Ser588	160	7.5	1:1000 TBS-Tween	1:4000 TBS-Tween
GSK3 $\beta$	Ser9	46	12	1:1000 TBS-Tween	1:4000 TBS-Tween

- v. All proteins besides ATM were transferred to Immobilon™ PVDF membranes for 60 minutes at 200 V and 200 mA using a transfer buffer containing 25.0 mM Tris-Base, 192 mM Glycine and 20% (v/v) methanol.
- vi. The ATM protein was transferred to Immobilon™ PVDF membranes for 90 minutes at 200 V and 200 mA using transfer buffer containing 25.0 mM Tris-Base, 192 mM Glycine and 10% (v/v) methanol.

The longer transfer time and less methanol used in the transfer buffer were used to ensure the capture of larger proteins like ATM which is 350 kDa.

- vii. After transfer, the membranes were washed in methanol and left to air-dry to assist binding of protein to the membranes. The dry membranes were stained with Ponceau-Red reversible stain to monitor adequate transfer of proteins and verify equal loading.
- viii. After removing the Ponceau-Red stain, the membranes were washed thoroughly three times with TBS-Tween (Tris-buffered saline containing 0.1% Tween-20) and blocked in TBS-Tween containing 5% fat free milk powder for 90 minutes. Thereafter the membrane was once again washed thoroughly with TBS-tween and incubated at 4°C in the respective primary antibodies overnight.
- ix. After the overnight incubation, the membranes were washed three times with TBS-Tween, followed by 60 minute incubation at room temperature in the appropriate secondary antibody linked to horse-radish peroxidase (HRP), (Cell Signaling, MA, USA).
- x. After exposure to the HRP-linked secondary antibody, the membranes were washed three times with TBS-Tween and treated to Clarity Western ECL (Bio-Rad, CA, USA) prior to exposure to Amersham Hyperfilm to capture the chemiluminescent light emission.
- xi. Membranes were prepared as mentioned in (ix) above using the ChemiDoc™. (Bio-Rad, CA, USA). The ChemiDoc is sensitive to the proteins being exposed as it allows

one to either pick up intense bands (protein bands which are quite prominent and are exposed within seconds) without over exposing the membrane and obtains a more crisp image and it can pick up faint bands easily (bands which are difficult to pick up using the Amersham Hyperfilm or bands that will take longer to expose, often the case with phosphorylated proteins).

- xii. The film was subjected to laser-scanning and densitometry using suitable software (UN-SCAN-IT, Silkscience, USA) to analyze the intensity of the bands in pixels.

### **3.3. Commercial Aortic endothelial cells (AECs)**

Adult rat AECs were commercially purchased from VEC technologies (NY, USA) and delivered in 75 ml tissue culture flasks coated with fibronectin. The AECs were cultured in endothelial cell basal medium-2 (EGM-2MV) until confluent, later supplemented with 10% FBS. Once confluent the cells were trypsinized and centrifuged at 1000 rpm, 4°C for 3 minutes. The supernatant was aspirated and the pellets were collected and stored away for future use. The cell pellets were stored in a cryo-vial containing a solution made up of 90% FBS, 5% AEC media and 5% DMSO (Figure 3.3). The cell suspension was stored in liquid nitrogen until needed. The commercially purchased AECs were subjected to staining with Dil-Ac-LDL to measure the purity of the cells in culture. AECs were considered a pure culture when more than 80% of the total cell population stained positively with Dil-Ac-LDL.

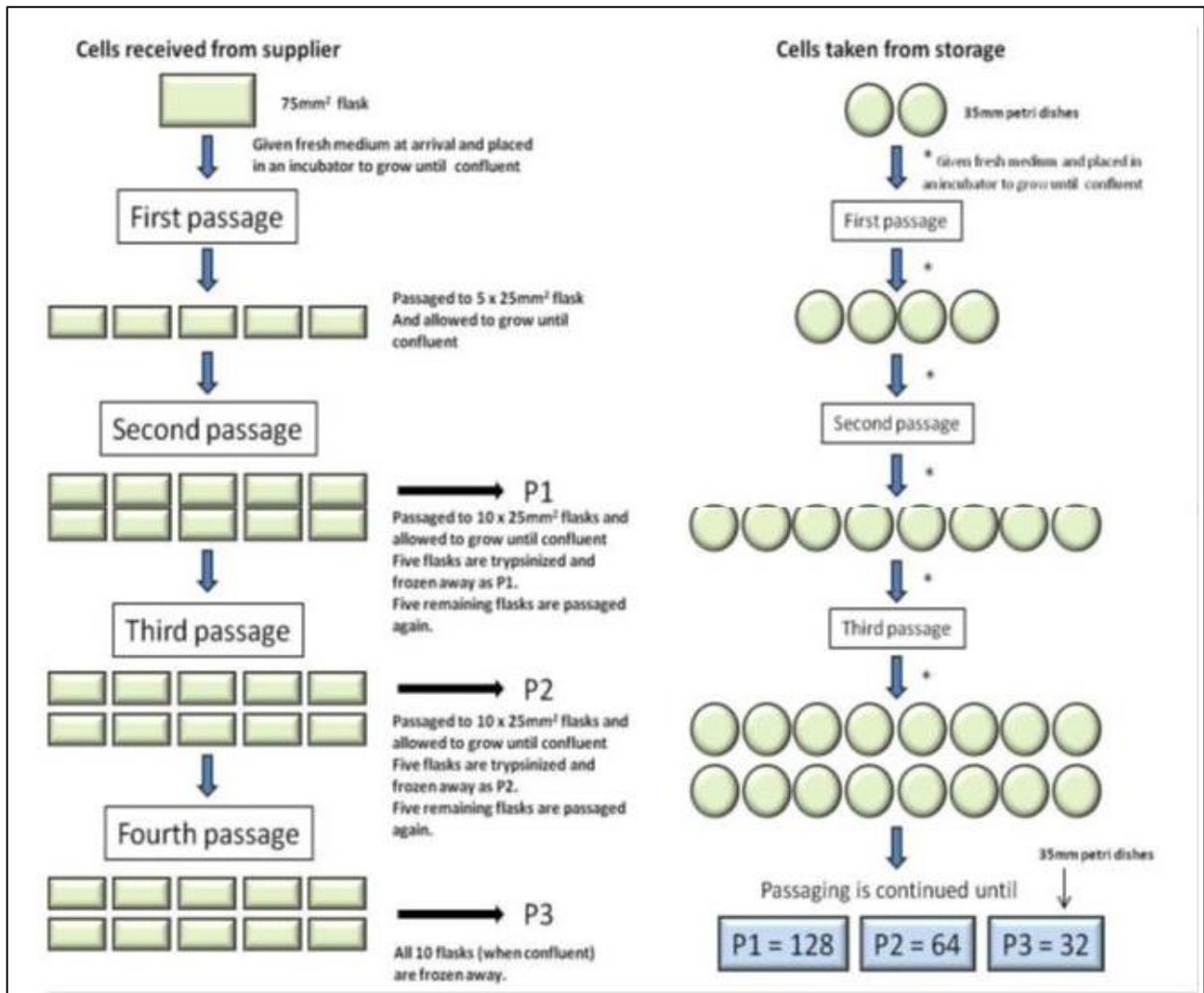


Figure 3.3: Diagram depicting the procedure used to passage and label the cells [Genis, A., 2014].



### **3.4. AEC treatment groups:**

#### **3.4.1. Insulin dose response curve:**

The AECs were washed twice with sterile PBS. Afterwards the AECs were serum starved by incubating them for 15 min at physiological conditions with sterile PBS. The PBS was aspirated and the cells were washed once with fresh PBS. The AECs were separated into three treatment groups which included a control, baseline group (treated with PBS), a 10 nM and a 100 nM insulin (Sigma-Aldrich, MO, USA) group. The insulin was prepared by dissolving the Zinc (anhydrous) insulin powder in 10mM HEPES buffer pH 7.4 to a final concentration of 10  $\mu$ M before further diluting it to 10 nM and 100 nM concentrations. The cells were treated for 15 min under standard incubation conditions. After the treatment period, the AECs were washed once with PBS and lysates were prepared for western blot analyses as described earlier. The cells from approximately 20 randomly chosen 35mm petri dishes were pooled for each experimental group. Protein lysates were prepared from 10 petri dishes, which yielded two sets of protein lysates per group.

#### **3.4.2. Stimulation and inhibition of the phosphatidylinositol-3 kinase (PI3-K) signalling pathway with emphasis on the ATM protein**

AECs were washed twice with PBS followed by a 15 min incubation in fresh PBS at physiological conditions to serum starve these cells. Afterwards the cells were washed once with PBS and separated into seven different treatment groups. These groups included a control, baseline group (PBS), 10 nM insulin, vehicle (DMSO), 3  $\mu$ M KU-60019 (Selleckchem; Texas, USA), 3  $\mu$ M KU-60019 with 10 nM insulin, 100 nM wortmannin, 100 nM wormannin with 10 nM insulin. All solutions were made up in sterile PBS. DMSO was used as the vehicle control because it was used to dissolve the ATM inhibitor KU-

60019 as well as wortmannin, the PI3-K inhibitor. AECs assigned to the control, KU-60019, DMSO and wortmannin groups were treated for 30 min, whereas the AECs assigned to the insulin treatment group were first incubated for 15 min in fresh PBS before the addition of insulin. Both the KU-60019 with insulin and the wortmannin with insulin groups were exposed to the respective inhibitors for 15 min before the addition of 10 nM insulin for a further 15 min. Following this, the cells were either used to measure the NO production, determine the cell viability after treatment or to make protein lysates.

### **3.4.3. 4,5-diaminofluorescein-2/diacetate (DAF-2/DA)**

DAF-2/DA (Calbiochem, EMD Millipore Corporation, CA, USA) was used to determine NO production by the cells. DAF-2/DA is a cell permeable, NO-specific fluorescent probe that is hydrolyzed by cytosolic esterases when it enters through the cell membrane [Strijdom et al., 2006]. Once in the cell, the probe traps NO in the presence of oxygen and emits a fluorescent signal at 515 nm [López-Figueroa et al., 2001].

In DAF-2/DA experiments approximately three AEC petri dishes (35 mm) were assigned to each treatment group. Once the cells have been treated, DAF-2/DA (2µl/ml PBS) was added to the AECs and incubated for two hours under standard conditions. Thereafter the cells were trypsinized and transferred to a 15 ml conical tube containing 1 ml cell staining buffer. The cells were centrifuged at 1000 rpm for 3 min at 4°C. The supernatant was aspirated and the pellet dissolved in 750 µl PBS before being transferred to a flow cytometry tube (BD Falcon, 5 ml polystyrene round bottom tube; BD Biosciences, MA, USA). NO production was measured using the FACS Calibur-BD (BD Biosciences, CA, USA) in the FL1-H channel. An absolute control (untreated and unstained) was added to each experiment. It consisted of a single 35 mm petri dish with a confluent AEC culture,

which had been treated with PBS for 30 min after the serum starvation step, but with the omission of DAF-2/DA. Additionally, a positive control was added to each DAF-2/DA experiment. In the positive control protocol, AECs were treated with DAF-2/DA for one hour, after which diethylamine nonoate (DEA/NO; Sigma-Aldrich, Schnellendorf, Germany), the NO donor, was added to the AECs and incubated for two hours. In summary, the AECs were incubated for three hours at standard conditions.

#### **3.4.4. Propidium iodide**

Propidium iodide (PI; Sigma-Aldrich, Schnellendorf, Germany) was used to determine the viability of the cells. PI cannot enter intact, healthy viable cells as it is a membrane impermeable probe. If a cell dies due to necrosis, it is expected that PI would be able to penetrate the injured cell membrane, move to the nucleus where it binds to nucleic acids, which produces the fluorescent signal observed in a population of non-viable cells [Nicoletti et al., 1991 and Al-Rubeai et al., 1997]. If a cell population is healthy there would be very low or no fluorescent signal.

After treatment the AECs were trypsinized and transferred to a 15 ml conical tube containing 1 ml cell staining buffer. The cells were centrifuged at 1000 rpm for 3 min at 4°C. Thereafter the supernatant was aspirated and the pellet re-suspended in 990 µl PBS and transferred to a flow cytometry tube. Propidium iodide aliquots were prepared in PBS to obtain a stock concentration of 500 µM. Thereafter, 10 µl of the stock solution was added to the FACS tube containing the AECs to obtain a final concentration of 5 µM. The AECs were then incubated for 15 min under standard conditions. Cell viability was measured using the FL2-H channel on the FACS Calibur-BD. The viability of the cells was measured by the increase in fluorescence intensity emitted by necrotic cells.

### **3.4.5. Statistical analysis:**

All data were analyzed with GraphPad Prism™ version 5.0. Data are presented as mean  $\pm$  standard error of the mean (SEM). A One-Way ANOVA with a Bonferroni post-test was used to analyze more than two groups. A Student's t-test was used to compare two sets of data. A probability (p) value being less than 0.05 ( $p < 0.05$ ) was considered significant.

## Chapter 4: Isolation of aortic endothelial cells

For the purpose of this research, one of the aims was to isolate and harvest a primary culture of vascular aortic endothelial cells (AECs). The purpose of this aim was to determine if it was possible to isolate and harvest primary AECs in our laboratory and use them for experimental research. Based on the success of the AEC isolation technique, the next aim would then be to isolate AECs from the thoracic region of the aorta in animals fed a high-fat diet to induce an insulin resistant model.

Before isolating the AECs, extensive research was completed on the different isolation procedures published over the past 20-30 years. This has created a pool of different isolation techniques for new researchers. An extensive review of the literature has revealed three major endothelial cell isolation techniques, or variations thereof. The first technique uses collagenase to digest the matrix that keeps the endothelial cells attached to the SMCs [Smith, 1989; Gordon et al, 1991; Marin et al, 2001; Chen, S., et al, 2004; Kobayashi, M. et al, 2005; Hu et al. 2009]. The second technique also uses collagenase, but is coupled with scraping of the endothelial cells away from the SMCs [Zhang, X., et al, 2007]. The third technique consists of cutting the vascular arteries into rings and allowing the endothelial cells to move off the explant and onto the bottom of the petri dish previously treated with an extracellular matrix attachment substance [Nicosia et al, 1994; Kreisel et al, 2001; Magid et al, 2003; Chao et al, 2003; Hu et al. 2009]. This technique is aimed at separating the endothelium from the rest of the vascular wall; if successful, the attached cells remain behind when the vessel is removed from the petri dish after a certain period of time.

One of the biggest challenges in isolating cells for primary cultures is the risk of contamination by other cell types located in the same organ or tissue. When isolating ECs from blood vessels, the main contaminating culprits are SMCs and fibroblasts. Therefore, researchers have been focussing on the design of techniques aimed at maintaining a pure EC culture as far as possible. Magid et al, used fluorescence-activated cell sorting (FACS) by flow cytometry to separate endothelial cells from non-endothelial cells followed by re-culturing while Hu et al, used serial dilution to purify the endothelial cell culture. According to their protocol the cells were diluted to 5 cells/ml after they were isolated and cultured in a 96-well plate [Magid et al, 2003; Hu et al. 2009]. For the most part researchers have been using acetylated low density lipoprotein (Ac-LDL) coupled to a fluorescent probe 1,1'-dioctadecyl-1,3,3,3',3'-tetramethyl-indocarbocyanine (Dil; Dil-Ac-LDL) to identify their cells as being endothelial cells [Chen, S., et al, 2004; Nicosia et al, 1994; Gordon et al, 1991; Magid et al, 2003, Kreisel et al., 2001] as well as using specific fluorescent antibodies to detect endothelial specific markers, namely: VCAM-1 and ICAM-1 [Marin et al, 2001], von Willebrand factor/Factor VIII [Chen, X., et al, 2013; Smith, 1989; Nicosia et al, 1994; Gordon et al, 1991, Magid et al, 2003], angiotensin converting enzyme (ACE), CD31 [Chen, S., et al, 2004] and CD43 [Chen, X., 2013]. Upon the satisfaction of the purity of an endothelial cell culture after rigorous methods to prove there are no contaminants present, the endothelial cells are often used between passages three and six for experimental purposes.

In this research study, two methods were identified and tested to isolate thoracic AEC. The first being the vascular ring method followed by the collagenase method. In this protocol, all buffers and equipment were autoclaved to ensure sterility; the lamina flow chamber was exposed to 5 min ultraviolet light before all surfaces were wiped down with 70% ethanol. The bottom surface of the lamina flow chamber was covered in linen savers to capture any excess blood. Male Wistar rats were anaesthetized with 160 mg/kg sodium

pentobarbital. The rats were sprayed with 70% ethanol to sterilize them before placing them in the lamina flow chamber. Once the rats failed to respond to a foot pinch, they were sacrificed by exsanguination. The aorta was removed by cutting the aorta out between the third aortic arch to above the left kidney. The distal and the proximal ends of the aorta were trimmed off to remove the jagged edges. The aorta was cleaned of all perivascular adipose tissue (PVAT).

#### **4.1. The vascular ring method**

After the removal of PVAT the aorta was inverted using a suture and forceps. Thereafter the aorta was cut into rings and placed in a 35 mm petri dish previously coated with attachment factor and containing 2 ml Dulbecco's Modified Eagle Medium (DMEM) supplemented with 1% penicillin-streptomycin (Pen-Strep) and 20% fetal bovine serum (FBS). The aortic rings remained in culture for 4 days receiving fresh DMEM media containing all supplements every 2 days. This was to ensure the cells would detach from the aortic rings and onto the attachment factor where they would migrate and grow. On the sixth day after the initial isolation the cells in culture were detached with 0.25% trypsin-EDTA and re-seeded until the cells became confluent. Thereafter the cells were stained with Dil-Ac-LDL for assessment of endothelial purity. Cardiac microvascular cells were used as a known endothelial cell control for positive staining by Dil-Ac-LDL. Cells were treated with 10 µg/ml Dil-Ac-LDL diluted in DMEM and incubated for 4 hours at standard conditions (37°C, 5% CO<sub>2</sub>, 40-60% humidified). The excess Dil-Ac-LDL probe was washed away with phosphate buffer saline (PBS), the cells were trypsinized with 0.25% trypsin-EDTA and centrifuged to collect the pellets. Each pellet was resuspended in 750 µl PBS and transferred to a FACS tube. The fluorescence intensity was used to measure the percentage the total cell population which stained positive with the probe Dil-Ac-LDL. The

fluorescence emitted by the cells was measured using the FACS Calibur-BD. The size (forward scatter) and granularity (side scatter) of the cells in culture were measured for 10000 events (refers to the cell population measured; figure 4.1).

In this experiment there were three sample groups namely (i) the unstained control group: commercially purchased endothelial cells that were not treated with Dil-Ac-LDL; (ii) positive control group: commercially purchased endothelial cells stained with Dil-Ac-LDL; and (iii) the cells isolated from the aortas (experimental group); these cells were treated with Dil-Ac-LDL under the same conditions as the positive control group.

The fluorescence intensity of each culture was measured with the FACS Calibur-BD, and analyzed with the WinMD software (Purdue University Cytometry Laboratories; IN, USA). The mean fluorescence intensity measurements of the commercially purchased endothelial cells are shown in figure 4.1. The area with the highest density (figure 4.1 A) on the scatterplot was gated to analyze the cell population in this area exclusively. On the histogram (figure 4.1 B), the unstained control cells emitted low fluorescence intensity, which is an indication of autofluorescence of the cells. When the cells were treated with Dil-Ac-LDL (positive control cells), the mean fluorescence intensity showed a significant right shift (figure 4.1 C), indicating a high degree of endothelial cell purity. 93 % of the cells in the positive control sample stained Dil-Ac-LDL, indicating that the vast majority of the cells in these samples were pure endothelial cells (figure 4.1 C).

For the experimental groups (i.e. cells harvested from the aortas), it was observed that the cell population expressed using the scatterplot showed a greater degree of cell granularity (as indicated by the upward shift of the cell population; figure 4.2 B) compared to the commercially purchased endothelial cells (figure 4.2 A). Additionally, not all of the cells in the experimental samples were contained within the gated region. It was also observed that although there was a slight shift in the mean fluorescence to the right compared to the



unstained control only 0.8% of the cells in the experimental control were positively stained with Dil-Ac-LDL in comparison to the positive control (figure 4.3). The data present are indicative of four to six different experiments (n = 4 - 6).

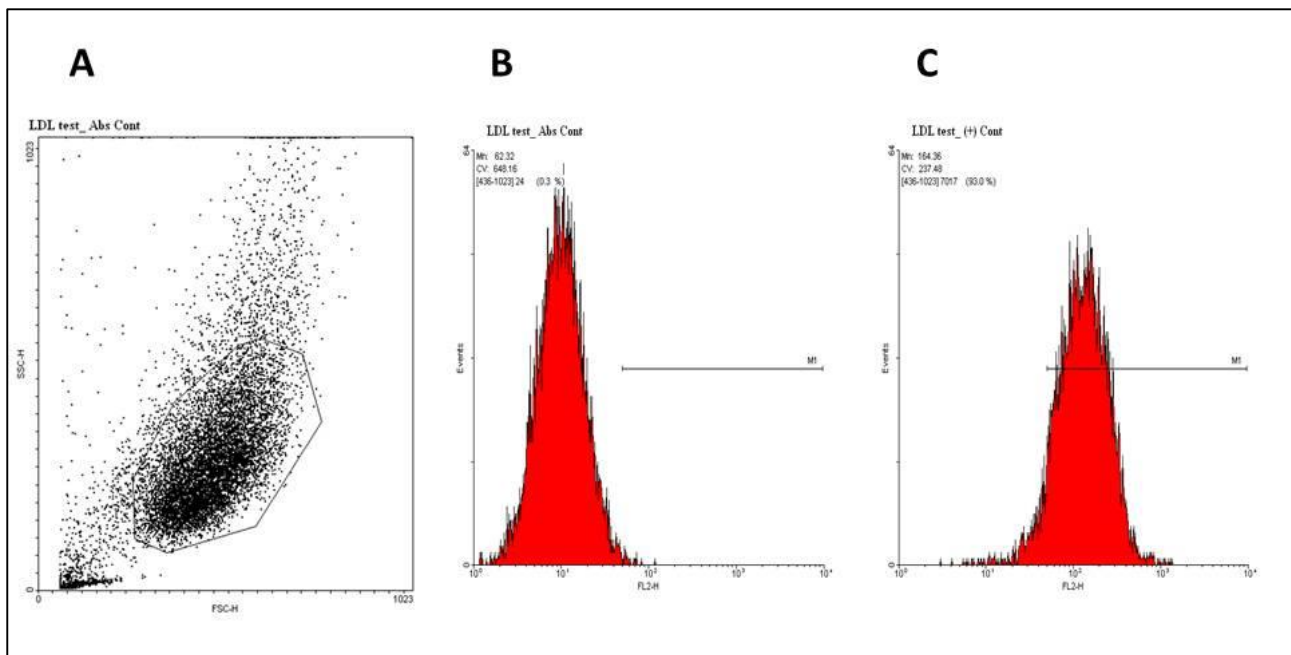


Figure 4.1: Validation of the endothelial cell purity of commercially purchased AECs with flow cytometric analysis of fluorescence intensity after staining with the endothelial-specific marker, Dil-Ac-LDL. (A) Representative scatterplot of the cells with forward scatter (cell size) and side scatter (cell granularity) on the x-axis and y-axis respectively. The round circle indicates the gated population of the sample which was analysed. (B) Mean fluorescence intensity of an unstained control sample showing the autofluorescence of the cells. The horizontal line (M1) is inserted at the point of maximum fluorescence of the unstained control sample. (C) Mean fluorescence intensity of a sample treated with Dil-Ac-LDL showing a clear right shift in the mean fluorescence intensity and the % cells that stained positively with the probe, as determined by M1, was 93% compared to the unstained control.

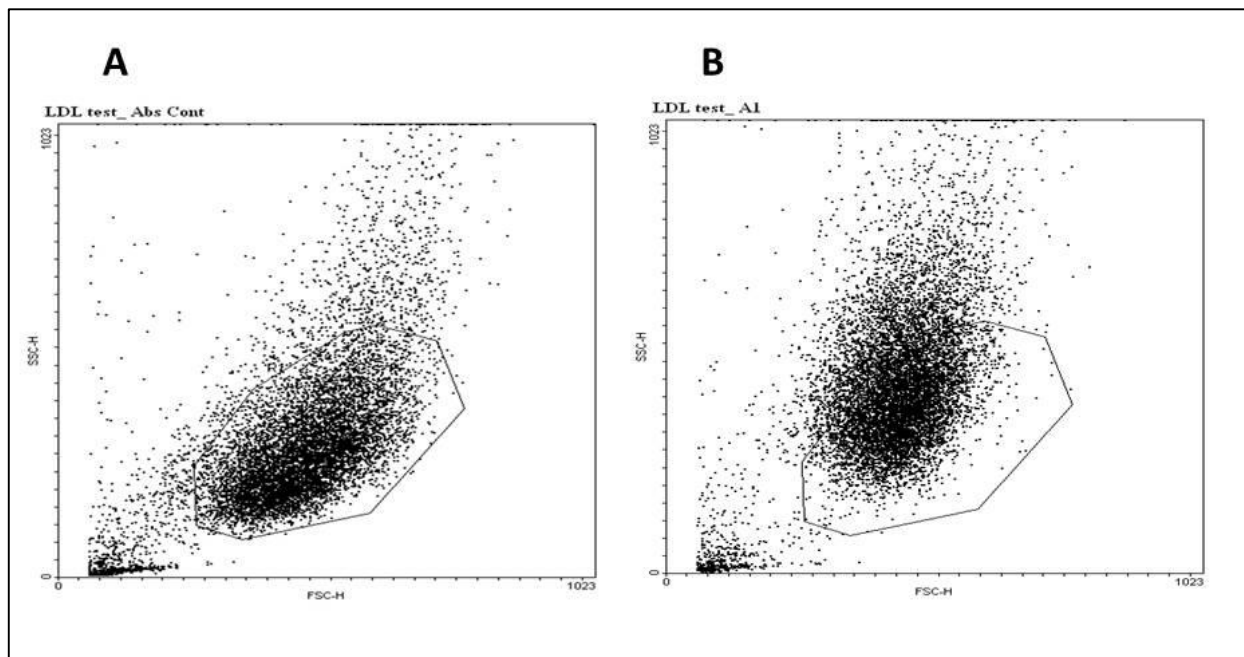


Figure 4.2: (A) Representative scatterplot of the commercial endothelial cells with forward scatter (cell size) and side scatter (cell granularity) on the x-axis and y-axis respectively. The round circle indicates the gated population of the sample which was analysed. (B) Representative scatterplot of the experimental cells with forward scatter (cell size) and side scatter (cell granularity) on the x-axis and y-axis respectively.

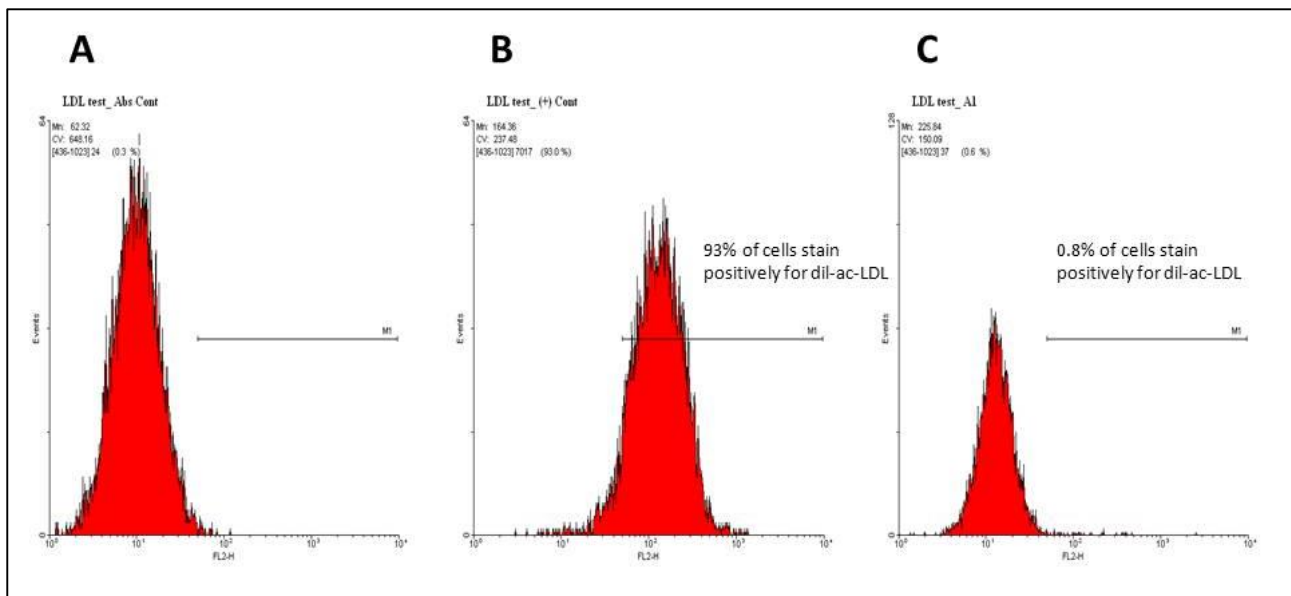


Figure 4.3: Validation of the endothelial cell purity by comparing the endothelial cells isolated from rat thoracic aorta with commercially purchased AECs with flow cytometric analysis of fluorescence intensity after staining with the endothelial-specific marker, Dil-Ac-LDL. (A) Representative histogram of the unstained commercially purchased AECs with a mean fluorescence between  $10^0$  and  $10^1$ . (B) Mean fluorescence of the commercially purchased AECs stained positively with Dil-Ac-LDL compared to the unstained population. The horizontal line (M1) was inserted at the point of maximum fluorescence of the unstained control sample. (C) Mean fluorescence of the experimental cell population stained with Dil-Ac-LDL. The mean fluorescence was between both the unstained control and the positive control, 0.8% of the gated experimental cell population were stained positively with Dil-Ac-LDL as determined by M1.

## 4.2. Collagenase method

After the PVAT was removed the lumen of the aorta was rinsed with 1000 I.U/ml Heparin diluted in PBS. Thereafter the thoracic region of the rat aorta was ligated to a 26-gauge needle at the proximal end and ligated closed at the distal end. The lumen was filled with 3 mg/ml collagenase type 2 dissolved in serum free DMEM. The rat aortas filled with collagenase-DMEM solution were incubated under standard conditions for 45 min. Following this, the distal end of the aorta was cut open above the thread used to ligate the lumen closed. The lumen was flushed with 5 ml DMEM solution to capture the endothelial cells that dissociated from the vascular wall due to the enzymatic action of the collagenase in a 15 ml conical tube. The cell suspension was centrifuged at 1200 rpm for 5 min at 4 °C. The cell pellet was collected and resuspended in 2 ml endothelial cell growth medium (EGM-2 MV) supplemented with 20% FBS. The cell suspension was plated in a 35 mm petri dish coated with attachment factor and incubated at standard conditions. Two hours after the cell culture was incubated, they received fresh media. The cell culture was incubated for six days, receiving fresh media every two days before it was trypsinized with 0.25% trypsin-EDTA and replated in a 35 mm petri dish until they reached confluency. Finally the cells were passaged every two days or when confluent.

The purity of the endothelial cells isolated using the collagenase method, were determined according to three different tests. The first test was based on cell morphology, (were the cells isolated in the laboratory mimic normal endothelial cell in size and shape). The second test was based on the positive staining of these cells with Dil-Ac-LDL. Thirdly, the expression of the enzyme eNOS was determined.

### 4.2.1. Cell morphology

After the cells were isolated from the lumen of the rat aorta they were often observed to gather together like a bunch of grapes and as time progressed and the cells properly attached to the attachment factor (a gelatine substance) on the surface of the petri dish and began to migrate and multiply (figure 4.4). Cells were allowed to grow and become confluent before they were passaged to the next generation.

### 4.2.2. Dil-Ac-LDL staining

Between the 3<sup>rd</sup> and 6<sup>th</sup> generations, the cells isolated were stained with Dil-Ac-LDL to determine the purity of the endothelial cell culture. After the cells were stained with Dil-Ac-LDL, they were either analysed with flow cytometry or by fluorescent microphotography to determine positive staining of the experimental cells. Figure 4.5 (A) represents the commercially purchased AECs which were used as both the unstained and the positive control. Most of the cells on the scatterplot (B) fell within the same region as the commercially purchased endothelial cells, although the experimental cells were observed to be slightly bigger and more granular than the commercial AECs. Once again, an unstained control was commercial cells that were not treated with Dil-Ac-LDL and autofluoresced between  $10^0$  and  $10^1$  on the log scale (figure 4.5.C). A horizontal line (M1) was placed on the histogram at the highest mean fluorescence of the unstained cell population. The commercial cells stained with Dil-Ac-LDL had a shift in mean fluorescence intensity to the right compared to the unstained control (Figure 4.5.D). The percentage of cells stained positive with Dil-Ac-LDL as determined by M1 was 97.8%. To test the purity of the experimental cells isolated using the collagenase method the experimental control was subjected to the same conditions as the positive control. In the representative example given in Figure 4.5.E, 84.8% of the cells of the experimental sample stained

positively with Dil-Ac-LDL. These results indicate high endothelial cell purity. The data presented in this section are representative of approximately 10 different AEC isolations.

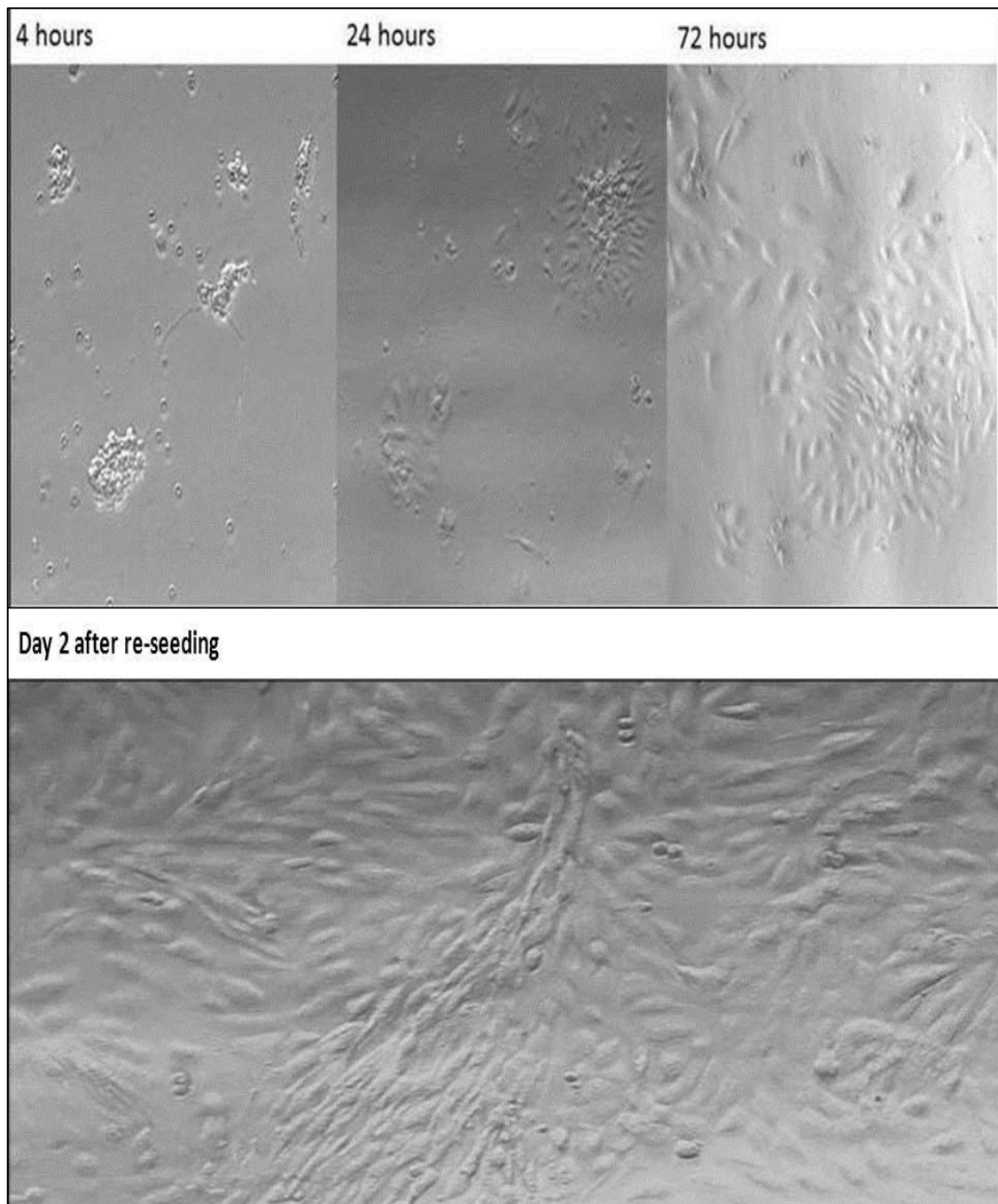


Figure 4.4: Cells isolated from the lumen of the thoracic region of male Wistar rats. Successful isolation of the experimental cells was determined based on the presence of cell colonies often clumped together like a bunch of grapes. Thereafter the viability and the growth of the cells were documented daily until the cell culture reached confluency. The morphology of the cells was often shaped like a cobblestone which is a characteristic of vascular endothelial cells.



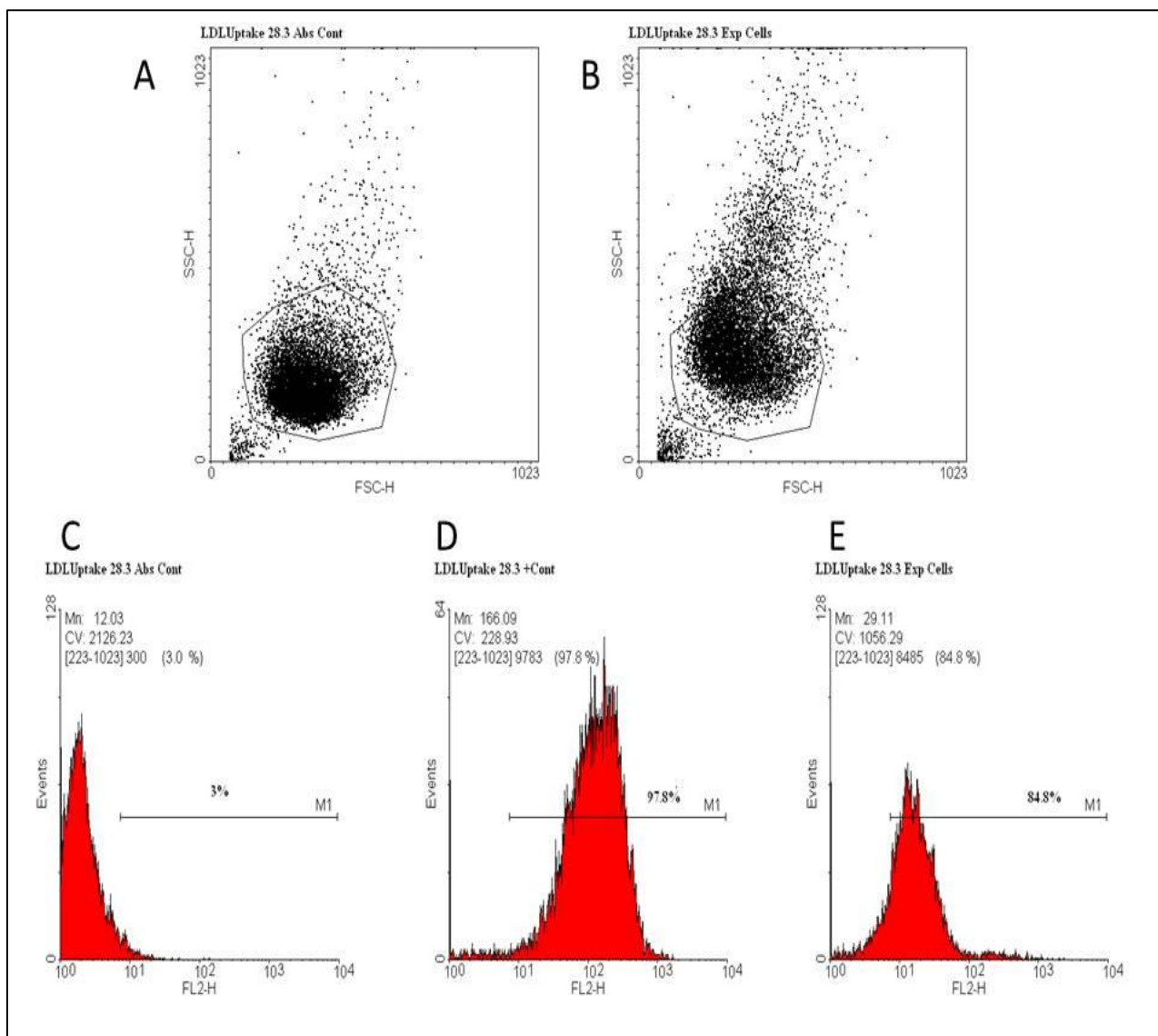


Figure 4.5: Validation of the endothelial cell purity of commercially purchased AECs and AECs isolated using the collagenase method with flow cytometric analysis of fluorescence intensity of the endothelial-specific marker, Dil-Ac-LDL. (A and B) Representative scatterplot of the cells with forward scatter (cell size) and side scatter (cell granularity) on the x-axis and y-axis respectively. The round circle indicates the gated population of the sample which was analysed. (C) Mean fluorescence intensity of an unstained control sample showing the autofluorescence of the cells. The horizontal line (M1) is inserted at the point of maximum fluorescence of the unstained control sample. (D) Mean fluorescence intensity of a sample treated with Dil-Ac-LDL showing a clear right shift in the mean fluorescence intensity and the % cells that stained positively with the probe, as

determined by M1, was 97.8% compared to the unstained control. (E) Mean fluorescence intensity of an experimental sample treated with Dil-Ac-LDL showing a shift to the right in the mean fluorescence intensity, 84.8% of the cells in the experimental sample stained positively with Dil-Ac-LDL.

#### 4.2.3. Cell cultures stained with Dil-Ac-LDL: Microphotographic analysis

Photographic images were taken of the experimental cells in culture. First images were taken of endothelial cells cultured in a 35 mm petri dish (figure 4.6). The cells were stained with Dil-Ac-LDL for 4 hours under standard conditions. Pictures were taken with a Nikon LDM camera (Nikon; Tokyo, Japan) in the Department of Biomedical Sciences, Stellenbosch University. The Dil-Ac-LDL staining was analysed with a red filter, and the magnification was set at 10x objective. In separate analyses, images were taken at the Central Analytical Facility (CAF), Stellenbosch University. Endothelial cells were grown in a Borosilicate coverglass system (Nunc, NY, USA). The “Carl Zeiss Confocal LSM 780 Elyra S1 with SR-SIM super resolution platform” microscope (Carl Zeiss, Jena, Germany) was used to photograph the cells stained positively with Dil-Ac-LDL. Images were taken at a magnification of 60 (figures 4.7, 4.8 and 4.9). Images were taken of the same sample area with and without the background. Figures 4.7 and 4.8 are of the experimental cells isolated using the collagenase method and the cells in figure 4.9 are commercially purchased AECs (the colour of the fluorescence was changed to differentiate between the two different cell types). In figure 4.7 the big bold patches of red is the Dil-Ac-LDL that was unable to stain cells and could not be washed away properly with PBS. The red fluorescence at a lower intensity in cells which have been successfully stained with the probe. In figure 4.8 cells were stained with Dil-Ac-LDL but it was also observed that there were other cell types contaminating the cell culture, as they did not fluoresce. Figure 4.9 are commercial AECs stained with Dil-Ac-LDL. The Dil-Ac-LDL is the ring structure in the centre of the cells surrounding the nucleus. As can be seen, all the cells present in this image are stained positively with the probe.

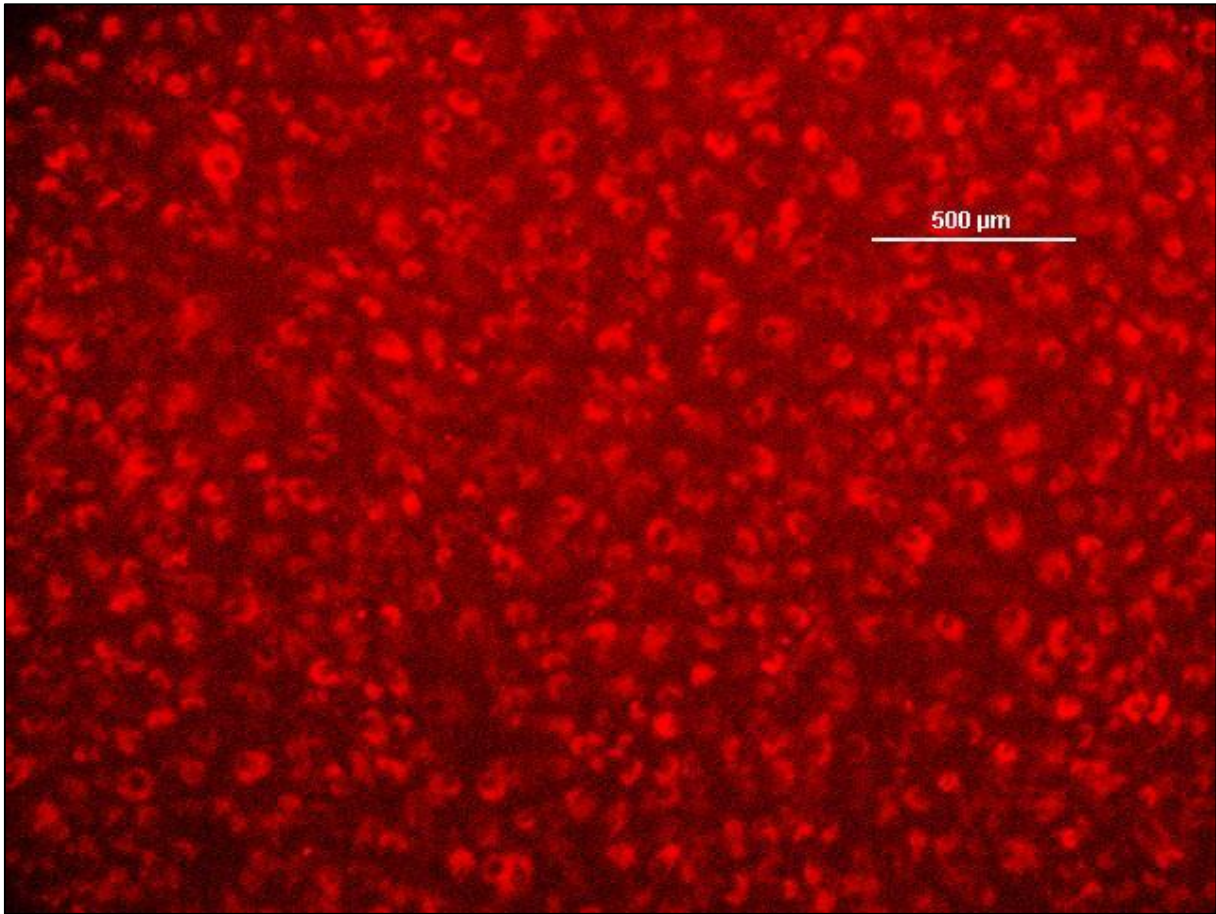


Figure 4.6: Isolated endothelial cells in culture after being stained with Dil-Ac-LDL. The image was taken using a Nikon LDM fluorescent camera.

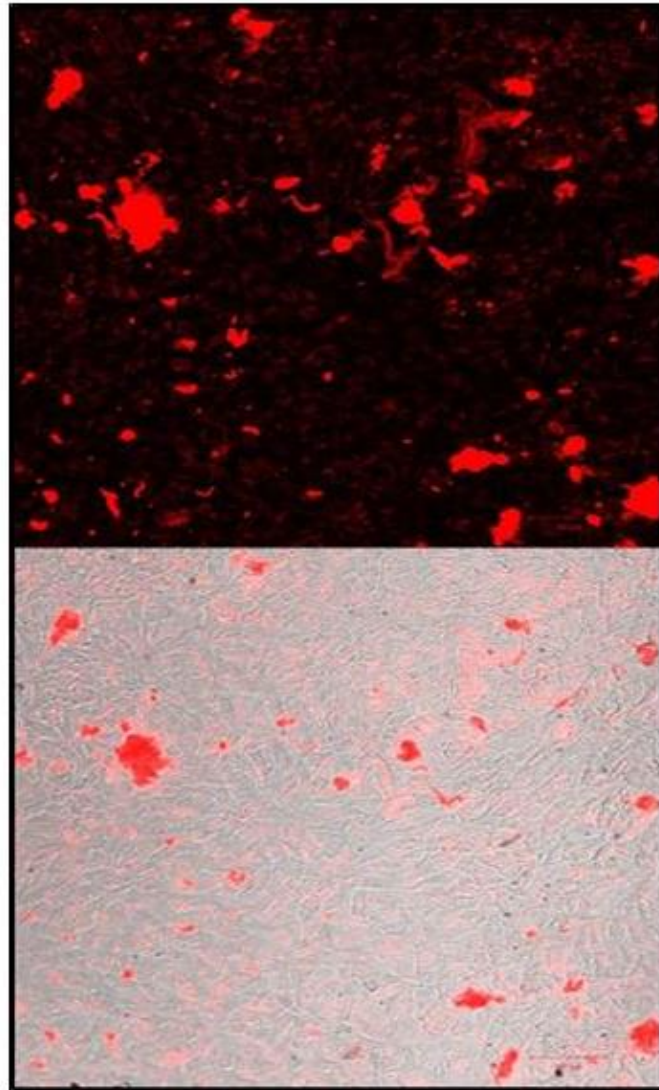


Figure 4.7: AECs (experimental control) were cultured in an eight chamber borosilicate coverglass system (Nunc, NY, USA) stained with Dil-Ac-LDL, the bar is 10  $\mu\text{m}$  and the magnification 60x. AECs were isolated using the collagenase method. Images were taken with a Carl Zeiss Confocal (LSM 780 Elyra S1 with SR-SIM super resolution platform) microscope (Carl Zeiss, Jena, Germany). The concentration of the probe used was 10  $\mu\text{g/ml}$  Dil-Ac-LDL.

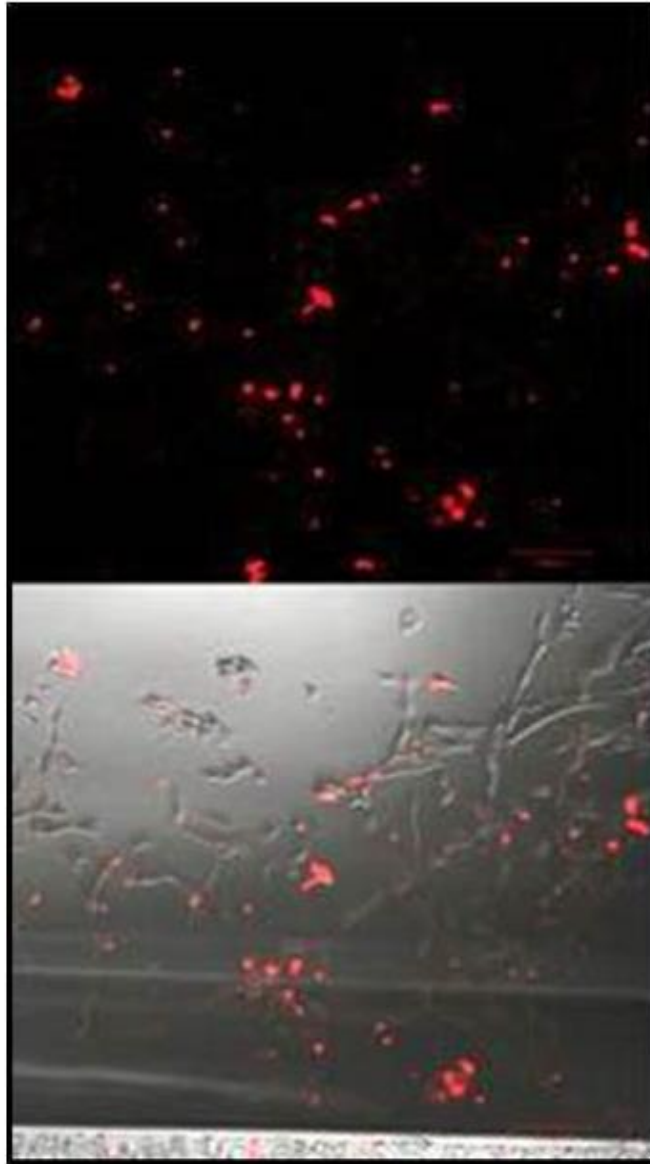


Figure 4.8: Cells stained with Dil-Ac-LDL, 60x magnification. AECs (experimental control) were cultured in an eight chamber borosilicate coverglass system and stained with Dil-Ac-LDL, the bar is 10  $\mu\text{m}$ . AECs were isolated using the collagenase method. Images were taken with a Carl Zeiss Confocal (LSM 780 Elyra S1 with SR-SIM super resolution platform) microscope. The concentration of the probe used was 10  $\mu\text{g}/\text{ml}$  Dil-Ac-LDL.



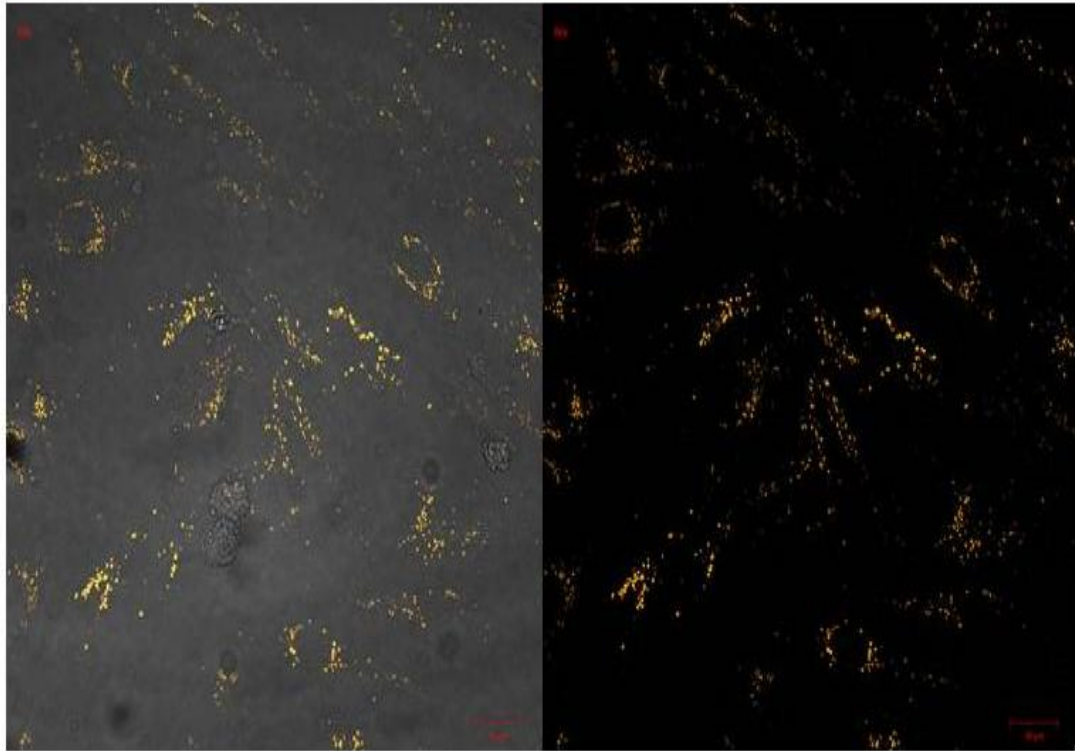


Figure 4.9: Commercial AECs stained with Dil-Ac-LDL, 60x magnification. The commercial AECs were cultured in an eight chamber borosilicate coverglass system and stained with Dil-Ac-LDL, the bar is 10  $\mu\text{m}$ . Images were taken with a Carl Zeiss Confocal (LSM 780 Elyra S1 with SR-SIM super resolution platform) microscope. The concentration of the probe used was 10  $\mu\text{g/ml}$  Dil-Ac-LDL.

#### 4.2.4. Western blot analysis

Cell cultures isolated using the collagenase method that were successfully identified as AECs were passaged until generation five. At this generation there were enough cells to prepare protein lysates. Protein lysates were prepared and the cytoplasmic fractions were used for western blot analysis to determine the presence of the eNOS enzyme and protein kinase B (PKB/Akt). The size of eNOS is 140 kDa and ubiquitously expressed by endothelial cells. eNOS is also activated by PKB/Akt which is upstream from eNOS in the insulin signalling pathway. PKB/Akt is a 60 kDa protein. A 7.5% SDS-PAGE gel was prepared and lysates from both commercial AECs and experimental cells were analysed. After separation, the proteins were transferred to a PVDF membrane as described in Materials and Methods and probed for total eNOS. As can be observed in figure 4.10 only the commercial AECs expressed total eNOS and not the experimental cells (Figure 4.10). Secondly, a 7.5% SDS-PAGE gel was prepared to detect PKB/Akt. Only lysates prepared from experimental cells were loaded and separated. The proteins were transferred to a PVDF membrane and probed for total PKB/Akt. All the lysates contained PKB/Akt in the cytoplasmic fractions (figure 4.11).



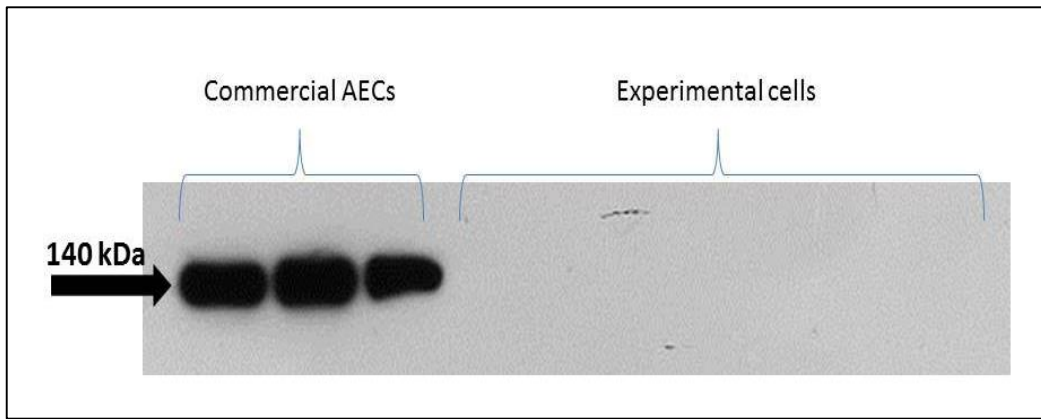


Figure 4.10: Total eNOS expression differences among the commercially purchased AECs and the experimental cells (endothelial cells isolated using the collagenase method).

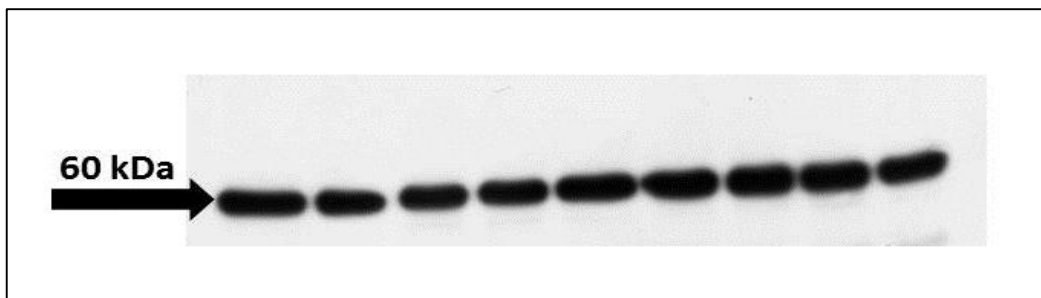


Figure 4.11: Total PKB-Akt expression in experimental cells isolated from the thoracic region of the rat aorta.

### 4.3. Summary and Discussion

The growth rate of the cells isolated using the vascular ring method took 2 weeks to reach confluency before the cells could be passaged to the next generation. Due to this long incubation period and that almost none of the cells in culture were stained positively with Dil-Ac-LDL, it was concluded that this isolation procedure was unsuccessful. Therefore, the isolation of AECs using the vascular ring method was aborted. In comparison, the cells isolated using the collagenase method took one week to reach confluency before they could be passaged to the next generation. The morphology of the cell culture mirrored what is often observed in a known culture of AECs and the fact that most of cells isolated using this technique were stained positively with Dil-Ac-LDL indicated that the collagenase method used to isolate endothelial cells could be very useful in the future. But with this technique, it is not always possible to obtain a pure AEC culture as some cultures only had a 50% positive staining rate, which was not sufficient for cardiovascular studies which require the use of these cells. Furthermore, the fact that these cells did not express the eNOS enzyme is disconcerting as this is a major positive marker for endothelial cells. The results were also confusing, especially after morphological and Dil-Ac-LDL tests have identified these cell types as being endothelial cells. Thus to conclude, both the vascular ring method and the collagenase method were regarded as unsuccessful and would require more optimization in the future than what time allowed for this project.

It was therefore decided to use commercially purchased AECs to complete the other remaining aims presented in the beginning.

## Chapter 5: Flow Cytometry Results

In Ataxia telangiectasia (AT) patients, the number one cause of death is cancer. Cancer is known as the uncontrollable cell division of abnormal cells often arising from mutations in its DNA.

Vara et al. (2004) described the role of PKB/Akt in cancer cells as an inhibitor of apoptosis as it phosphorylates Bad and caspase-9 [Vara et al., 2004 and Hemmings and Restuccia, 2012]. Li and Yang (2010) investigated the occurrence of apoptosis in MDA-MB-453 cells (breast cancer cells) and PC-3 cells (a prostate cancer cell line) when treated with the ATM inhibitor Ku-55933. What they observed was that under serum starvation conditions Ku-55933 had the ability to induce apoptosis in both cells lines [Li and Yang, 2010 and Yang et al., 2011]. Duan et al. (2011) studied the relationship between autophagy and apoptosis. What they observed in their data was that under glucose restrictions autophagy was induced and resulted in apoptosis in both ataxia telangiectasia (AT) skin fibroblasts and normal human skin fibroblasts [Duan et al., 2011]. In glucose restriction, the AMP/ATP ratio increases the activation of AMPK, an energy sensor, via LKB1 or ATM. Once activated, AMPK has the potential to activate p53, which mediates senescence, autophagy, apoptosis and growth arrest [Duan et al., 2011]. Yang et al, (2011) wrote that ATM<sup>-/-</sup> mice experience a decrease in pancreatic beta cell mass and an increase in pancreatic beta cell death as they age when compared to age matched controls [Yang et al., 2011]. This could be a possible reason for the development of diabetes often experienced by ATM patients. Furthermore when combined with rapamycin the two inhibitors (rapamycin and Ku-55933) together induces apoptosis and cancer cell proliferation better than on their own [Yang et al., 2011].

Madamanchi et al. (2010) hypothesized in their literature review that apoptosis in ATM heterozygous (ATM+/-) ApoE null (ApoE-/-) macrophages are a result of mitochondrial DNA (mtDNA) damage [Madamanchi et al., 2010]. Furthermore, they concluded that macrophages that undergo apoptosis in the vascular wall contribute to plaque progression and instability in atherosclerosis [Madamanchi et al., 2010 and Li, H. et al., 2014]. Under physiological conditions, another contributor to apoptosis is reactive oxygen species (ROS). At basal conditions, ROS regulates many signalling pathways regarding maintaining vascular tone, inducing apoptosis and controlling cell growth and inflammatory responses [Li, H. et al., 2014]. When ROS exceeds the available antioxidants present in the body, oxidative stress arises and contributes to the onset of cardiovascular disease.

As discussed in the literature review the ATM protein is a sensor and regulator of ROS within all cell types. Based on the literature, mtDNA damage, increased ROS and hyperglycaemia can all lead to the development of cardiovascular disease. Cardiovascular pathologies such as atherosclerosis are associated with a decrease in NO production which is a marker of endothelial dysfunction and a disruption in vascular homeostasis.

Therefore, in this chapter the effects of the different stimulators (insulin) and inhibitors (Ku-60019 and wortmannin) on AEC were determined by measuring the NO production and the viability of these cells after treatment. The protocol followed is as described in the methods chapter.

### **5.1. AEC viability: Propidium iodide staining (necrosis)**

In figure 5.1 necrosis of AECs was measured with the use of propidium iodide staining. The AECs were previously treated with insulin, an ATM inhibitor Ku-60019 a combination of Ku-60019 and insulin, wortmannin and a combination of wortmannin with insulin. The aim of staining the cells with propidium iodide was to detect any cell death that may have

occurred due to treatment of these cells with one or a combination of the drugs used. Cell viability was measured using a density plot (figure 5.1). In the representative density plot shown in figure 5.1, the sub-population in the bottom left quadrant are the viable cells of the sample (88.8% of the total population were viable cells in this particular sample) and the sub-population in the bottom right quadrant are the non-viable necrotic cells (10% of the total cell population). 10 nM insulin, 3  $\mu$ M Ku-60019 and 100 nM wortmannin had no effect on the necrosis, therefore on cell viability, of the AECs (figure 5.2).

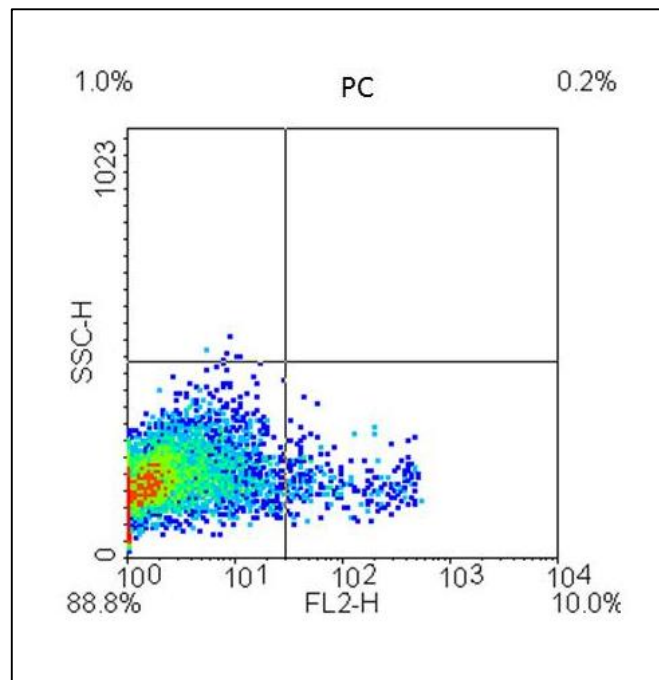


Figure 5.1: Density plot used to determine the percentage of viable and non-viable cells in a total AECs population. The Y-axis represents propidium iodide fluorescence. The bottom left quadrant contains the viable (non-propidium iodide staining) cells (88.8% of the total AEC population) and the bottom right quadrant contains the non-viable, propidium iodide staining cells (10% of the total AEC population).

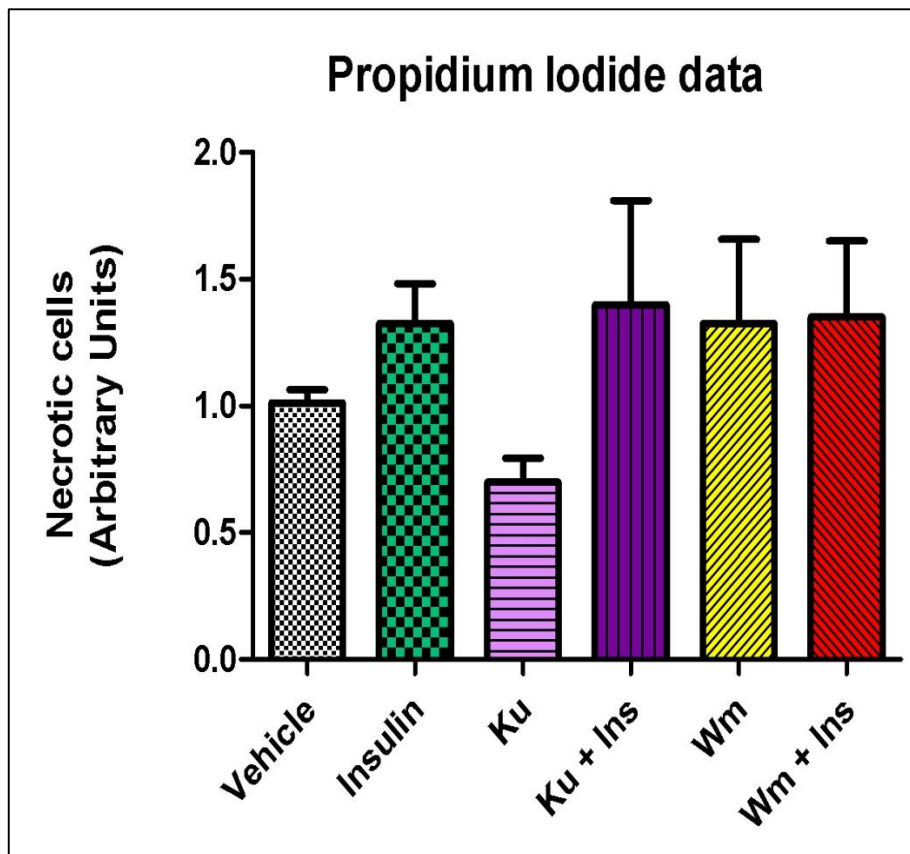


Figure 5.2: The effects of insulin, Ku-60019 and wortmannin on the development of necrosis (% cells staining positively with propidium iodide) in AECs. Ins = insulin; Ku = Ku-60019; Wm = wortmannin.

## 5.2. NO-production

The effects of 10 nM insulin, 3  $\mu$ M Ku-60019, and 100 nM wortmannin on NO production was detected by measuring the fluorescence intensity of DAF-2/DA. 3  $\mu$ M Ku-60019 significantly increased the amount of NO produced compared to the vehicle (DMSO), (Ku 3  $\mu$ M:  $1.326 \pm 0.08906$  vs. vehicle:  $0.9981 \pm 0.02958$ ;  $p < 0.05$ ) (figure 5.3). 10 nM insulin produced significantly more NO than the wortmannin with insulin group (Ins 10 nM:  $1.186 \pm 0.04962$  and Wm 100 nM with Ins 10 nM:  $0.7964 \pm 0.07332$ ;  $p < 0.01$ ) (figure 5.3). Therefore, wortmannin inhibited the NO production induced by insulin but KU did not.



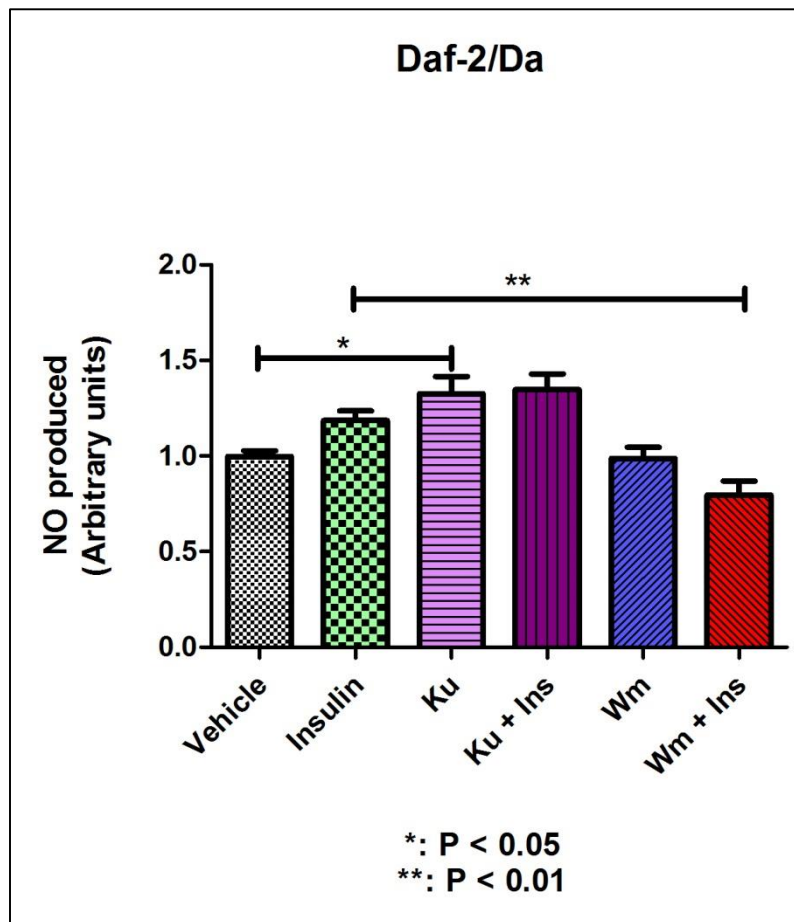


Figure 5.3: The effects of insulin, Ku-60019 and wortmannin on the production of NO (as determined by the arithmetic mean of the fluorescence intensity) in AECs. Approximately 3-4 petri dishes were assigned to each treatment group. Ins = Insulin (10 nM); Ku = Ku-60019 (3  $\mu$ M); Wm = wortmannin (100 nM).

### 5.3. Summary and Discussion

Based on the data insulin, Ku-60019 and wortmannin had no significant effect on necrosis in the AECs in comparison to the vehicle.

The decrease observed in NO produced by the AECs in the wortmannin + insulin-groups compared to the insulin treated groups, indicates the inhibitory effect of wortmannin on the PI3-K signalling pathway. Furthermore, the data concerning the insulin treatment group and the wortmannin treatment groups confirms the need for eNOS enzyme activation at Ser1177 by PKB/Akt in response to insulin treatment. Surprisingly the inhibition of the ATM protein by its inhibitor Ku-60019 led to an increase in NO production. This aspect of the role of ATM in cardiovascular health and disease has not been researched before. One could speculate that the increased NO production seen in figure, 5.4 could be a result of an increase in eNOS expression when ATM is inhibited. According to Kobayashi, T. et al. (2007), treatment with insulin increases the expression of eNOS mRNA thereby increasing NO availability. Logically, with the increase in NO there is an increase in vasodilation which, is often observed at the onset of diabetes. As diabetes progresses the availability of NO decreases and the endothelium becomes dysfunctional [Kobayashi, T. et al., 2007]. Additionally, if NO is produced in the presence of superoxide anions the two react to produce peroxynitrite which is also a marker of oxidative stress and endothelial dysfunction. Furthermore, these observations could contribute to the insulin resistance, hyperglycaemia and diabetes observed in AT patients.

## Chapter 6: Western blot analysis

The glucose uptake pathway is controlled by both Protein kinase B (PKB/Akt) and AMP-activated protein kinase (AMPK). According to Young et al. (2005) AMPK can be activated by oxidative stress and cardiovascular pathologies such as ischemia. Ischemia is characterized by the insufficient blood flow and delivery of oxygen and glucose to tissues such as the heart muscle [Young et al., 2005]. During ischemia, the ratio of AMP/ATP increases which is necessary to phosphorylate and activate the AMPK protein alpha subunit at Thr172. According to Li and Keane (2010) AMPK phosphorylates eNOS to release NO resulting in increased vasodilation and decreased apoptosis in order to promote vascular homeostasis [Li and Keane, 2010].

In the AMPK signalling pathway, AMPK is activated by upstream proteins such as LKB1 and Ca<sup>2+</sup>/calmodulin-dependent protein kinase kinase (CaMKK), in response to a decrease in ATP, or by the pharmacological AMPK activator aminoimidazole carboxamide ribonucleotide (AICAR); [Fu et al., 2008]. According to Amatya et al, (2012) when DNA damage occurs the AMPK protein is activated in an LKB1 independent manner and in an ATM-dependent manner by the DDR in human glioma cells (M059K and M059J), [Amatya et al., 2012].

Once activated, AMPK directly mediates the translocation of glucose transporter 4 (GLUT4) vesicles from the cytoplasm to the cell membrane. During metabolic stress AMPK-mediated glucose uptake is the primary method of maintaining glucose homeostasis when insulin is unable to mediate glucose uptake via the phosphatidylinositol 3 kinase (PI3-K)-PKB/Akt signalling pathway [Young et al., 2005]. In contrast to AMPK-mediated glucose uptake, the insulin PI3-K-PKB/Akt signalling pathway involves more

proteins in the glucose uptake pathway. As discussed previously in the first chapter, the proteins involved in the insulin mediated glucose uptake pathway include insulin receptor substrate-1 (IRS-1), PI3-K, phosphatidylinositol 4,5-bisphosphate (PIP2) / phosphatidylinositol 3,4,5-trisphosphate (PIP3), Phosphatidylinositol dependent kinase (PDK1), PKB/Akt, Akt substrate, 160 kDa (AS160) and the GLUT4 protein itself. It was also found that the AS160 protein is not only a PKB/Akt substrate but an AMPK substrate as well. AS160 inhibition occurs by AMPK phosphorylation when mice muscle tissue (extensor digitorum longus) is treated with AICAR [Treebak et al., 2006].

In this chapter the protein expression and phosphorylation of various proteins involved in the glucose uptake pathway were investigated by treating AECs with insulin, the ATM inhibitor Ku-60019 and PI3-K inhibitor wortmannin. The proteins of interest were: PI3-K/P83, Phosphatase and tensin homolog (PTEN), PKB/Akt, AS160, Glycogen synthase kinase 3 beta (GSK3 $\beta$ ), AMPK, Ataxia telangiectasia mutated (ATM), and eNOS.

## **6.1. Insulin dose response experiments**

Insulin dose response experiments were completed as described in the methods chapter. AECs were treated with two different insulin concentrations (10 nM and 100 nM) to determine the lowest concentration that would result in the phosphorylation / activation of PKB/Akt at Ser473 and eNOS at Ser1177. For both PKB/Akt and eNOS,  $\beta$ -tubulin was probed for to ensure there was equal loading.

### **6.1.1. PKB/Akt**

In figure 6.1, it was observed that 100 nM insulin did not cause a significant increase in PKB/Akt phosphorylation compared to 10 nM insulin or the control group. Although not

statistically significant, there was an increase in the phosphorylation of PKB/Akt with the increase in insulin concentration (Figure 6.1, A) compared to the amount of total PKB/Akt protein expressed in the AECs (figure 6.1, B). The increase in PKB/Akt phosphorylation was confirmed by the phosphorylated over total ratios observed in figure 6.1 (C). For both the eNOS and the PKB/Akt proteins 10 nM insulin was enough to induce phosphorylation of these proteins compared to the control group (figure 6.1 and 6.2).

### 6.1.2. eNOS

In figure 6.2 representative western blots are shown to demonstrate eNOS phosphorylation at Ser1177 after insulin treatment (figure 6.2, A). 100 nM insulin did not increase the phosphorylation of eNOS compared to 10 nM insulin and the control group. 10 nM insulin significantly decreased total eNOS expression compared to the control group (Control:  $1.00 \pm 0.03$  vs. Insulin 10 nM:  $0.72 \pm 0.03$   $p=0.0004$ ) (figure 6.2, B). 100 nM insulin statistically increased the phosphorylation over total ratio compared to the control (Control:  $1.00 \pm 0.15$  vs. Insulin 100 nM:  $1.67 \pm 0.14$ ;  $p=0.0205$ ) (figure 6.2, C).

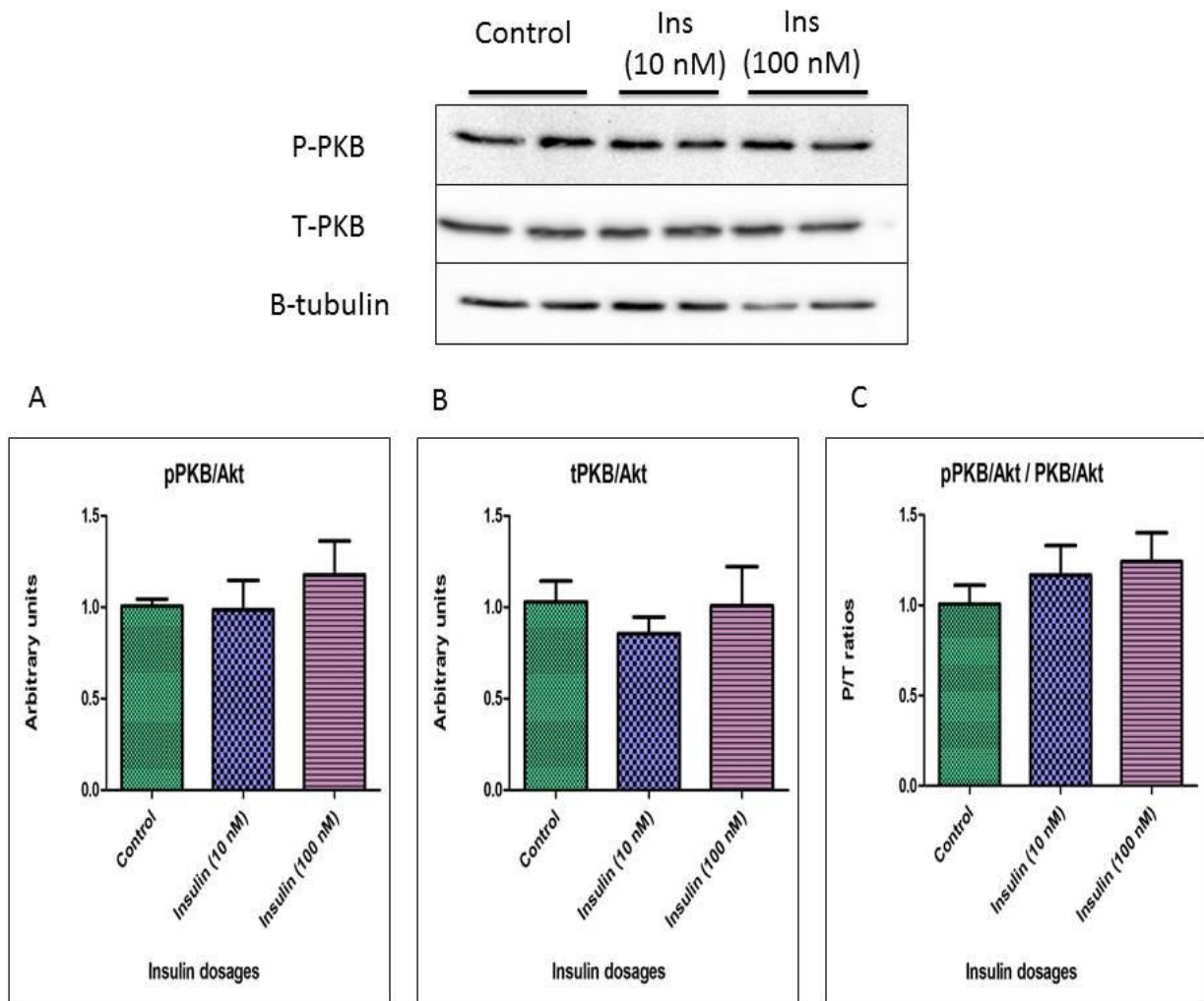


Figure 6.1: PKB/Akt insulin dose response. (A) Phosphorylated PKB/Akt expressed in the cytosol of the AECs. (B) Total PKB/Akt protein expressed in the AECs. (C) The phosphorylated over total ratios, the amount of phosphorylated protein in the AECs exceeded that of the total PKB/Akt proteins in response to insulin. All data were corrected for  $\beta$ -tubulin. N=4

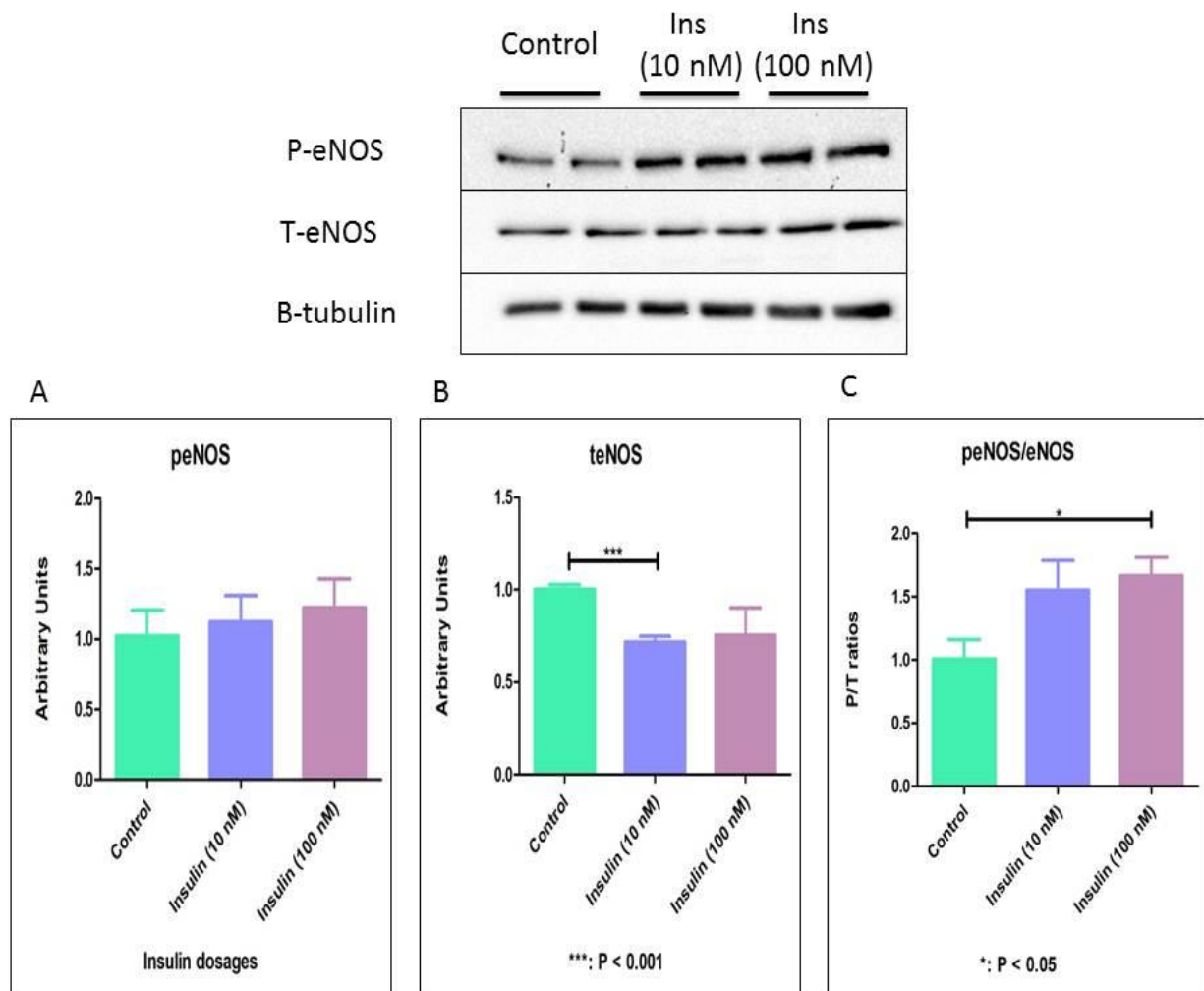


Figure 6.2: eNOS insulin dose response. (A) Phosphorylated eNOS proteins expressed in AECs. (B) Total eNOS protein present in AECs, contrary to the literature the addition of insulin appears to down-regulate the expression of eNOS in the 10 nM insulin group ( $p=0.004$ ). (C) Phosphorylated over total ratios, 100 nM insulin had the highest ratio compared to the control ( $p=0.0205$ ). All data were corrected for  $\beta$ -tubulin.

\*:  $P < 0.05$  and \*\*\*:  $P < 0.001$ .  $N=4$

## 6.2. Stimulation and inhibition of the phosphatidylinositol-3 kinase (PI3-K) signalling pathway in aortic endothelial cells with emphasis on the ATM protein

### 6.2.1. PI3-K/P85

The P85 protein is one of the first proteins to be activated in response to insulin in the insulin-signalling pathway. In figure 6.3 (A) changes in phosphorylation of P85 were observed in response to 10 nM insulin and 3  $\mu$ M Ku-60019 (Ku) compared to the vehicle. 10 nM insulin significantly increased phosphorylation of P85 ( $1.365 \pm 0.078$  vs.  $0.99 \pm 0.003$ ,  $p = 0.0033$ ). This phosphorylation could be inhibited by 100 nM Wm ( $1.36 \pm 0.08$  vs.  $0.93 \pm 0.08$ ,  $p = 0.0073$ ) (figure 6.3, A). 3  $\mu$ M Ku however, could not inhibit the phosphorylation induced by 10 nM insulin ( $1.46 \pm 0.16$  vs.  $1.36 \pm 0.08$ ,  $p = 0.03$ ). Surprisingly, Ku alone induced phosphorylation of P85 ( $1.36 \pm 0.08$  vs.  $0.99 \pm 0.003$ ,  $p = 0.0057$ ). 10 nM Insulin was also able to increase the expression of P85 ( $1.26 \pm 0.06$  vs.  $0.99 \pm 0.003$ ,  $p = 0.0061$ ). Unexpectedly, the expression of P85 was also increased by 100 nM Wm ( $2.06 \pm 0.39$  vs.  $0.99 \pm 0.003$ ;  $p = 0.0353$ ) (figure 6.3, B). Calculating the phosphorylated to total ratio highlighted that 100 nM Wm will inhibit the phosphorylation induced by 10 nM insulin ( $1.10 \pm 0.12$  vs  $0.58 \pm 0.09$ ;  $p = 0.0116$ ) (Fig 6.3 C).

### 6.2.2. PTEN

PTEN is a phosphatase protein, which dephosphorylates PIP3 or inhibits its phosphorylation by accepting a phosphate group from PIP3 [Mukherjee et al., 2013]. As shown in Fig 6.4 B, 10 nM insulin resulted in upregulation of PTEN from  $0.99 \pm 0.003$  to  $1.19 \pm 0.02$ ,  $p < 0.001$ . None of the other interventions changed either the phosphorylation or expression of PTEN.



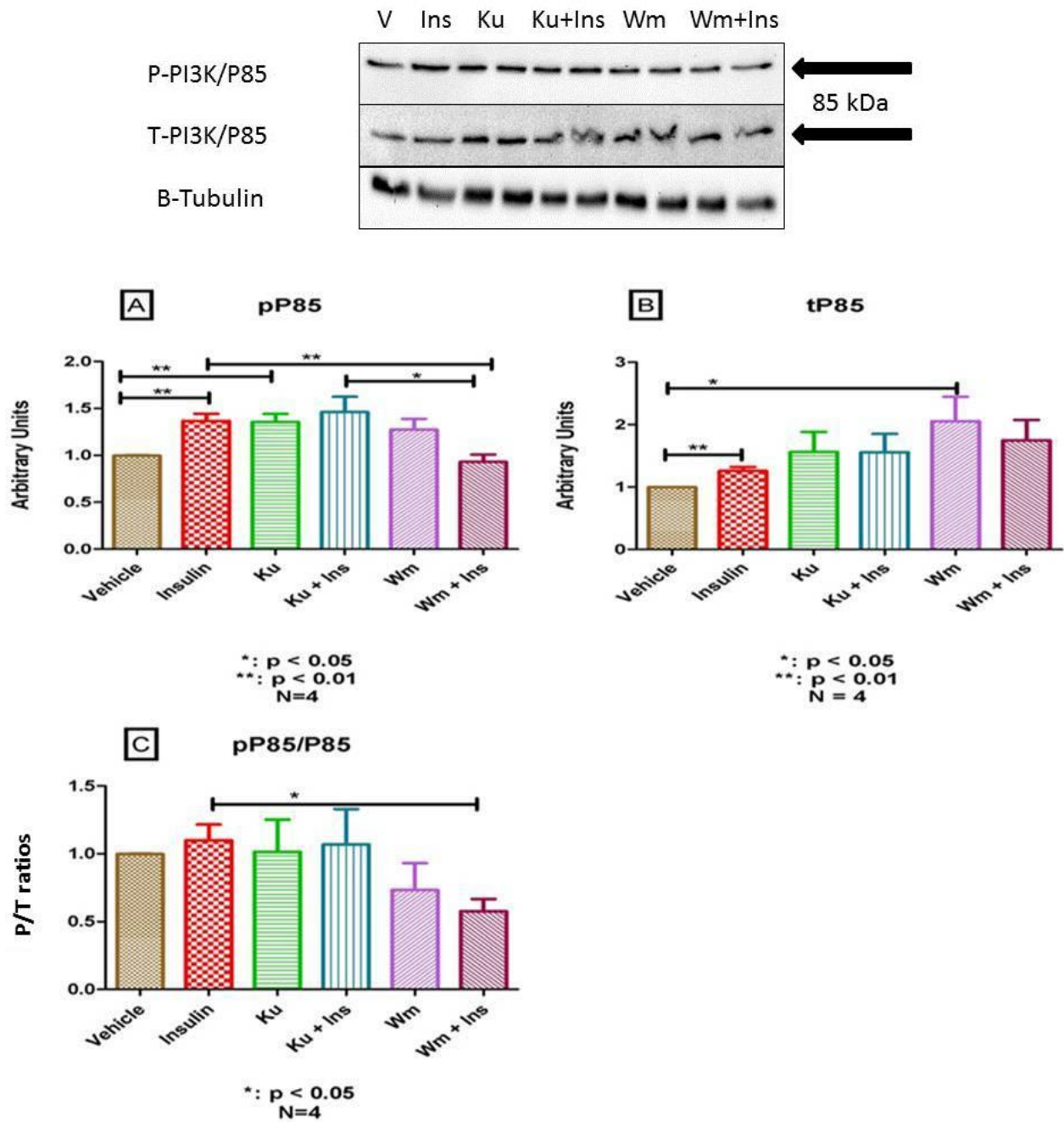


Figure 6.3: P85 protein activation and inhibition (A) Phosphorylated P85, (B) total P85 and (C) the phosphorylated/total P85 ratio after the stimulation with insulin, Ku-60019 and wortmannin with or without insulin respectively. All data were corrected for  $\beta$ -tubulin.

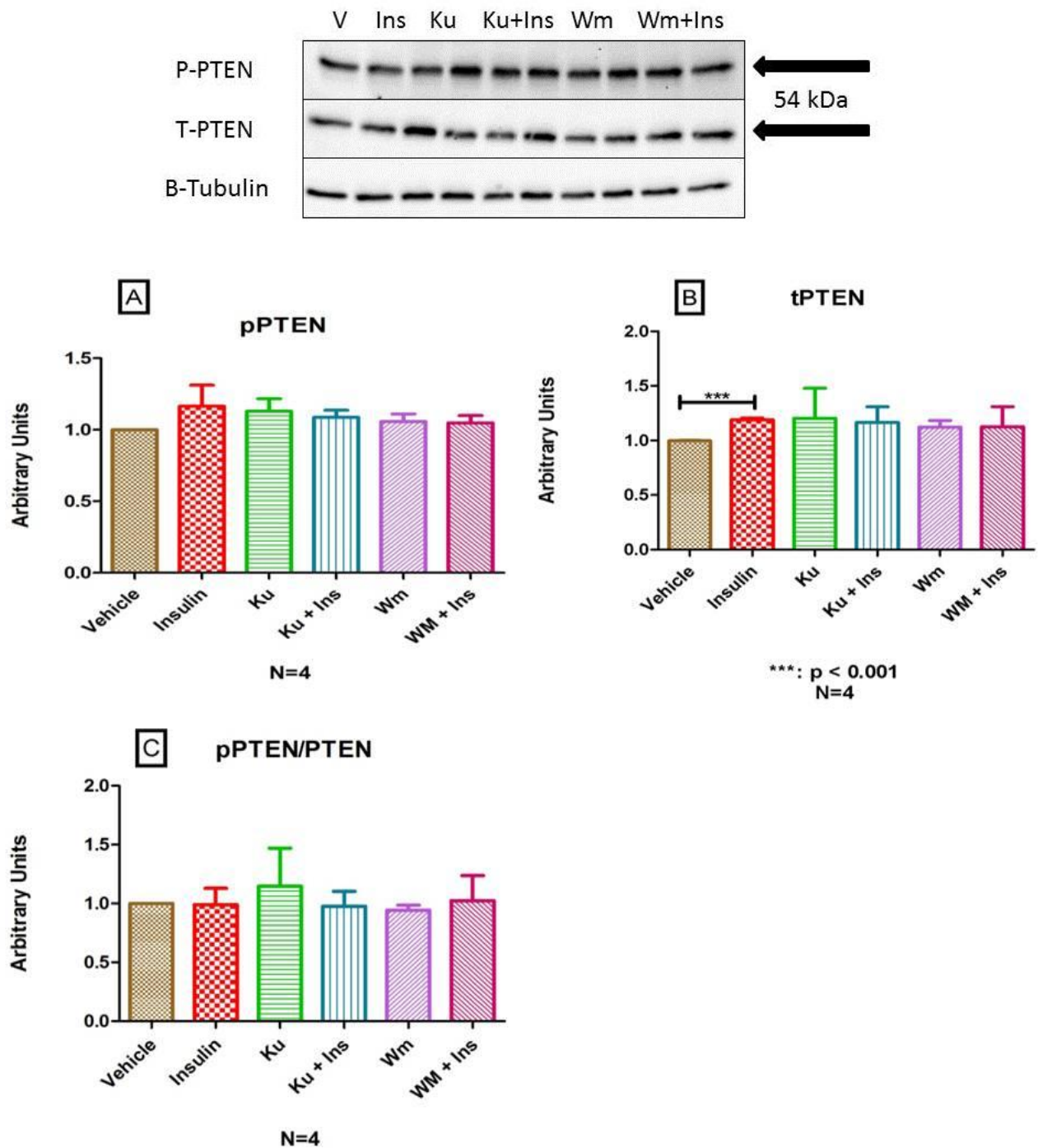


Figure 6.4: PTEN protein activation and inhibition (A) Phosphorylated PTEN, (B) total PTEN and (C) the phosphorylated/total PTEN ratio after the stimulation with insulin, Ku-60019 and wortmannin with or without insulin respectively. All data were corrected for  $\beta$ -tubulin.

### 6.2.3. PKB/Akt

PKB/Akt is a protein that is not only involved in the glucose uptake but also in angiogenesis, cell growth and proliferation and glycogen synthesis. PKB/Akt is phosphorylated in the presence of insulin. As can be observed in figure 6.5, 10 nM insulin significantly increased the phosphorylation of PKB/Akt compared to the vehicle group ( $1.34 \pm 0.14$  vs.  $0.99 \pm 0.003$ ;  $p=0.0388$ ) and this phosphorylation could be inhibited by 100 nM wortmannin ( $1.34 \pm 0.14$  vs.  $0.89 \pm 0.04$ ;  $p=0.0175$ ) (figure 6.5, A). 10 nM insulin, 3  $\mu$ M Ku and 100 nM Wm had no significant impact on the total protein expression of PKB/Akt (figure 6.5, B). However, a significant decrease was observed in the phosphorylated over total protein ratios (figure 6.5, C). AECs treated with 100 nM Wm had significantly less PKB/Akt phosphorylated over total ratios ( $0.73 \pm 0.11$  vs.  $0.99 \pm 0.003$ ;  $p=0.0468$ ) and 100 nM Wm decreased the phosphorylated over total ratio compared to 10 nM insulin ( $0.85 \pm 0.04$  vs.  $1.00 \pm 0.02$ ;  $p=0.0166$ ) (figure 6.5, C).

### 6.2.4. GSK3 $\beta$

As mentioned GSK3 $\beta$  activity is inhibited by insulin by phosphorylation at Ser9 [Jensen et al., 2011]. 10 nM insulin significantly increased the phosphorylation of GSK3 $\beta$  ( $2.12 \pm 0.02$  vs.  $0.99 \pm 0.005$ ;  $p=0.0003$ ). Both 3  $\mu$ M Ku ( $1.24 \pm 0.005$  vs.  $2.12 \pm 0.02$ ;  $p=0.0005$ ) and 100 nM wortmannin ( $0.62 \pm 0.17$  vs.  $2.12 \pm 0.02$ ;  $p=0.0128$ ) significantly inhibited the insulin-stimulated phosphorylation (figure 6.6, A). Both 10 nM insulin and 100 nM Wm attenuated the expression of GSK3 $\beta$  (vehicle:  $0.99 \pm 0.005$  vs. 10 nM Ins:  $0.88 \pm 0.005$ ;  $p=0.0035$  vs. 100 nM:  $0.79 \pm 0.03$ ;  $p=0.0213$ ) (figure 6.6, B). This effect was synergistic as a combination of Wm and Ins lowered the expression even more. ( $0.88 \pm 0.005$  vs.  $0.62 \pm 0.02$ ;  $p=0.0037$ ) (figure 6.6, B).

Calculating the ratio between phosphorylated and total protein also showed an effect of Ku on GSK3 $\beta$ . A significant increase in the phosphorylated over total ratio was observed between the vehicle and the 3  $\mu$ M Ku ( $0.99\pm 0.005$  vs.  $1.46\pm 0.06$ ;  $p=0.0164$ ) although no significant effect on either the phosphorylation or the expression was observed. The stimulatory effect of insulin as well as the inhibitory effect of Wm on the stimulation of insulin was clearly seen in this calculation: 10 nM Ins ( $2.42\pm 0.02$  vs.  $0.99\pm 0.005$ ;  $p=0.0002$ ) and 100 nM Wm with 10 nM insulin ( $1.02\pm 0.30$  vs.  $2.42\pm 0.02$ ;  $p=0.0442$ ) (figure 6.6, C).

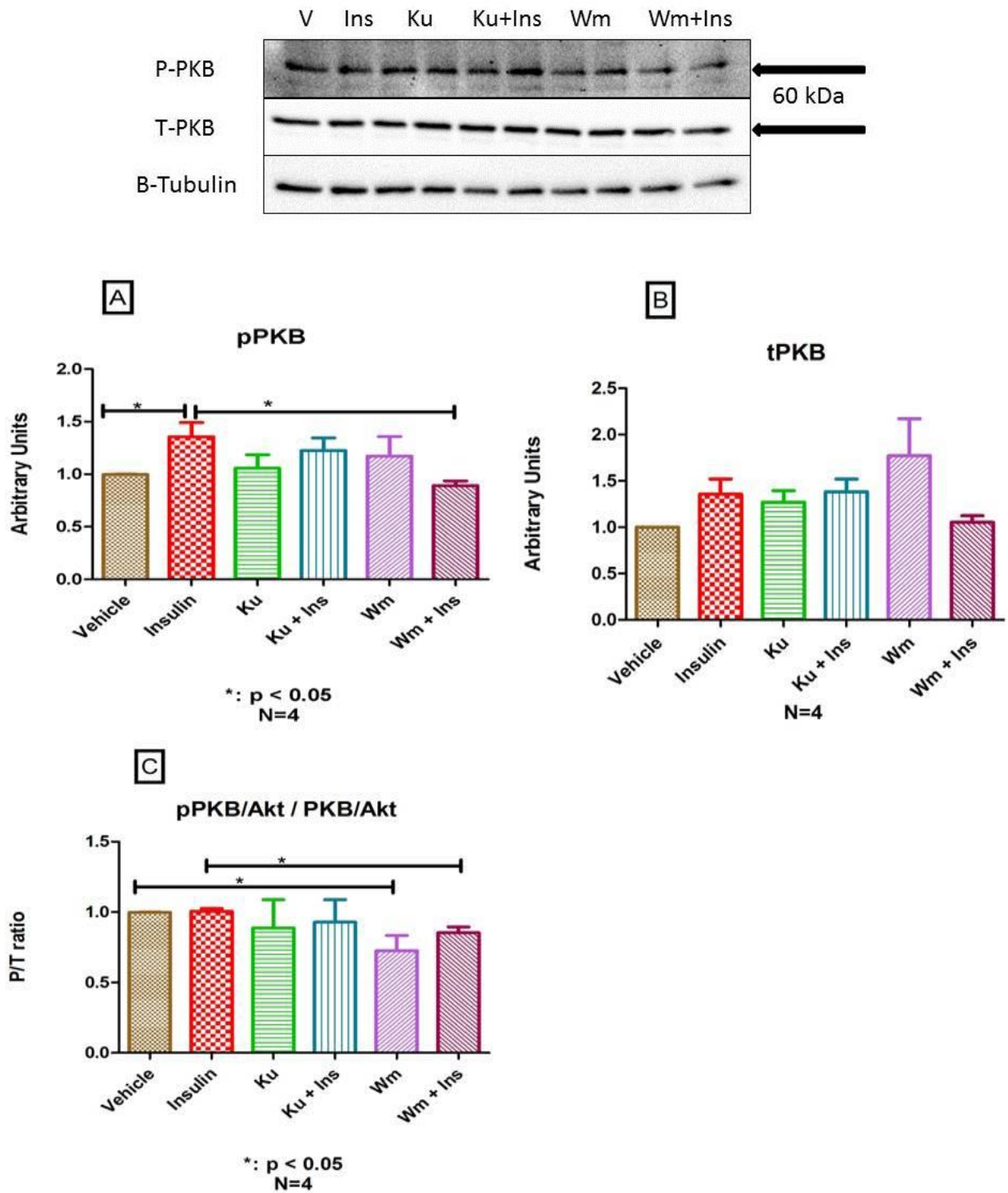


Figure 6.5: PKB/Akt protein activation and inhibition (A) Phosphorylated PKB/Akt, (B) total PKB/Akt and (C) the phosphorylated/total PKB/Akt ratio after the stimulation with insulin, Ku-60019 and wortmannin with or without insulin respectively. All data were corrected for  $\beta$ -tubulin.



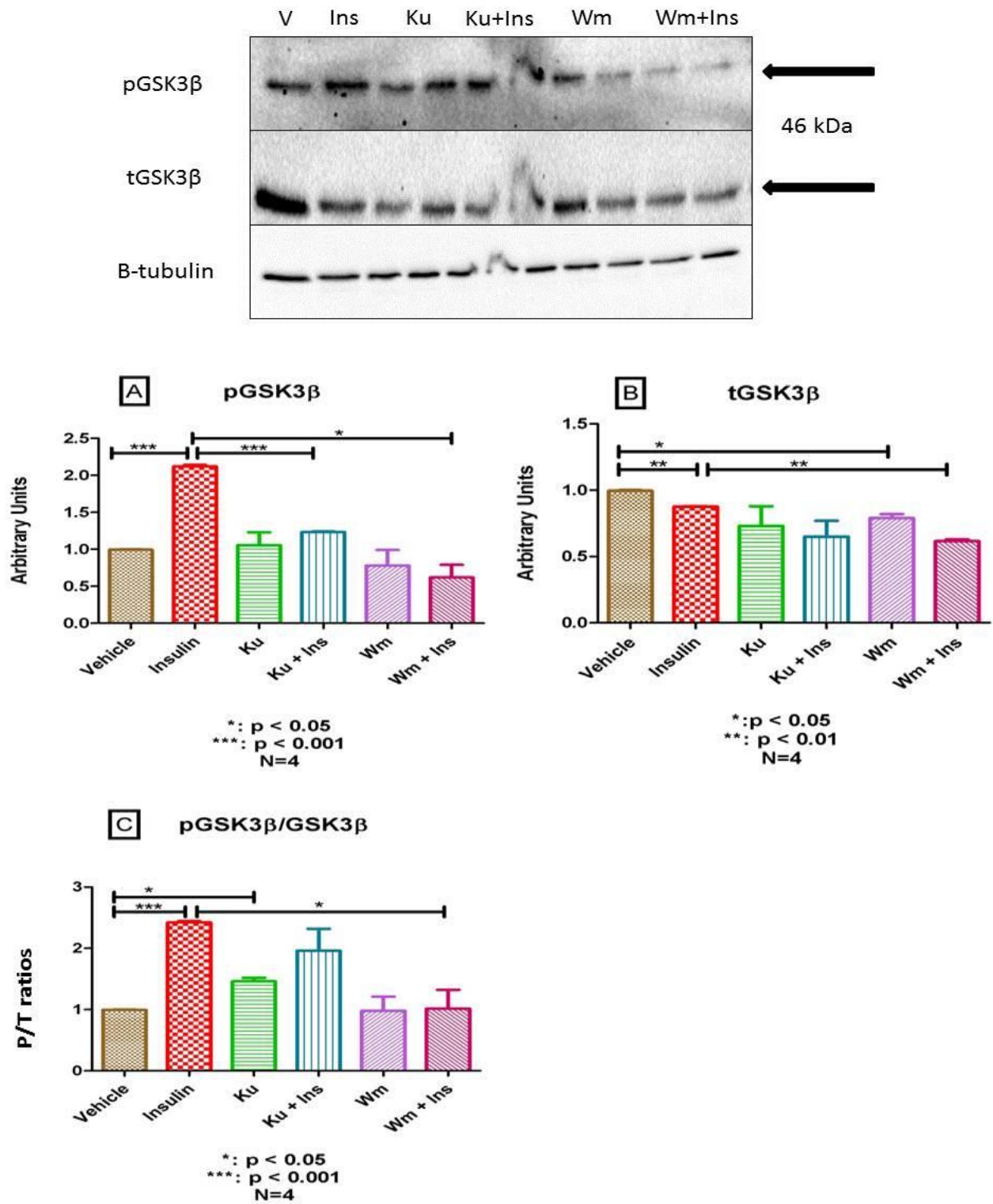


Figure 6.6: GSK3β protein activation and inhibition (A) Phosphorylated GSK3β, (B) total GSK3β and (C) the phosphorylated/total GSK3β ratio after the stimulation with insulin, Ku-60019 and wortmannin with or without insulin respectively. All data were corrected for β-tubulin.

### 6.2.5. AMPK

AMPK is the energy sensor in all tissue types and replenishes ATP when it has been depleted. AMPK is activated by an increase in AMP/ATP ratios and thus does not normally respond to insulin. In figure 6.7 A, the expected decrease in AMPK phosphorylation after stimulation with insulin was demonstrated ( $0.67 \pm 0.001$  vs.  $0.99 \pm 0.005$ ;  $p=0.0002$ ). The ATM inhibitor Ku, abolished this inhibition ( $0.95 \pm 0.029$  vs.  $0.67 \pm 0.001$ ;  $p<0.05$ ) but the PI3-K inhibitor Wm, unexpectedly, did not ( $0.83 \pm 0.006$  vs.  $0.99 \pm 0.005$ ;  $p=0.0022$ ) (figure 6.7, A).

10 nM insulin significantly attenuated the expression of total AMPK ( $0.90 \pm 0.004$  vs.  $0.99 \pm 0.005$ ;  $p=0.0049$ ) (figure 6.7, B).

Calculating the ratio of phosphorylated to total protein therefore showed an increase in the ratio stimulated by insulin ( $1.33 \pm 0.03$  vs.  $0.99 \pm 0.005$ ;  $p=0.0063$ , Fig 6.7, C). This calculation highlighted the effect of Ku both alone ( $0.58 \pm 0.02$  vs.  $0.99 \pm 0.005$ ;  $p=0.0018$ ) and by inhibiting the increase induced by insulin ( $1.33 \pm 0.03$  vs.  $0.59 \pm 0.12$ ;  $p=0.026$ ) (Fig 6.7, C).

### 6.2.6. ATM

There were no significant differences in either the expression or the phosphorylation of ATM under the conditions examined (figure 6.8 A and B). However, calculating the ratio of phospho to total protein, showed an attenuation of this ratio in the presence of wortmannin ( $0.43 \pm 0.11$  vs.  $0.99 \pm 0.005$ ;  $p=0.036$ ) (Fig 6.8 C).

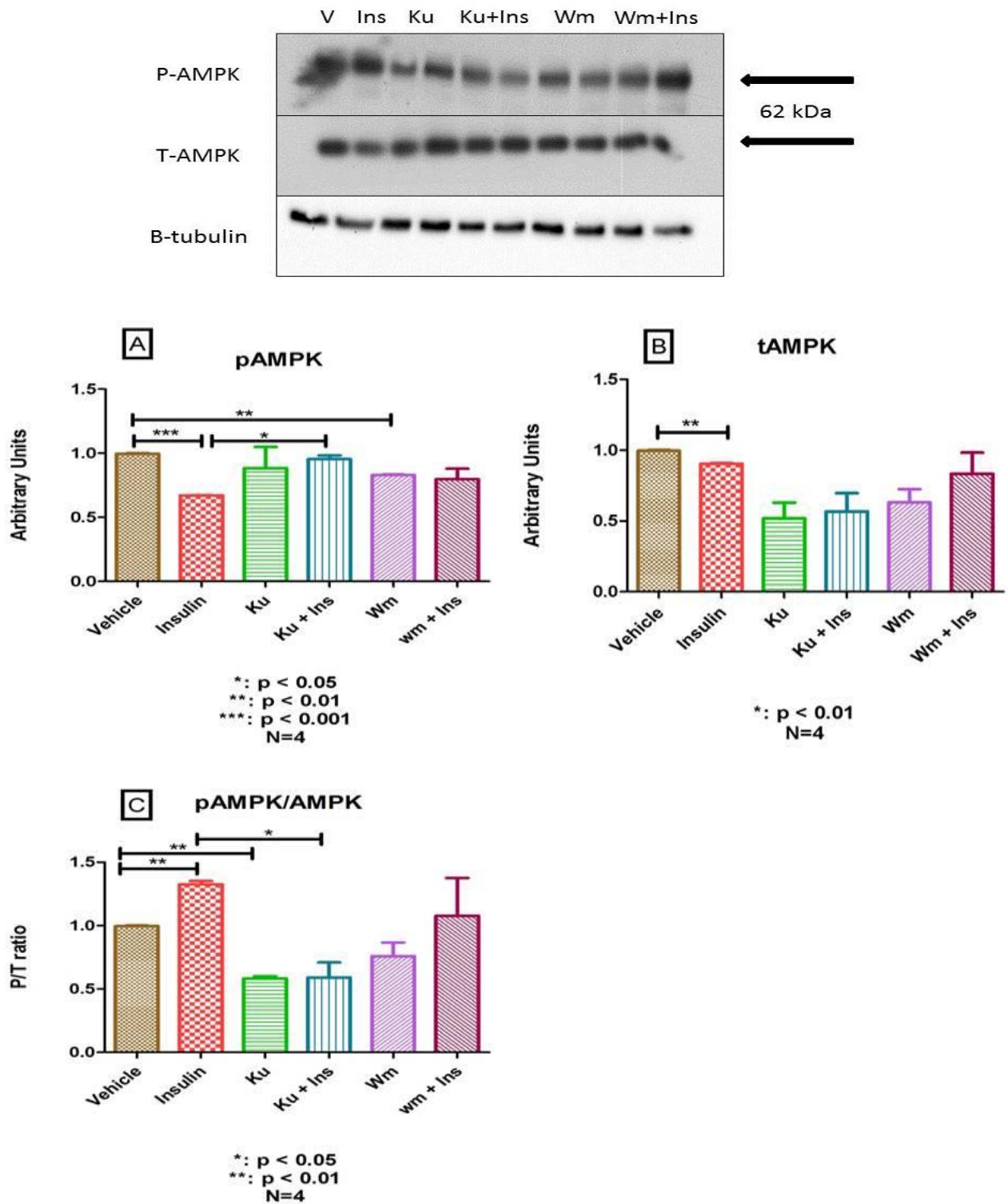


Figure 6.7: AMPK protein activation and inhibition (A) Phosphorylated AMPK, (B) total AMPK and (C) the phosphorylated/total AMPK ratio after the stimulation with insulin, Ku-60019 and wortmannin with or without insulin respectively. All data were corrected for  $\beta$ -tubulin.



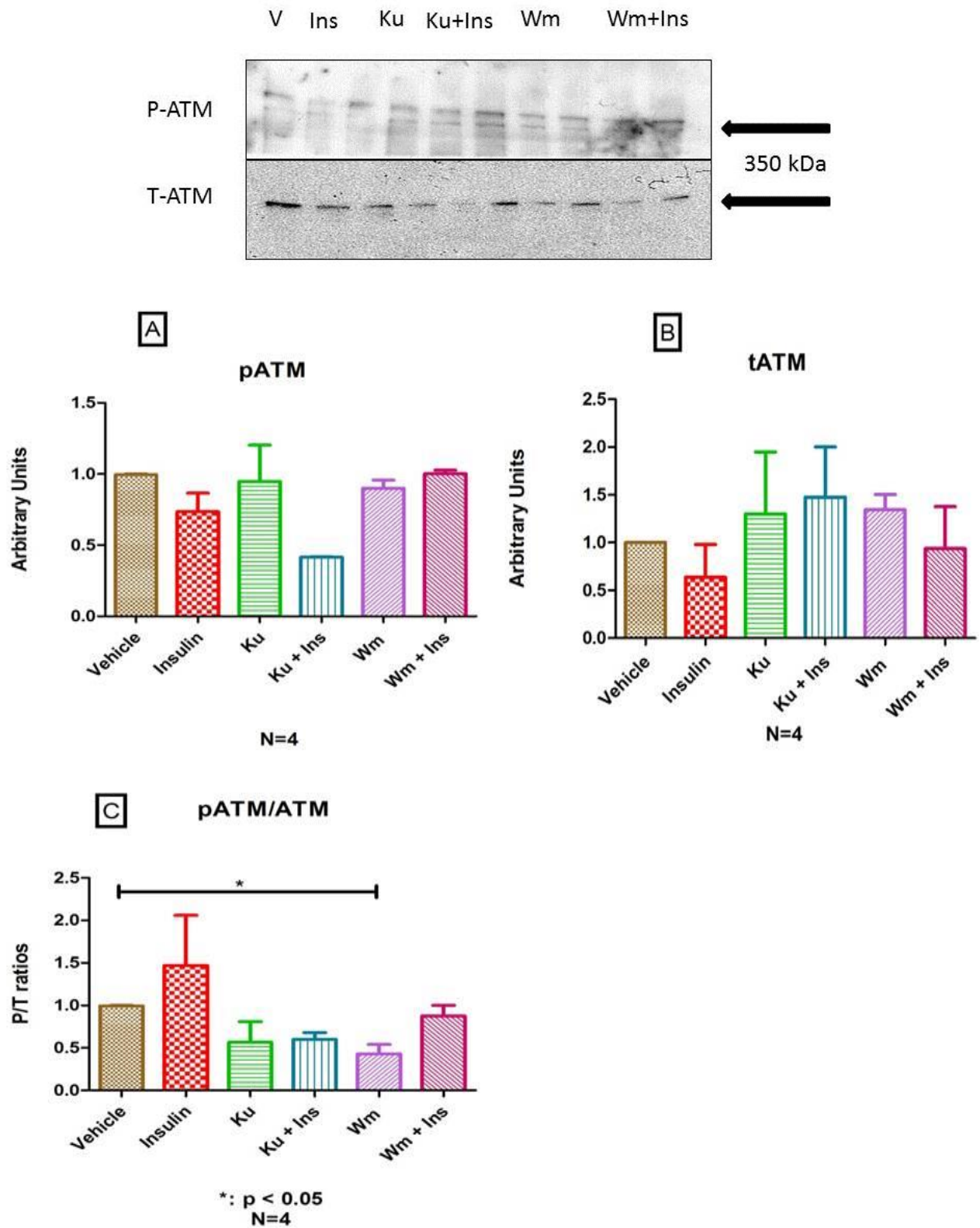


Figure 6.8: ATM protein activation and inhibition (A) Phosphorylated ATM, (B) total ATM and (C) the phosphorylated/total ATM ratio after the stimulation with insulin, Ku-60019 and

wortmannin with or without insulin respectively. In the absence of  $\beta$ -tubulin data were corrected using the stain-free technology provided by Bio-Rad (Bio-Rad, CA, USA)

#### **6.2.7. eNOS activation and inhibition**

As shown in figure 6.9 A, 100 nM wortmannin (Wm) significantly increased the phosphorylation of eNOS compared to the vehicle ( $2.75 \pm 0.35$  vs.  $0.99 \pm 0.01$ ;  $p=0.0280$ ) (6.9, A). There was a significant increase in the expression of total eNOS (figure 6.9, B) in AECs treated with a combination of 100 nM Wm and 10 nM insulin (Ins) compared to the 10 nM insulin alone ( $2.83 \pm 0.47$  vs.  $0.94 \pm 0.23$ ;  $p < 0.05$ ) (figure 6.9, B). Furthermore, the ratio of eNOS phosphorylation over the total eNOS protein between the various groups compared to the vehicle showed no significant differences (figure 6.9, C).

### 6.2.8. AS160

The AS160 protein, a negative regulator of GLUT4, is believed to be inactivated by phosphorylation mediated by PKB/Akt. Insulin, which mediates AS160 inactivation did not significantly affect the phosphorylation of AS160 (figure 6.10, A). In figure 6.10 (A) there appears to be a discrepancy in the phosphorylation of the AS160 protein as increased phosphorylation is observed in the Ku, Ku + Ins, Wm and Wm + Ins treatment groups. 100 nM Wm induced significantly more AS160 phosphorylation than 3  $\mu$ M Ku ( $6.60 \pm 0.64$  vs.  $1.0 \pm 0.05$ ;  $P < 0.01$ ) (figure 6.10, A). 3  $\mu$ M Ku + 10 nM Ins phosphorylated the AS160 protein profoundly more than the 100 nM Wm + 10 nM Ins treatment ( $5.46 \pm 0.29$  vs.  $1.03 \pm 1.03$ ) (figure 6.10, A). In figure 6.10, B it can be observed that 100 nM wortmannin attenuated the expression of AS160 ( $0.81 \pm 0.01$  vs.  $1.00 \pm 0.01$ ;  $p = 0.0003$ ). It was also observed that 100 nM Wm resulted in a significantly higher phosphorylated over total AS160 ratio compared to 3  $\mu$ M Ku ( $7.54 \pm 1.24$  vs  $1.04 \pm 0.01$ ;  $p = 0.0345$ ) (figure 6.10, C).

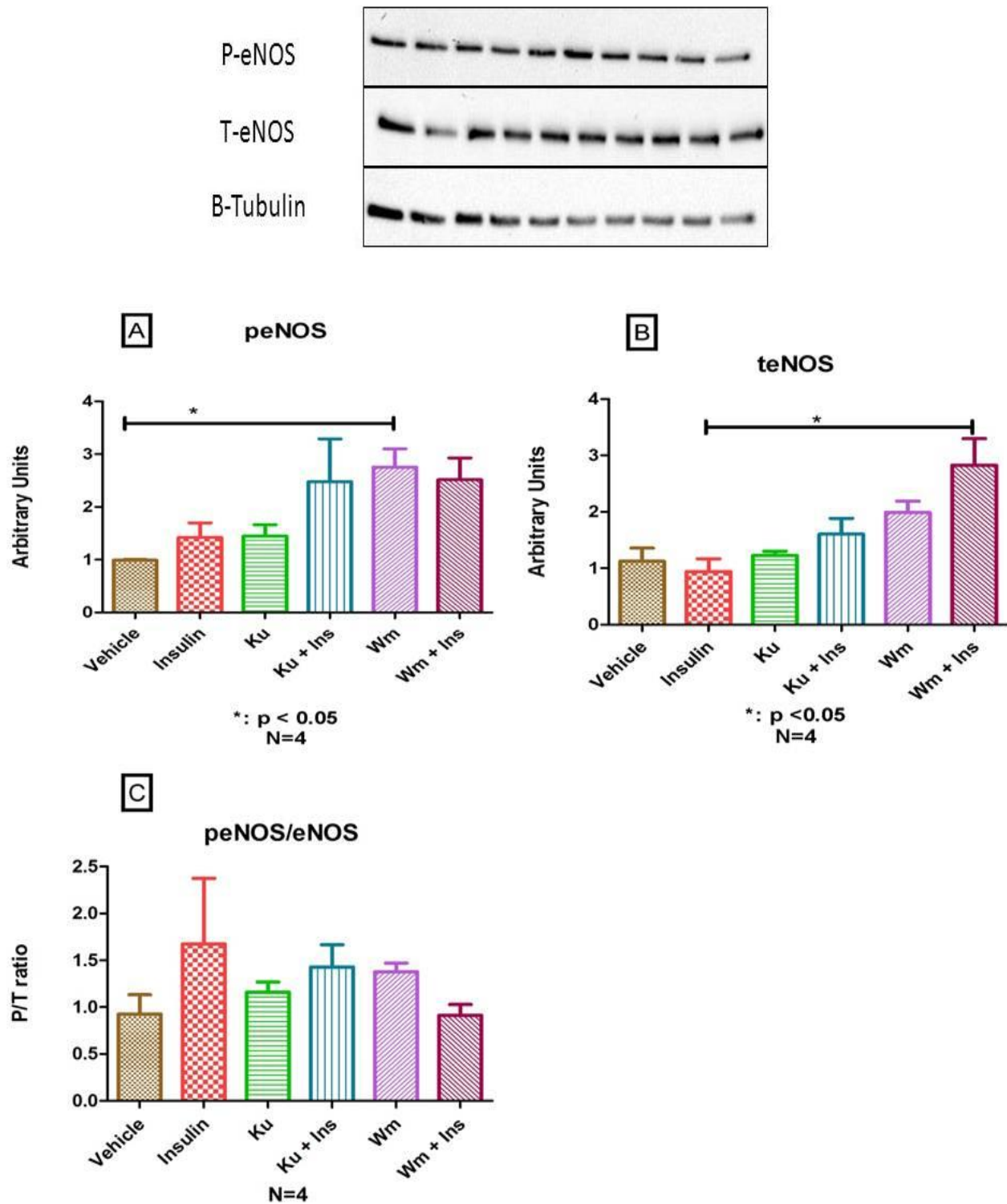


Figure 6.9: eNOS protein activation and inhibition. (A) Phosphorylated eNOS, (B) total eNOS and (C) the phosphorylated/total eNOS ratio after the stimulation with insulin, Ku-60019 and wortmannin with or without insulin respectively. All data were corrected for  $\beta$ -tubulin.

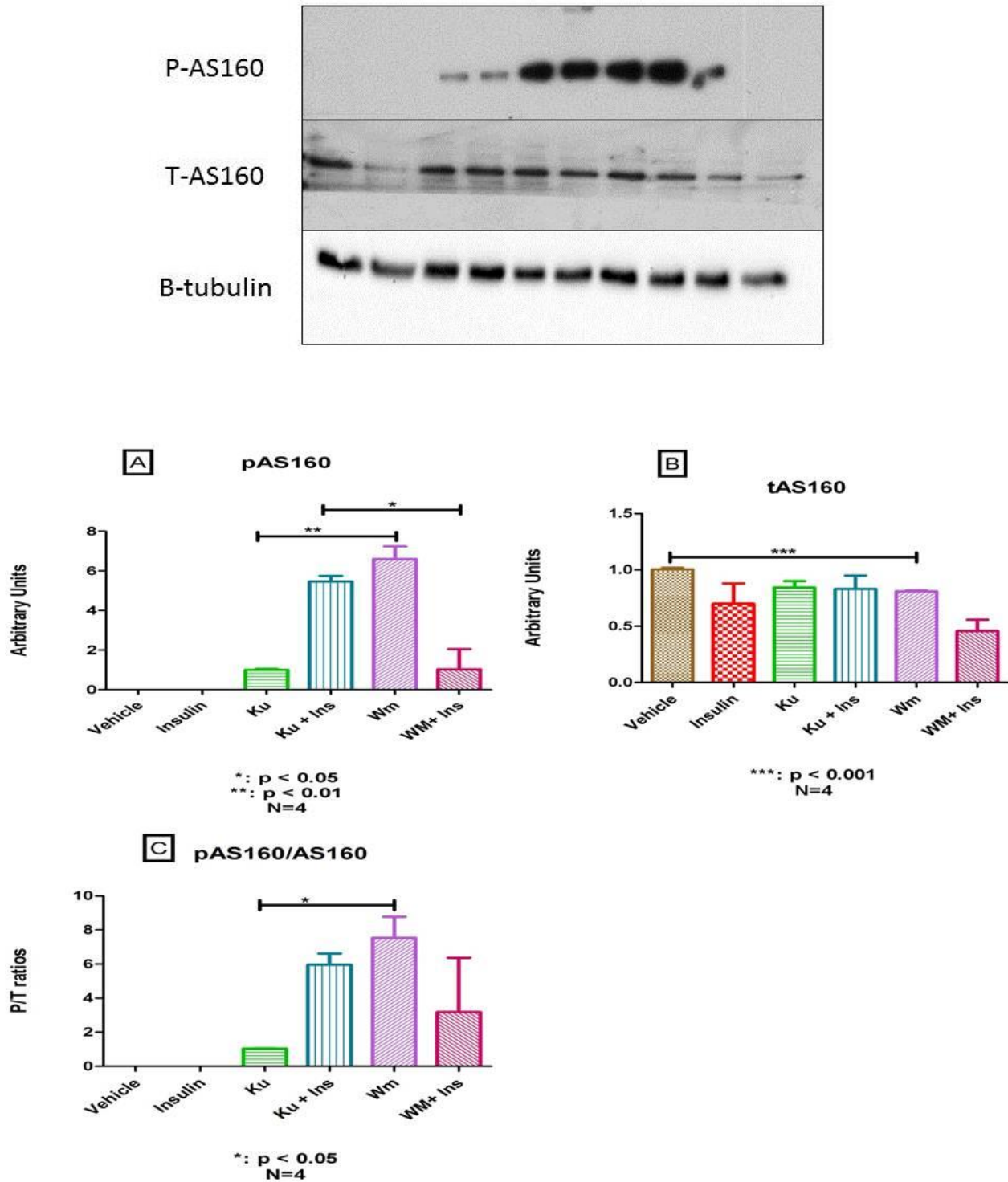


Figure 6.10: AS160 protein activation and inhibition (A) Phosphorylated as160, (B) total AS160 and (C) the phosphorylated/total AS160 ratio after the stimulation with insulin, Ku-60019 and wortmannin with or without insulin respectively. All data were corrected for  $\beta$ -tubulin.

### 6.3. Summary and Discussion

PKB/Akt and AMPK kinase are two proteins both involved in NO production and glucose utilization by endothelial cells. The shared effector proteins are the eNOS enzyme and AS160 respectively. Insulin is known to activate PKB/Akt via PI3-K but recently it has been postulated that ATM activation may be a prerequisite for PKB/Akt activation [Shiloh, 2003 and Ching et al., 2013]. As discussed in the literature review, ATM activity may therefore be important in endothelial function or dysfunction. This part of the current study utilized insulin as activator of these pathways and Ku-60019 as a specific ATM inhibitor. Wortmannin, well known for its ability to inhibit PI3-K, also has inhibitory effects on ATM at the concentrations used [Menotta et al., 2012; Yang and Kastan, 2000]. Measurement of the activity and expression of the proteins involved in these signalling pathways was used to try to dissect possible interactions.

It was firstly demonstrated that stimulation of AEC's with insulin resulted in both PKB/Akt and eNOS phosphorylation. As it is known that 100 nM insulin is a pharmacological concentration that masks any synergistic effects, therefore 10 nM insulin was used in this study. Additionally, the concentration of insulin used in this study was not based on whether the 10 nM or 100 nM insulin concentrations caused the more significant increase in phosphorylated PKB/Akt and eNOS or in P/T PKB/Akt and eNOS ratios. But was the lowest concentration which could be used that caused an increase in the P/T ratio of both PKB/Akt and eNOS.

Stimulating AEC's with 10 nM insulin resulted in enhanced phosphorylation of the P85 regulatory subunit of PI3-K that was indeed inhibited by wortmannin but not by Ku indicating that the effect of insulin on PI3-K is not mediated by ATM. However, Ku alone also enhanced phosphorylation of P85 indicating that the ATM protein may indeed interact with PI3-K by attenuating its activity under basal conditions [Vinięgra et al., 2005].

The effect of insulin was accompanied by phosphorylation of PKB/Akt that was again inhibited by wortmannin, probably through the inhibition of PI3-K, but not by Ku, indicating again that the phosphorylation of PKB/Akt by insulin in endothelial cells is not mediated by ATM. Still distal to PKB/Akt in the insulin-signalling pathway is the phosphorylation of GSK3 $\beta$ , measured as a read out of PKB/Akt activity. Indeed, stimulation with 10 nM insulin also resulted in phosphorylation of GSK3 $\beta$  that was inhibited by wortmannin, but in this instance, also by Ku indicating that events downstream of PKB/Akt activation is affected by ATM. The ratio of phospho/total GSK3 $\beta$  corroborates this as it was enhanced with insulin and attenuated by wortmannin but inhibition of ATM by Ku also enhanced this ratio. This may indicate that ATM has an inhibitory effect on the actions of activated PKB/Akt or it may also be that ATM normally regulates the expression of GSK3 $\beta$ . It is known that the expression of GSK3 $\beta$  is regulated by PKB/Akt and vice versa through the activity of the Wnt signalling pathway [Wymann and Marone; 2005].

As no effects of any intervention were seen on the phosphorylation of expression of PTEN, it was concluded that this phosphatase did not play a role in any of the effects investigated. However, our results showed a downregulation of PTEN expression induced by stimulation with 10 nM Insulin, corroborating previous reports that there exists a negative feedback mechanism on PKB/Akt activity through the PI3-K-PKB/Akt-mTOR pathway on the level of PTEN expression [Song et al., 2012 and Yu, Y. et al., 2011].

The expected attenuation of phosphorylation of AMPK through inhibition by PKB/Akt was observed after stimulation with 10 nM insulin but because insulin also resulted in lower expression of AMPK, the phospho/total ratio was significantly enhanced. Not only was the insulin-stimulated effect inhibited by inhibition of ATM but Ku alone also attenuated the phospho/total AMPK ratio confirming previous observations that ATM leads to activation of AMPK [Fu et al., 2008]. In addition, both wortmannin and Ku resulted in lower expression



of AMPK. This effect may be because both inhibitors will inhibit the activity of ATM which is known to regulate the expression of AMPK through activation of P53 [Armata et al., 2010].

Stimulation of AEC's with 10 nM insulin did not result in either phosphorylation or expression of ATM itself. However, the phospho/total ratio clearly showed that 100 nM wortmannin significantly attenuated the activation of ATM corroborating previous observations [Goodarzi and Lees-Miller, 2004.]

10 nM insulin could in the end not stimulate the phosphorylation of eNOS significantly. A small effect of inhibition of both PI3-K and ATM with wortmannin was observed as this was manifested in the phospho/total ratio of activity.

Conflicting results were also obtained at the level of phosphorylation of AS160 as, unexpectedly; wortmannin resulted in enhanced phosphorylation of AS160 as well as an increased phospho/total ratio. It is possible that inhibition of the activity of PKB/Akt may enhance activity of AMPK as also shown in Fig 6.8A and that AMPK may then phosphorylate AS160. This result would then lead us to conclude that, in AEC's; the AMPK pathway has a much stronger effect on AS160 activity than insulin via PKB/Akt. This is an observation that may be further investigated in future. An additional observation was that 10 nM insulin was not enough to enhance AS160 phosphorylation but simultaneous inhibition of ATM enhanced the effect of insulin, now resulting in significant phosphorylation. This again points to our previous conclusion that ATM has an inhibitory effect on the actions of PKB/Akt. In addition, we demonstrated that inhibition of PI3-K-PKB/Akt attenuated AS160 expression in AECs.



## Chapter 7: Discussion and Conclusion

### 7.1. Literature review

Ataxia telangiectasia (AT) is a well-characterized neurodegenerative disease and most of the nuclear functions of the ataxia telangiectasia mutated (ATM) protein has been investigated. The localization, role and function in various tissue types including neurons [Li et al., 2009 and Marinoglou, 2012] have been investigated extensively in AT patients and AT animal models.

After the well-established function of ATM in the nucleus was concluded, researchers began to investigate the role of ATM in oxidative stress, associating oxidative stress with DNA damage, mitochondrial DNA damage and dysfunction as well as mitochondrial uncoupling [Madamanchi et al., 2010; Mookerjee et al., 2010 and Yu et al., 2013]. Many researchers have designated the function of ATM in the mitochondria to be that of an oxidative stress sensor that activates other proteins to alleviate and down regulate the detrimental effects of oxidative stress.

In the current study, the role of ATM was investigated in AECs. Few studies have explored the function of the ATM protein in the cytosol in relation to glucose homeostasis, insulin sensitivity and diabetes among ATM null (ATM<sup>-/-</sup>), ATM heterozygous (ATM<sup>+/-</sup>) and ATM wild type (ATM<sup>+/+</sup>) tissue types. Often in tissue culture studies, disease states have to be simulated via *in vitro* induction by for example the addition of pharmacological inhibitors or inflammatory cytokines. Very little data is available on experiments completed in tissue culture whereby AECs were isolated from animal or human models with pathologies such as diet induced insulin resistance, diabetes or atherosclerosis. Therefore, the first aim of the present study was not only to isolate a pure aortic endothelial culture but also to

establish a method of isolating AECs that would consistently yield a pure culture of AECs. Flowing from this first aim, and depending on its success, we aimed to isolate AECs from diseased animals that are insulin resistant, diabetic; hyperglycaemic, obese and may have other symptoms of the metabolic syndrome.

## **7.2. Aortic endothelial cell (AEC) isolation**

The data presented in chapter 4 indicates that our attempts to isolate AECs from healthy adult male Wistar rats were reasonably successful. A major advantage of setting up an in-house endothelial cell isolation technique is the fact that the researcher can conduct experiments on true primary cells that have not been exposed to multiple passages and storage in liquid nitrogen for long periods before they are used. Another advantage is that of saving of time and money as it eliminates the necessity to buy commercially available endothelial cells and passage them into respective parental groups as described in figure 3.3. However, most importantly, is the possibility of isolating these cells from diseased animals and age matched controls in order to observe physiological differences in protein expression and function of the AECs without inducing these pathologies *in vitro*.

The limitations experienced in the present research project included the inconsistency in obtaining a pure AEC culture, particularly experienced with the vascular ring model. The biggest set-back, however, was the lack of detectable eNOS expression as observed in the western blots (figure 4.10). Furthermore, determining the non-endothelial cell types that contaminate the cell cultures has proven to be difficult because often smooth muscle cells, fibroblasts and endothelial cells possess a few of the same protein markers making the search for anti-fibroblast or anti-smooth muscle cell specific antibodies even harder. According to Azuma et al. (2009) thoracic AECs both *in vitro* and *in vivo* have the potential

to transdifferentiate into smooth muscle cells and that some of the endothelial cells both in the aorta or after isolation by means of enzyme digestion possess both endothelial cell markers and smooth muscle cell markers [Azuma et al., 2009]. Unfortunately, we were therefore unable to meet all the strict criteria we had set for ourselves, and the lack of detectable expression of the eNOS protein resulted in the decision to rather conduct the experiments in the second part of the study on commercially purchased AECs.

### **7.3. Nitric oxide production and AEC viability in response to insulin, Ku-60019 and wortmannin**

As observed in figure 5.3 there was a significant increase in NO production when the ATM protein was inhibited by Ku-60019. The beneficial impact of increased NO production (especially eNOS-derived) includes maintaining vascular homeostasis, promoting angiogenesis, initiating DNA repair by activating p53 [Goodman et al., 2004], inhibiting smooth muscle cell proliferation and many other functions in the respiratory system, inflammation responses and nervous system [Mian et al., 2013]. Conversely, high (excessive) NO concentrations can be harmful as it readily reacts with superoxide anions to generate peroxynitrite. According to Munoz et al. (2009), reactive oxygen species (ROS) and reactive nitrogen species (RNS) can exert both protective and harmful effects. Examples of these include cell death due to high concentrations of ROS, preconditioning by the heart towards ischemic injury or “sudden death” in response to ischemia-reperfusion [Munoz et al., 2009]. As observed in figure 5.2 the effects of Ku-60019, wortmannin and insulin treatment did not significantly affect the viability of the AECs. As the AECs were only exposed to Ku-60019 and wortmannin for 30 min and insulin for 15 min it is unknown, what prolonged exposure to these inhibitors or insulin will do to the viability of the AECs or their production of NO in a time dependent manner.

The increase in NO production observed by the inhibition of ATM as is in chapter 5 may not be a result of eNOS activation alone, as according to the western blot data (figure 6.9) inhibition of ATM by Ku-60019 did not affect the phosphorylation and activity of the eNOS protein. This could suggest that the inhibition of the ATM protein in the AECs may lead to the activation of one of the other NOS isoforms (iNOS or nNOS). One of the unexplained results in our study is that inhibition of ATM with Ku resulted in a significant increase in NO production. As this is totally contrary to what we expected, this observation will be further investigated because it indicates a significant regulatory role for ATM in AECs and possibly its vasoconstrictory effects.

#### **7.4. The relationship between ATM and eNOS function in the insulin-signalling pathway.**

We have demonstrated for the first time, a relationship between endothelial ATM protein kinase and the generation of NO. The study was expanded to investigate central proteins that may be involved in this reaction. The signalling pathways involved in NO production and glucose utilization form a network of interrelationships. Central to both pathways is the activity of 2 protein kinases, PKB/Akt and AMPK. Both these kinases are known to phosphorylate the eNOS enzyme to produce NO on the one hand and AS160 to induce GLUT 4 translocation and glucose uptake on the other hand. Activation of the ATM protein is postulated to be a prerequisite for PKB/Akt activation and it may result in activation of AMPK.

A second important observation was that inhibition of ATM significantly enhanced phosphorylation of the p85 regulatory subunit of PI3-K. This would imply that ATM

normally has an inhibitory effect on p85 phosphorylation and therefore PI3-K activation. We base this assumption on previous publications showing that Ku does not inhibit PI3-K [Vecchio et al., 2014]. This again indicates that ATM has a hitherto unexplored regulatory role in endothelial function.

## **7.5. Conclusion**

In the present study it has been established that the AECs express the ATM protein. Unexpectedly, ATM inhibition by Ku-60019 increased NO production within the AECs without significantly increasing the phosphorylation of eNOS in the PI3-K signalling pathway. In addition to this, inhibition of the ATM protein did not result in a decrease in PKB/Akt phosphorylation indicating that the interaction between PKB/Akt and eNOS within the PI3-K signalling pathway is quite complex and requires further investigation into the exact mechanisms by which ATM regulates PKB/Akt and eNOS.

## References

Al-Rubeai, M., Welzenbach, K., Lloyd, D.R. and Emery, A.N. "A Rapid Method for Evaluation of Cell Number and Viability by Flow Cytometry" *Cytotechnology* 24 (1997) 161-168.

Amatya, P.N., Kim, H., Park, S., Youn, C., Hyun, J., Chang, I., Lee, J., You, H. "A Role of DNA-Dependent Protein Kinase for the Activation of AMP-Activated Protein Kinase in Response to Glucose Deprivation" *Biochimica et Biophysica Acta* 1823 (2012) 2099–2108.

Andrisse, S., Koehler, R.M., Chen, J.E., Patel, G.D., Vallurupalli, V.R., Ratliff, B.A., Warren, D.E., Fisher, J.S. "Role of GLUT1 in Regulation of Reactive Oxygen Species" *Redox Biology* 2 (2014) 764–771.

Armata, H.L., Golebiowski, D., Jung, D. Y., Ko, H.J., Kim, J.K. and Sluss, H. K. "Requirement of the ATM/p53 Tumor Suppressor Pathway for Glucose Homeostasis" *Molecular And Cellular Biology* 30 (2010) 24:5787–5794.

Azuma, K., Ichimura, K., Mita, T., Nakayama, S., Jin, W.L., Hirose, T., Fujitani, Y., Sumioshi, K., Shimada, K., Daida, H., Sakai, T., Mitsumata, M., Kawamori, R. and Watada, H. "Presence of  $\alpha$ -Smooth Muscle Actin-Positive Endothelial Cells in the Luminal Surface of Adult Aorta" *Biochemical and Biophysical Research Communications* 380 (2009) 620–626.

Bakkenist, C.J. and Kastan, M.B. "DNA Damage Activates ATM through Intermolecular Autophosphorylation and Dimer Dissociation" *Nature* 421 (2003) 499-506.

Basu, S.K., Goldstein, J.L., Anderson, R.G.W. and Brown, M.S. "Degradation of cationized low density lipoprotein and regulation of cholesterol metabolism in homozygous familial hypercholesterolemia fibroblasts" *Cell Biology* 73 (1976) 3178-3182.

Bensimon, A., Aebersold, R. and Shiloh, Y. "Beyond ATM: The Protein Kinase Landscape of the DNA Damage Response" *FEBS Letters* 585 (2011) 1625-1639.

Bradford, M.M. "A Rapid and Sensitive Method for the Quantification of Microgram Quantities of Protein Utilizing the Principle of Protein-Dye Binding" *Analytical Biochemistry* 72 (1976) 248-254.

Bretón-Romeros, R. and Lamas, S. "Hydrogen Peroxide Signaling in Vascular Endothelial Cells" *Redox Biology* 2 (2014) 529-534.

Carnicer, R., Crabtree, M.J., Sivakumaran, V., Casadei, B., and Kass, D.A. "Nitric Oxide Synthases in Heart Failure" *Antioxidants & Redox Signaling* 18 (2013) 9:1078-1099.

Chao, W.T., Fan, S.S., Chen, J.K. and Yang, V.C. "Visualizing Caveolin-1 and HDL in Cholesterol-Loaded Aortic Endothelial Cells" *Journal of Lipid Research* 44 (2003) 1094-1099.

Chen, B.P.C., Li, M., Asaithamby, A. "New Insights into the Roles of ATM and DNA-Pkcs in the Cellular Response to Oxidative Stress" *Cancer Letters* 327 (2012) 103-110.

Chen, C., Zhang, L., Huang, N., Huang, B. and Kornbluth, S. "Suppression of DNA-Damage Checkpoint Signaling by Rsk-Mediated Phosphorylation of Mre11" *PNAS* 110 (2013) 51:20605–20610.

Chen, S., Segal, M. and Agarwal, A. "Lumen Digestion" Technique for Isolation of Endothelial Cell from Heme Oxygenase-1 Knockout mice" *BioTechniques* 37 (2004) 84-89.

Chen, X., Chen, Q., Wang, L. and Li, G. "Ghrelin induces cell migration through GHSR1a-Mediated PI3-K/Akt/eNOS/NO Signaling Pathway in Endothelial Progenitor Cells" *Metabolism Clinical and Experimental* 62 (2013) 743-752.

Ching, J.K., Luebbert, S.H., Collins IV, R.L., Zhang, Z., Marupudi, N., Banerjee, S., Hurd, R.D., Ralston, L. and Fisher, J.S. "Ataxia Telangiectasia Mutated Impacts Insulin-Like Growth Factor-1 Signalling in Skeletal Muscle" *Experimental Physiology* 98 (2013) 2:526–535.

Coyle, C.H., Martinez, L.J. Coleman, M. C. Spitz, D. R., Weintraub, N.L. and Khalid N. Kader, K.N. "Mechanisms of H<sub>2</sub>O<sub>2</sub>-Induced Oxidative Stress in Endothelial Cells" *Free Radical Biology & Medicine* 40 (2006) 2206–2213.

D'Souza, A.D., Parish. A.I., Krause, D.S., Kaech, S.M. and Shadel, G.S. "Reducing Mitochondrial ROS Improves Disease-related Pathology in a Mouse Model of Ataxia-Telangiectasia" *The American Society of Gene & Cell Therapy* 21 (2013) 1:42–48.

Dandona, P. and Aljada, A. "A Rational Approach to Pathogenesis and Treatment of Type 2 Diabetes Mellitus, Insulin Resistance, Inflammation, and Atherosclerosis" *The American Journal of Cardiology* 90 (2002) 5A:27G-33G.

Ditch, S. and Paull, T.T. "The ATM Protein Kinase and Cellular Redox signalling: Beyond the DNA Damage Response" *Trends in Biochemical Sciences* 37 (2012) 1:15-22.

Duan, X., Ponomareva, L., Veeranki, S. and Choubey, D. "IFI16 Induction by Glucose Restriction in Human Fibroblasts Contributes to Autophagy through Activation of the ATM/AMPK/p53 Pathway" *PLoS ONE* 6 (2011) 5:e19532- e19532.



Eguez, L., Lee, A., Chavez, J.A., Miinea, C.P., Kane, S., Lienhard, G.E. "Full Intracellular Retention of GLUT4 Requires AS160 Rab GTPase Activating Protein" *Cell Metabolism* 2 (2005) 263-272.

Förstermann, U. and Sessa, W.C "Nitric Oxide Synthases: Regulation and Function" *European Heart Journal* 33 (2012) 829–837.

Fu., X., Wan., S., Lyu, Y.L., Liu, L.F. and Qi, H. "Etoposide Induces ATM-Dependent Mitochondrial Biogenesis through AMPK Activation" *PLoS ONE* 3 (2008) 4:1-10.

Genis, A. "Exposure of Cardiac Microvascular Endothelial Cells to Harmful Stimuli: A Study of the Cellular Responses and Mechanisms" Stellenbosch University (2014) 1-469.

Gingras, A., Kennedy, S.G., O'Leary, M.A., Sonenberg, N. and Hay, N. "4E-BP1, a Repressor Of mRNA Translation, is Phosphorylated And Inactivated by the Akt(PKB) Signaling Pathway" *Genes and Development* 12 (1998) 502–513.

Golding, S.E., Rosenberg, E., Valerie, N., Hussaini, I., Frigerio,, M., Cockcroft,, X.F., Chong,, W.Y., Hummersone, M., Rigoreau, L., Meneer, K.A., O'Connor, M.J., Povirk, L.F., van Meter, T. and Valerie, K. "Improved ATM Kinase Inhibitor KU-60019 Radiosensitizes Glioma Cells, Compromises Insulin, AKT and ERK Prosurvival Signaling, and Inhibits Migration and Invasion" *Molecular Cancer Therapeutics* 8 (2009) 10:2894-2902.

Goodarze, A.A. and Lees-Miller, S.P. "Biochemical characterization of the ataxia-telangiectasia mutated (ATM) protein from human cells" *DNA repair* 3 (2004) 753-767.

Goodman, J.E., Hofseth, L.J., Hussain, S.P. and Harris, C.C. "Nitric Oxide and p53 in Cancer-Prone Chronic Inflammation and Oxyradical Overload Disease" *Environmental and Molecular Mutagenesis* 44 (2004) 3–9.

Gordon, E.L., Danielsson, P.E., Nguyen, T. and Winn, H.R. "A Comparison of Primary Cultures of Rat Cerebral Microvascular Endothelial Cells to Rat Aortic Endothelial Cells" *In Vitro Cellular & Developmental Biology* 27A (1991) 312-326.

Greiwe, J.S., Kwon, G., McDaniel, M.L. And Semenkovich, C.F. "Leucine and Insulin Activate P70 S6 Kinase through Different Pathways in Human Skeletal Muscle" *American Journal of Physiology –Endocrinology and Metabolism* 281 (2001) E466–E471.

Guo, Z., Deshpande, R. and Paull, T.T. "ATM Activation in the Presence of Oxidative Stress" *Cell Cycle* 9 (2010) 24:4805-4811.

Halaby, M., Hibma, J.C., He, J. and Yang, D. "ATM Protein Kinase Mediates full Activation of Akt and Regulates Glucose Transporter 4 Translocation by Insulin in Muscle Cells" *Cellular Signalling* 20 (2008) 1555–1563.

Hammond, E.M. and Giaccia A.J. "The Role of ATM and ATR in the Cellular Response to Hypoxia and Re-oxygenation" *DNA Repair* 3 (2004) 1117-1122.

He, A., Liu, X., Liu, L., Chang, Y., Fang, F. "How Many Signals Impinge on GLUT4 Activation by Insulin?" *Cellular Signalling* 19 (2007) 1-7.

Hemmings, B.A. and Restuccia, D.F. "PI3-K-PKB/Akt Pathway" *Cold Spring Harb Perspect Biol* 4 (2012) 1-3.

Hickson, I., Zhao, Y., Richardson, C.J., Green, S.J., Martin, N.M.B., Orr, A.I., Reaper, P.M., Jackson, S.P., Curtin, N.J. and Smith, G.C.M. "Identification and Characterization of a Novel and Specific Inhibitor of the Ataxia-Telangiectasia Mutated Kinase ATM" *American Association for Cancer Research* 64 (2004) 9152–9159.

Hirsch, E., Costa, C. and Ciruolo, E. "Phosphoinositide 3-Kinase as a Common Platform for Multi-Hormone Signaling" *Journal of Endocrinology* 194 (2007) 243-256

Hotamisligil, G.S., Peraldi, P., Budavari, A., Ellis, R., White M.F., Spiegelman, B.M. "IRS-1 Mediated Inhibition of Insulin Receptor Tyrosine Kinase Activity in TNF-alpha and Obesity-Induced Insulin Resistance" *Science* 271 (1996) 665-668.

Hu, S., Song, Z., Zheng, Q and Nie, J. "Differences in the Primary Culture, Purification and Biological Characteristics Between Endothelial Cells and Smooth Muscle Cells from Rat Aorta" *Journal of Nanjing Medical University* 23 (2009) 4:241-246.

Huang, X., Sun, M., Li, D., Liu, J., Guo, H., Dong, Y., Jiang, L., Pan, Q., Man, Y., Wang, S. and Li, J. "Augmented NADPH oxidase activity and p22phox expression in monocytes underlie oxidative stress of patients with type 2 diabetes mellitus" *Diabetes Research and Clinical Practice* 91 (2011) 371-380.

Irrazabal CE., Burg MB., Ward SG. and Ferraris JD. "Phosphatidylinositol 3-Kinase Mediates Activation of ATM by High NaCl and by Ionizing Radiation: Role in Osmoprotective Transcriptional regulation" *PNAS* 103 (2006) 23:8e cell882-8887.

Jackson, S.P. and Bartek, J. "The DNA-Damage Response in Human Biology and Disease" *Nature* 461(2009) 1071-1078.

Jaffe, E.A., Nachman, R.L., Becker, C.G. and Minick, C.R. "Culture of Human Endothelial Cells Derived from Umbilical Veins" *The Journal of Clinical Investigation* 52 (1973) 2745-2756.

Jensen, J., Rustad, P.I., Kolnes, A.J. and Lai, Y. "The Role of Skeletal Muscle Glycogen Breakdown for Regulation of Insulin Sensitivity By Exercise" *Frontiers in Physiology* 2 (2011) 112:1-11.

Joshi, M.S., Berger, P.J., Kaye, D.M., Pearson, J.T., Bauer, J.A., Ritchie, R.H. "Functional Relevance of Genetic Variations of Endothelial Nitric Oxide Synthase and Vascular Endothelial Growth Factor in Diabetic Coronary Microvessel Dysfunction" *The Authors Clinical and Experimental Pharmacology and Physiology* © (2013) Wiley Publishing Asia Pty Ltd.

Kerr, B.A. and Byzova T.V. "The Dark Side of the Oxidative Force in Angiogenesis" *Nature Medicine* 18 (2012) 1184–1185.

Khalil, H.S., Tummala, H., Chakarov, S., Zhelev, N., Lane, D.P. "Targeting ATM Pathway for Therapeutic Intervention in Cancer" *Bio. Discovery* 1 (2012) 1-13.

Khang, YH., Cho, S., Kim, HR. "Risks for Cardiovascular Disease, Stroke, Ischaemic Heart Disease, and Diabetes Mellitus Associated with the Metabolic Syndrome using the new Harmonised Definition: Findings from Nationally Representative Longitudinal Data From an Asian Population" *Atherosclerosis* 213 (2010) 579–585.

Khanna, K., Lavin, M.F. Jackson, S. P. and Mulhern. T.D. "ATM, a Central Controller of Cellular Responses to DNA Damage" *Cell Death and Differentiation* 8 (2001) 1052-1065.

Kobayashi, M., Inoue, K., Warabi, E., Minami, T and Kodama, T. "A Simple Method of Isolating Mouse Aortic Endothelial Cells" *Journal of Atherosclerosis and Thrombosis* 12 (2005) 138-142.

Kobayashi, T., Taguchi, K., Takenouchi, Y., Matsumoto, T. and Kamata, K. "Insulin-Induced Impairment via Peroxynitrite Production of Endothelium-Dependent Relaxation and Sarco/Endoplasmic Reticulum Ca<sup>2+</sup> - ATPase Function in Aortas from Diabetic Rats" *Free Radical Biology & Medicine* 43 (2007) 431–443.

Kreisel, D., Krupnick, A.S., Szeto, W.Y., Popma, S.H., Sankaran, D., Krasinskas, A.M., Amin, K.M. and Rosengard, B.R. "A Simple Method for Culturing Mouse Vascular Endothelium" *Journal of Immunological Methods* 254 (2001) 31-45.

Kubota, T., Kubota, N., Kumagai, H., Yamaguchi, S., Kozono, H., Takahashi, T., Inoue, M., Itoh, S., Takamoto, I., Sasako, T., Kumagai, K., Kawai, T., Hashimoto, S., Kobayashi, T., Sato, M., Tokuyama, K., Nishimura, S., Tsunoda, M., Ide, T., Murakami, K., Yamazaki, T., Ezaki, O., Kawamura, K., Masuda, H., Moroi, M., Sugi, K., Oike, Y., Shimokawa, H., Yanagihara, N., Tsutsui, M., Terauchi, Y., Tobe, K., Nagai, R., Kamata, K., Inoue, K., Kodama, T., Ueki, K. and Kadowaki, T. "Impaired Insulin Signaling in Endothelial Cells Reduces Insulin-Induced Glucose Uptake by Skeletal Muscle" *Cell Metabolism* 13 (2011) 294–307.

Kuliszewski, M.A., Ward, M.R., Kowalewski, J.W., Smith, A.H., Stewart, D.J., Kutryk, M.J., Leong-Poi, H. "A Direct Comparison of Endothelial Progenitor Cell Dysfunction in Rat Metabolic Syndrome and Diabetes" *Atherosclerosis* 226 (2013) 58-66.

Kuo, W.W., Huang, C.Y., Chung, J.G., Yang, S.F., Tsai, K.L., Chiu, T.H., Lee, S.D. and Ou, H.C. "Crude Extracts of *Solanum Lyratum* Protect Endothelial Cells Against Oxidized Low-Density Lipoprotein-Induced Injury by Direct Antioxidant Action" *Journal of Vascular Surgery* 50 (2009), 4:849-860.

Levine, A.J., Munoz-Sanjuan, I., Bell, E., North, A.J. and Brivanlou, A.H. "Fluorescent Labeling of Endothelial Cells Allows in Vivo, Continuous Characterization of The Vascular Development of *Xenopus Laevis*" *Developmental Biology* 254 (2003) 50–67.

Li, C and Keaney Jr, J.F. "AMP-Activated Protein Kinase: A Stress-Responsive Kinase with Implications for Cardiovascular Disease" *Current Opinion in Pharmacology* 10 (2010) 111–115.

Li, H., Horke, S. and Forstermann, U. "Vascular Oxidative Stress, Nitric Oxide and Atherosclerosis" *Atherosclerosis* 237 (2014) 208-219.

Li, J., Han, Y.R., Plummer, M.R. and Herrup, K. "Cytoplasmic ATM in Neurons Modulates Synaptic Function" *Current Biology* 19 (2009) 24: 2091–2096.

Li, Y. and Yang, D. "The ATM Inhibitor KU-55933 Suppresses Cell Proliferation and Induces Apoptosis by Blocking Akt in Cancer Cells with Overactivated Akt" *Molecular Cancer Therapy* 9 (2010) 1:113-125.

Liu, H., Yang, H., Wang, D., Liu, Y., Liu, X., Li, Y., Xie, L. and Wang, G. "Insulin Regulates P-Glycoprotein in Rat Brain Microvessel Endothelial Cells via an Insulin Receptor-Mediated PKC/NF-KB Pathway but not a PI3K/Akt Pathway" *European Journal of Pharmacology* 602 (2009) 277–282.

López-Figueroa, M.O., Caamaño, C., Marin, R., Guerra, B., Alonso, R., Morano, M. I., Akil, H. and Watson, S.J. "Characterization of Basal Nitric Oxide Production in Living Cells" *Biochimica et Biophysica Acta* 1540 (2001) 253-264.

Madamanchi, N.R., Zhou, R., Vendrov, A.E., Niu, X. and Runge, M.S. "Does Oxidative DNA Damage Cause Atherosclerosis and Metabolic Syndrome? New Insights into Which Came First – the Chicken or the Egg" *Circ Res.* 107 (2010) 8: 940–942.

Magid, R., Martinson, D., Hwang, J., Jo, H. and Galis, Z.S. "Optimization of Isolation and Functional Characterization of Primary Murine Aortic Endothelial Cells" *Endothelium* 10 (2003) 103-109.

Mahmoudi, M., Mercer, J., Bennett, M. "DNA damage and repair in atherosclerosis" *Cardiovascular Research* 71 (2006) 259 – 268.

Marin, V., Kalpnaski, G., Grès, S., Farnarier, C. and Bongrand, P. "Endothelial Cell Culture: Protocol to Obtain and Cultivate Human Umbilical Endothelial Cells" *Journal of Immunological Methods* 254 (2001) 183-190.

Marinoglou, K. "The Role of The DNA Damage Response Kinase Ataxia Telangiectasia Mutated in Neuroprotection" *Yale Journal of Biology and Medicine* 85 (2012) 469-480.

Mead, JR. and Ramji, DP. "The Pivotal Role of Lipoprotein Lipase in Atherosclerosis" *Cardiovascular Research* 55 (2002) 261–269.

Menotta, M., Biagiotti, S., Bianchi, M., Chessa, L. and Magnani, M. "Dexamethasone Partially Rescues Ataxia Telangiectasia-mutated (ATM) Deficiency in Ataxia Telangiectasia by Promoting a Shortened Protein Variant Retaining Kinase Activity" *The Journal of Biological Chemistry* 287 (2012) 49:41352–41363.

Mercer, J.R., Cheng, K.K., Figg, N., Gorenne, I., Mahmoudi, M., Griffin, J., Vidal-Puig, A., Logan, A., Murphy, M.P. and Bennett, M. "DNA Damage Links Mitochondrial Dysfunction to Atherosclerosis and the Metabolic Syndrome" *Circulation Research* 107 (2010) 1021-1031.

Mian A.I., Aranke, M. and Bryan, N.S. "Nitric Oxide and its Metabolites in the Critical Phase of Illness: Rapid Biomarkers in the Making" *The Open Biochemistry Journal* 7 (2013) 24-32.

Miles, P.D., Treuner, K., Latronica, M., Olefsky, J.M. and Barlow, C. "Impaired Insulin Secretion in a Mouse Model of Ataxia Telangiectasia" *American Journal of Physiology-Endocrinology and Metabolism* 293 (2007) E70–E74.

Mookerjee, S.A., Divakaruni, A.S., Jastroch, M and Brand, M.D. "Mitochondrial Uncoupling and Lifespan" *Mechanism of Aging and Development* 131 (2010) 463-472.

Mukherjee, A., Misra, S., Howlett, N.G. and Karmakar, P. "Multinucleation Regulated by the Akt/PTEN Signaling Pathway is a Survival Strategy for Hepg2 Cells" *Mutation Research* 755 (2013) 135– 140.

Munoz, J.P., Chiong, M., L García, L., Troncoso, R., Toro, B., Pedrozo, Z., Diaz-Elizondo, J., Salas, D., Parra, V., Núñez, M.T., Hidalgo, C. and Lavandero, S. "Iron Induces Protection and Necrosis in Cultured Cardiomyocytes: Role of Reactive Oxygen Species and Nitric Oxide" *Free Radical Biology & Medicine* 48 (2010) 526–534.

Nickenig, G. and Harrison, D.G. "The AT1-Type Angiotensin Receptor in Oxidative Stress and Atherogenesis : Part I: Oxidative Stress and Atherogenesis" *Circulation* 105 (2002) 393-396.

Nicoletti, I., Migliorati, G., Pagliacci, M.C., Grignani, F. and Riccardi, C. "A Rapid and Simple Method for Measuring Thymocyte Apoptosis by Propidium Iodide Staining and Flow Cytometry" *Journal of Immunological Methods* 139 (1991) 2:271-279.

Nicosia, R.F., Villaschi, S. and Smith, M. "Isolation and Characterization of Vasoformative Endothelial Cells from the Rat Aorta" " *In Vitro Cellular & Developmental Biology* 30A (1994) 394-399.

Ousset M., Bouquet, F., Fallone, F., Biard, D., Dray, C., Valet, P., Salles, B., Muller, C. "Loss of ATM Positively Regulates the Expression of Hypoxia Inducible Factor 1 (HIF-1) Through Oxidative Stress: Role in the Physiopathology of the Disease" *Cell Cycle* 9 (2010) 14: 2814-2822.

Pajunen, P., Rissanen, H., Härkänen, T., Jula, A., Reunanen, A., Salomaa, V. "The Metabolic Syndrome as a Predictor of Incident Diabetes and Cardiovascular Events in the Health 2000 Study" *Diabetes & Metabolism* 36 (2010) 395–401.



Peretz, S., Jensen, J., Baserga, R. and Glazer, P.M. "ATM-Dependent Expression of the Insulin-Like Growth Factor-I Receptor in a Pathway Regulating Radiation Response" *PNAS* 98 (2001) 4:1678-1681.

Ray, A., Huisman, MV., Tamsma, JT. "The Role of Inflammation on Atherosclerosis, Intermediate and Clinical Cardiovascular Endpoints in Type 2 Diabetes Mellitus" *European Journal of Internal Medicine* 20 (2009) 253–260.

Razani, B., Chakravarthy, M.V. and Semenkovich, C.F. "Insulin Resistance and Atherosclerosis" *Endocrinology Metabolism Clinics of North America* 37 (2008) 603–621.

Rocourt, C.R.B., Wua, M., Chen, B.P.C. and Cheng, W. "The catalytic subunit of DNA-dependent protein kinase is downstream of ATM and feeds forward oxidative stress in the selenium-induced senescence response" *Journal of Nutritional Biochemistry* 24 (2013) 781–787.

Savitsky, K., Bar-Shira, A., Gilad, S., Rotman, G., Ziv, Y., Vanagaite, L., Tagle, D.A., Smith, S., Uziel, T., Sfez, S., Ashkenazi, M., Pecker, I., Frydman, M., Harnik, R., Patanjali, SR., Simmons, A., Clines, G.A., Sartiel, A., Gatti, R.A., Chessa, L., Sanal, O., Lavin, M.F., Jaspers, NGJ., Talor, A.M.R., Arlett, C.F., Miki, T., Weissman, S.M., Lovett, M., Collins, F.S., Shiloh, Y. "A Single Ataxia Telangiectasia Gene with a Product Similar to PI-3 Kinase" *Science* 268 (1995) 1749-1753.

Schneider, JG., Finck, BN., Ren, J., Standley, KN., Takagi, M., Maclean, KH., Bernal-Mizrachi, C., Muslin, AJ., Kastan, MB. and Semenkovich, CF. "ATM-Dependent Suppression of Stress Signaling Reduces Vascular Disease in Metabolic Syndrome" *Cell Metabolism* 4 (2006) 377–389.

Schramm, A., Matusik, P., Osmenda, G., Guzik, T.J. "Targeting NADPH Oxidases in Vascular Pharmacology" *Vascular Pharmacology* 56 (2012) 216–231.

Semenkovich, CF. "Insulin Resistance and Atherosclerosis" *The Journal of Clinical Investigation* 116 (2006) 7:1813-1822.

Semlitsch, M., Shackelford, R.E., Zirkl, S., Sattler, W., Malle, E., "ATM Protects Against Oxidative Stress Induced By Oxidized Low-Density Lipoprotein" *DNA Repair* 10 (2011) 848– 860.

Shiloh, Y. "ATM and Related Protein Kinases: Safeguarding Genome Integrity" *Nature Reviews* 3 (2003) 155-168.

Smith, P. "Effect of Hypoxia upon the Growth and Sprouting Activity of Cultured Aortic Endothelium from the Rat" *Journal of Cell Science* 92 (1989) 505-512.

Song, M.S., Salmena, L. And Pandolfi, P.P. "The Functions and Regulation of the PTEN Tumour Suppressor" *Nature Reviews: Molecular Cell Biology* 13 (2012) 283-296.

Stracker, T.H., Roig, I., Knobel, P.A. and Marjanovi, M. "The ATM signalling network in development and disease" *Frontiers in Genetics* 4 (2013) 37:1-19.

Strijdom, H., Chamane, N., Lochner, A. "Nitric Oxide in the Cardiovascular System: A Simple Molecule with Complex Actions" *Cardiovascular Journal of Africa* 20 (2009) 5:303-310.

Strijdom, H., Jacobs, S., Hattingh, S., Page, C. and Lochner, A. "Nitric Oxide Production Is Higher in Rat Cardiac Microvessel Endothelial Cells than Ventricular Cardiomyocytes in Baseline and Hypoxic Conditions: A Comparative Study" *The FASEB Journal* 20 (2006) 314-316.

Stuehr, D.J., Wei, C., Wang, Z. and Hille, R. "Exploring the Redox Reactions between Heme and Tetrahydrobiopterin in the Nitric Oxide Synthases" *The Royal Society of Chemistry* (2005) 3427–3435.

Sumpio, B.E., Riley, J.T., Dardik, A. "Cells in Focus: Endothelial Cell " *The International Journal of Biochemistry & Cell Biology* 34 (2002) 1508–1512.

Taguchi, K., Matsumoto, T., Kamata, K., Kobayashi, T. "Akt/eNOS Pathway Activation in Endothelium-Dependent Relaxation is Preserved in Aortas from Female, but not from Male, Type 2 Diabetic Mice" *Pharmacological Research* 65 (2012) 56– 65.

Treebak, J.T., Glund, S., Deshmunkh, A., Klein, D.K., Long, Y.C., Jensen, T.E., Jorgensen, S.B., Viollet, B., Andersson, L., Neumann, D., Wallimann, T., Richter, E.A., Chibalin, A.V., Zierath, J.R., Wojtaszewski, J.F.P. "AMPK-Mediated AS160 Phosphorylation on AMPK Catalytic and Regulatory Subunits" *Diabetes* 55 (2006) 2051-2058.

Vara, J.A.F., Casado, E., de Castro, J., Cejas, P., Belda-Iniesta, C. and Gonzalez-Baron, M. "PI3-K/Akt Signalling Pathway and Cancer" *Cancer Treatment Reviews* 30 (2004) 193–204.

Vecchio, D., Daga, A., Carra, E., Marubbi, D., Baio, G., Neumaier, C.E., Vagge, S., Corvò, R., Pia Brisigotti, M., Louis Ravetti, J., Zunino, A., Mascelli, S., Raso, A. and Frosina, G. "Predictability, Efficacy and Safety of Radiosensitization of Glioblastoma-Initiating Cells by the ATM Inhibitor KU-60019" *International Journal of Cancer* 135 (2014) 479–491.

Venugopal, S.K., Devaraj, S., Yuhanna, I., Shaul, P., Jialal, I. "Demonstration That C-Reactive Protein Decreases eNOS Expression and Bioactivity in Human Aortic Endothelial Cells" *Circulation* 106 (2002) 1439-1441.

Viniegra, J.G., Martínez, N., Modirassari, P., Losa, J.H., Cobo, C.P., Lobo, V.J.S., Luquero, C.I.A., Álvarez-Vallina, L., Cajal, S.R., Rojas, J.M. and Sánchez-Prieto, R. “Full Activation of PKB/Akt in Response to Insulin or Ionizing Radiation is Mediated Through ATM” *The Journal Of Biological Chemistry* 280 (2005) 6:4029–4036.

Wang, H., Albadawi, H., Siddiquee, Z., Stone, J. M. Panchenko, M.P., Watkins, M.T. and Stone, J.R. “Altered Vascular Activation due to Deficiency of the NADPH Oxidase Component P22phox” *Cardiovascular Pathology* 23 (2014) 35–42.

Wang, S., Song, P. and Zou, MH. “AMP-Activated Protein Kinase, Stress Responses and Cardiovascular Diseases” *Clin Sci (Lond)*. 122 (2012), 12: 555–573.

Watters, D. “Oxidative Stress in Ataxia Telangiectasia” *Redox Report* 8 (2003) 1:23-29.

Weichhart, T. and Säemann, M.D. “The PI3K/Akt/mTOR Pathway in Innate Immune Cells; Emerging Therapeutic Applications” *Ann Rheum Dis* 67 (2008) iii70-iii74.

Wymann, M.P. and Marone, R. “Phosphoinositide 3-kinase in disease: timing, location, and scaffolding” *Current Opinion in Cell Biology* 17 (2005) 141–149.

Yang, D., and Kastan, M.B. “Participation of ATM in Insulin Signalling through Phosphorylation of eIF-4E-Binding Protein 1” *Nature Cell Biology* 2 (2000) 893-898.

Yang, D., Halaby, M., Li, Y., Hibma, J.C. and Burn, P. “Cytoplasmic ATM Protein Kinase: an Emerging Therapeutic Target for Diabetes, Cancer and Neuronal Degeneration” *Drug Discovery Today* 16 (2011) 7/8: 333-338.

Yang, Z. and Li, J. “Stimulation of Endothelin-1 Gene Expression by Insulin via PI3K” *Life Science* 82 (2008) 512-518.

Yin, D., Liu, M., Yang, G., Huang, J., Gui, M. "Effects of Simvastatin on Early Oxidative Stress and Endothelial Function in Apolipoprotein E-Deficient Mice" *Journal of Nanjing Medical University* 21 (2007) 6:359-362.

Young, L.H., Li, J., Baron, S.J. and Russell, R.R. "AMP-Activated Protein Kinase: A Key Stress Signaling Pathway in the Heart" *Trends in Cardiovascular Medicine* 15 (2005) 110–118.

Yu, E., Calvert, P.A., Mercer, J.R., Harrison, J., Baker, L., Figg, N.L., Kumar, S., Wang, J.C., Hurst, L.A., Obaid, D.R., Logan, A., West, N.E.J., Clarke, M.C.H., Vidal-Puig, A., Murphy, M.P., Bennett, M.R. "Mitochondrial DNA Damage Can Promote Atherosclerosis Independently of Reactive Oxygen Species Through Effects on Smooth Muscle Cells and Monocytes and Correlates With Higher-Risk Plaques in Humans" *Circulation* 128 (2013) 702-712.

Yu, Y., Yoon, S., Poulgiannis, G., Yang, Q., Ma, X.M., Villén, J., Kubica, N., Hoffman, G.R., Cantley, L.C., Gygi, S.P. and Blenis, J. "Phosphoproteomic Analysis Identifies Grb10 as an mTORC1 Substrate that Negatively Regulates Insulin Signaling" *Science* 332 (2011) 1322-1326.

Zhang, D., Contu, R., Latronico, M.V.G., Zhang, J.L., Rizzi, R., Catalucci, D., Miyamoto, S., Huang, K., Ceci, M., Gu, Y., Dalton, N.D., Peterson, K.L. Guan, K., Brown, J.H., Chen, J., Sonenberg, N. and Condorelli, G. "MTORC1 Regulates Cardiac Function and Myocyte Survival Through 4E-BP1 Inhibition in Mice" *The Journal of Clinical Investigation* 120 (2010) 2805-2816.

Zhang, X., Chen, S. and Wang, Y. "Honokiol Up-Regulates Prostacyclin Synthase Protein Expression and Inhibits Endothelial Cell Apoptosis" *European Journal of Pharmacology* 554 (2007) 1-7.

Zreikat, H.H., Harpe, S.E., Slattum, P.W., Mays, D.P., Essah, P.A., Cheang, K.I. “Effect of Renin–Angiotensin System Inhibition on Cardiovascular Events in Older Hypertensive Patients with Metabolic Syndrome” *Metabolism, Clinical and Experimental* 63 (2014) 392-399.

Websites:

What-When-How: “In Depth Tutorials and Information” <http://what-when-how.com/cardiomyopathies-from-basic-research-to-clinical-management/insulin-resistance-and-cardiomyopathy-metabolic-and-drug-induced-cardiomyopathies-part-1/>